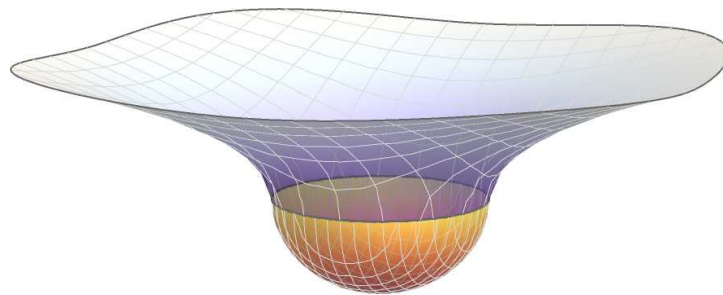# Ultraviolet improved black holes

Master Thesis

Sven Köppel

December 2014

First Supervisor: PD Dr. Piero Nicolini

Second Supervisor: Prof. Dr. Marcus Bleicher

Institute for Theoretical Physics &
Frankfurt Institute for Advanced Studies

GOETHE
UNIVERSITÄT
FRANKFURT AM MAIN

Vorliegende Version ist vom **December 11, 2014, 18:09**

Abstract

In this thesis, Planck size black holes are discussed. Specifically, new families of black holes are presented. Such black holes exhibit an improved short scale behaviour and can be used to implement gravity self-complete paradigm. Such geometries are also studied within the ADD large extra-dimensional scenario. This allows black hole remnant masses to reach the TeV scale. It is shown that the evaporation endpoint for this class of black holes is a cold stable remnant. One family of black holes considered in this thesis features a regular deSitter core that counters gravitational collapse with a quantum outward pressure. The other family of black holes turns out to nicely fit into the holographic information bound on black holes, and lead to black hole area quantization and applications in the gravitational entropic force. As a result, gravity can be derived as emergent phenomenon from thermodynamics.
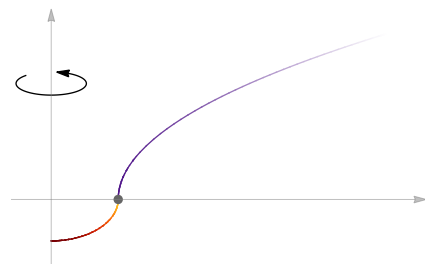
The thesis contains an overview about recent quantum gravity black hole approaches and concludes with the derivation of nonlocal operators that modify the Einstein equations to ultraviolet complete field equations.

About the front picture

This picture shows an embedding diagram for the self-regular black hole in the outstanding case $\alpha \to \infty$.
By intention, there are no units as this is purely illustrative. The 3d picture can be constructed by rotating the graphs shown on the right around its y axis. The color transition indicates the position of the black hole event horizon.
For more information about the computation of embedding diagrams, see appendix A.

Contents

Todo list

Chapter 1

Introduction

1.1 Motivation

This work is about the quest of contemporary physics on the smallest scales and biggest energies. By historical evolution, in the 20th century two opposing theories developed: For phenomena on the smallest scales (e.g. the constituents of an atom), quantum physics evolved. On the other hand, for phenomena on the biggest scales (e.g. the Universe), general relativity was formulated.

Combining these two worlds is a big quest in physics. A theory which describes effects from both the quantum and the gravitational world is a *Quantum Gravity* theory.
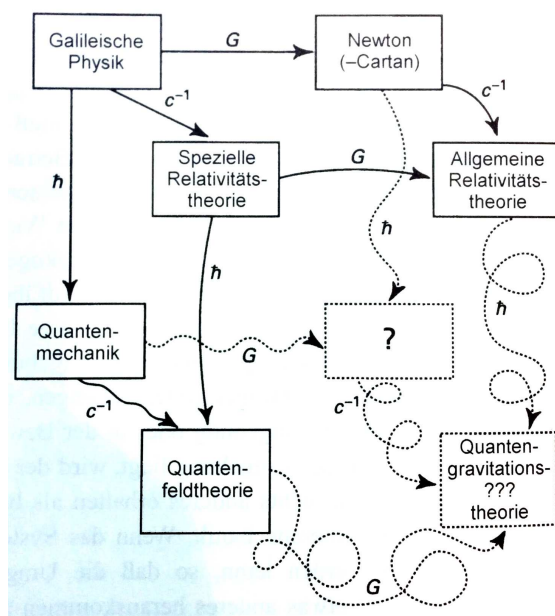
Figure 1.1: The *cube of physics*, a popular illustration about characteristic constants that describe the regime for physical phenomena. First appeared in a 1999 book from Roger Penrose [64].

The whirly lines shall encode how hard the author percieved the challenge to find or handle the theories the arrows point to. Appearently, Penrose finds a theory of Quantum Gravity hard to find.

Cube of Physics als Vektor machen

The combination of quantum mechanics and special relativity leads to Quantum Field Theory (QFT) and the formulation of the Standard Model of particle physics which is exceptionally

and unexpectedly successful. From the viewpoint of an high-energy physicist, three of the four fundamental interactions, namely the electromagnetic, weak and strong interactions can be joined into a unified theory, while gravity is simply the weakest and last interaction left as an "ordinary" classic field theory. A unification of the three Standard Model interactions is called grand unified theory (GUT). On the other hand, from the viewpoint of a relativist, General Relativity taught us that there is no background space where physics "takes place". This new principle leads to a bunch of new physics, where the most remarkable fact is perhaps the existence of black holes as regions of no escape in spacetime or even the existence of wormholes (Einstein-Rosen bridge). Certainly, General Relativity had the biggest impact on the science fiction genre.

Physics beyond the Standard Model is an uncomfortable job, because it still lacks experimental accessibility. One thing theorists can do is quantum field theory in curved space (QFTCS), the semiclassical approximation to quantum gravity where quantum fields interact with a classical background spacetime. In the *cube of physical theories*, as shown in figure 1.1, QFTCS is "one step" from QFT to Quantum Gravity, because 1-loop graviton contributions are included in the quantum energy momentum tensor at the right hand side of Einstein Field Equations.

Actually, QFTCS opened the door for the first quantum mechanical treatments of strong gravity objects, namely black holes. In the 1970s, this led to the Hawking's groundbreaking prediction of thermal radiation of Schwarzschild black holes. In terms of "theories", Hawking radiation is really interdisciplinary:

$$T_{\mathrm{H}} = \frac{\hbar\, c^3}{8\pi\, G\, M k_{\mathrm{B}}}$$

There are "ingredients" from Quantum Mechanics (Planck constant $\hbar$), Special Relativity (speed of light c), Gravitation (Newton's constant G) and Thermodynamics (Boltzmann constant k_B).

But Hawking's temperature also spots one of the inconsistencies of General Relativity: The temperature increases with decreasing mass M. As radiating black holes lose mass, they get hotter and hotter. At some point, the validity of QFTCS breaks down. The need for a better theory arises.

1.2   The problems and the approach

The breakdown of QFTCS is one of the problems addressed in this thesis. Other problems are

- The curvature singularity in the center of the Schwarzschild black hole, discussed in section 2.2.

- The hierarchy problem in the Standard model, discussed in section 2.3.

- The black hole–particle duality at high energies, where Quantum Mechanics and General Realtivity predict different length scales, discussed in section 3.1.

I propose black hole geometries with an improved short scale behaviour based on the self-complete paradigm of gravity. These modified geometries engage all three problems outlined above.

1.3 Outline

Chapter 2 is an introductory section about General Relativity. It will give an introduction to the formalism and shortly derive the Einstein equation. Then the first solutions on GR are shown and the different types of singularities and their origins are discussed. The large spatial extra dimension scenario is outlined.

Chapter 3 is devoted to the minimal length in physics. The particle–black hole duality is discussed and nonlocal gravity formalism is proposed. The generalized uncertainty principle is given as an example for minimal length physics.

In chapter 4, the formalism for a class of short-scale modified static isotropic black holes in higher dimensions is prepared. To do so, Einstein Equations are solved for an ideal static isotropic "blurred" matter ball that shall describe a "quasi-classical" mass point. Thermodynamical properties like temperature, heat capacity and entropy are derived and a nonlocal operator is determined in terms of a Fourier transform.

Chapter 5 and 6 are devoted to two classes of black holes that are based on the more generic class discussed in chapter 4. In these two chapters, physical properties and implications are discussed based on the formalism introduced before.

Chapter 2

Theoretical background

2.1 General Relativity

In this section, a short derivation of General Relativity (GR) is given. It is the geometrical theory of gravitational interaction from matter and the major framework used in this work. To do so, some core concepts of differential geometry on manifolds are retraced briefly in order to derive the Einstein Field Equations (EFE) by Hamiltonian's principle of least action. Exact definitions of the new vector concept are skipped in favour of condensing the ideas. In this text I follow the notations of [17, 46, 50, 80, 81]. They prefer abstract index notation as a more fundamental approach to introduce Riemannian geometry. In contrast, some tensors may also be derived by "index constraints" as done in [29]. This is less elegant but more straightforward.

2.1.1 Differential Geometry

In curved space geometry, intuition about well-known mathematical symbols like vectors as "position vectors" fails [81]. The mathematical approach is a differential description using the fact that manifolds M are locally flat (they look "nearly" flat). Thus the tangent vector V is introduced as a directional derivative operator. The components of such a vector may be denoted as

$$V(f) = V^\mu \frac{\partial f}{\partial x^\mu}. \tag{2.1}$$

The vector V maps functions $f \in C^\infty(M, \mathbb{R})$ to $\mathbb{R}$. With a fixed point $p \in M$, it defines the tangent vector space V_p. Introducing the dual space V_p^* and the dual dual space $V_p^{**} \cong V_p$ yields to the definition of tensors as a multilinear mappings from vectors and dual vectors into numbers [80].

2.1.2 Covariant Derivation Operator

As for two points $p, q \in M$, the tangent spaces V_p and V_q can not directly be compared. For example, defining for the vector V^μ a traditional derivative (cf. [50, page 208])

$$\frac{\partial V^\mu}{\partial x^\nu} = \lim_{h \to 0} \frac{V^\mu(x^1, \dots, x^\nu + h^\nu, \dots, x^n) - V^\mu(x^1, \dots, x^\nu + h^\nu, \dots, x^n)}{h^\nu} \tag{2.2}$$

fails as even x and $x + h$ may not be compared directly. As a solution, a covariant derivation operator ∇ by means of the parallel transport is derived. This operator will transform like a tensor.

While Wald [80, page 31] designates requirements for the covariant derivation (linearity, Leibnitz rule, index contraction commutativity, consistency with the index free notation and vanishing torsion tensor/commutativity) and derives the existence of a *connection coefficient* Γ^a_{bc}, one can also introduce the connection coefficient as the link in the parallel transport which shall be the "correct" way to denote the derivative (2.2):

$$V^\mu(x \to x + h) := V^\mu(x) - V^\lambda(x) \Gamma^\mu_{\nu\lambda} h^\nu. \tag{2.3}$$

By replacing the traditional difference $V^\mu(x) - V^\mu(x + h)$ by $V^\mu(x) - V^\mu(x \to x + h)$ in equation (2.2), one immediately ends up with the definition of the covariant derivative

$$\nabla_\mu V^\nu = \partial_\mu V^\nu + \Gamma^\nu_{\mu\sigma} V^\sigma. \tag{2.4}$$

The covariant derivative naturally extends when computing derivatives of tensors of arbitrary rank. For a (k, l) tensor T the derivative is given (without proof) by

$$\nabla_\alpha T^{\lambda_1 \dots \lambda_k}_{\mu_1 \dots \mu_l} = \partial_\alpha T^{\lambda_1 \dots \lambda_k}_{\mu_1 \dots \mu_l} + \sum_{i=1}^{k} \Gamma^{\lambda_i}_{\alpha\beta} T^{\lambda_1 \dots \beta \dots \lambda_k}_{\mu_1 \dots \mu_l} - \sum_{j=1}^{l} \Gamma^\beta_{\alpha\mu_i} T^{\lambda_1 \dots \lambda_k}_{\mu_1 \dots \beta \dots \mu_l}. \tag{2.5}$$

The indices $\lambda_1 \dots \beta \dots \lambda_k$ have to be read in a way that β replaces the index variable at that place. For example, the covariant derivative of a $(2, 2)$ tensor reads

$$\nabla_\alpha T^{\lambda\delta}_{\mu\nu} = \partial_\alpha T^{\lambda\delta}_{\mu\nu} + \Gamma^\lambda_{\alpha\beta} T^{\beta\delta}_{\mu\nu} + \Gamma^\delta_{\alpha\beta} T^{\lambda\beta}_{\mu\nu} - \Gamma^\beta_{\alpha\mu} T^{\lambda\delta}_{\beta\nu} - \Gamma^\beta_{\alpha\nu} T^{\lambda\delta}_{\mu\beta}. \tag{2.6}$$

2.1.3 The Metric

The connection symbol $\Gamma^\alpha_{\beta\gamma}$ introduced in equation (2.3) is still ambigous. As soon as one equippes the manifold with a metric $g_{\mu\nu}$, there is a special choice, constrained by the requirement that scalars shall be invariant under parallel transport (in colloquial terms, scalars are required to be the same in any coordinate system). The inner product of two arbitrary vectors $\boldsymbol{v}$ and $\boldsymbol{w}$ is a scalar and shall therefore also be invariant under any parallel transport $t^\alpha \nabla_\alpha$. This leads to

$$0 \overset{!}{=} t^\alpha \nabla_\alpha g_{\beta\gamma} v^\beta w^\gamma \quad \Rightarrow \quad 0 = \nabla_\alpha g_{\beta\gamma}. \tag{2.7}$$

A connection $\Gamma^\gamma_{\alpha\beta}$ is called *metric compatible* if it fulfills (2.7) and is torsion-free ($\Gamma^\gamma_{\alpha\beta} = \Gamma^\gamma_{(\alpha\beta)}$, with $\Gamma_{(\alpha\beta)}$ being the symmetric part of $\boldsymbol{\Gamma}$ according to eq. (F.3). See e.g. [17, page 99] for torsion).

These uniquely determined connection symbols are called *Christoffel symbols*. They allow for computing the parallel transport and the covariant derivative from the metric:

$$\Gamma^\delta_{\alpha\beta} = \frac{1}{2} g^{\delta\gamma} (\partial_\alpha g_{\beta\delta} + \partial_\beta g_{\alpha\delta} + \partial_\gamma g_{\alpha\beta}). \tag{2.8}$$

2.1.4 Curvature

It is important to remember that for a manifold M there exist different choices of coordinate systems, and only if one founds flat space coordinates that are applicable everywhere (that is, $\boldsymbol{\Gamma} = 0$ for all $p \in M$), the manifold is not curved. This reasoning does not work the other way, as the example of choosing polar coordinates (t, r, ϕ, θ) in flat space shows: Some entries are non-zero (e.g. $\Gamma^\phi_{r\phi} = 1/r$), but the space is still flat.

In favour to get a measure for spacetime curvature, one can analyse the "defects" of parallel transport around a closed loop with infinitesimal extend. It will be shown that the change is described by a $(1,3)$-curvature tensor called *Riemann curvature tensor*.

In the present setup (cf. figure 2.1), the vector V^μ is moved around the closed path $a \to b \to c \to d$ with infinitesimal spacings $+\Delta^\mu_1, +\Delta^\mu_2, -\Delta^\mu_1, -\Delta^\mu_2$. One can determine the missing part $\#$ when coming back to a by explicit computation of the vector V^μ at the space time points:

$$V^\mu(a) = V^\mu(a) \tag{2.9a}$$

$$V^\mu(b) = V^\mu(a \to a + \Delta_1) = V^\mu(a) - V^\alpha(a)\Gamma^\mu_{\beta\alpha}(a)\Delta^\beta_1 \tag{2.9b}$$

$$V^\mu(c) = V^\mu(b \to b + \Delta_2) = V^\mu(b) - V^\gamma(b)\Gamma^\mu_{\delta\gamma}(b)\Delta^\delta_2 \tag{2.9c}$$

$$V^\mu(d) = V^\mu(c \to c - \Delta_1) = V^\mu(c) - V^\epsilon(c)\Gamma^\mu_{\kappa\epsilon}(c)(-\Delta^\kappa_1) \tag{2.9d}$$

$$\#V^\mu(a) = V^\mu(d \to d - \Delta_2) = V^\mu(d) - V^\lambda(d)\Gamma^\mu_{\omega\lambda}(d)(-\Delta^\omega_2) \tag{2.9e}$$

Recursively inserting all equations into each other gives a long expression where all linear terms $\mathcal{O}(\Delta^\nu_i)$ vanish. All third powers $\mathcal{O}(\Delta^\nu_i \Delta^\xi_j \Delta^\rho_k)$ are ignored, so the result is proportional
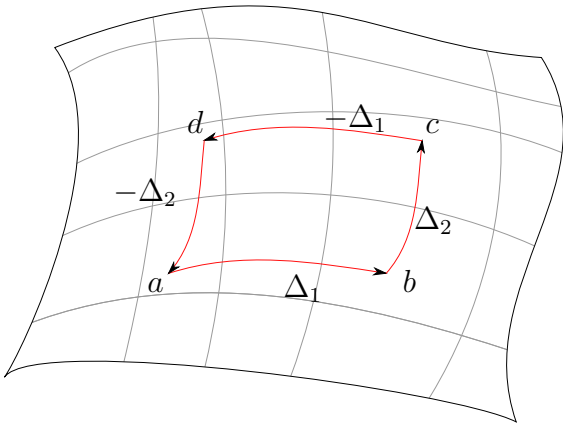

Figure 2.1: Illustration of the closed loop parallel transport on infinitesimal linear displacements Δ^μ_i. When performing the calculation in equation 2.9, on curved spacetimes one finds a defect which defines the Riemann tensor. This means that the vector at the beginning (point a) does not match the vector after the loop any more.

to second order terms $\mathcal{O}(\Delta_1^\gamma \Delta_2^\delta)$ after appropriate index relabeling. Note that the Christoffel symbols (also) depend on the point where they are evaluated at. They can be simply moved e.g. at the first insertion step 2.9b into 2.9c by $\Gamma(b) = \Gamma(a) + \partial_\nu \Delta_1^\nu \Gamma(a)$. One ends up with the definition of the Riemann tensor $R_{\alpha\beta\gamma}^\mu$ as a piece of the missing part

$$\# V^\mu(a) = V^\mu(a) \Big(\underbrace{\partial_\beta \Gamma_{\gamma\alpha}^\mu - \partial_\gamma \Gamma_{\beta\alpha}^\mu + \Gamma_{\gamma\alpha}^\delta \Gamma_{\beta\delta}^\mu - \Gamma_{\beta\alpha}^\delta \Gamma_{\gamma\delta}^\mu}_{R_{\alpha\beta\gamma}^\mu} \Big) \Delta_1^\gamma \Delta_2^\delta. \tag{2.10}$$

By tensor contraction, one can define the Ricci tensor $R_{\mu\nu} = R_{\mu\lambda\nu}^\lambda$ and finally the Ricci scalar $R = R_\lambda^\lambda$. This quantity is also called scalar curvature and it is the simplest invariant that gives information about flatness of space: As soon as $R = 0$ everywhere, the space is flat.

Most significance for the next section has the Einstein curvature tensor $\boldsymbol{G}$, defined by a linear combination of the Ricci tensor and the curvature scalar as

$$G_{\mu\nu} = R_{\mu\nu} + \frac{1}{2} g_{\mu\nu} R. \tag{2.11}$$

2.1.5 Einstein field equations

Einstein field equations (or shorter: Einstein's equations) can be derived from a variational principle (Hamliton principle $\delta S = 0$ on the action S). They can also be derived by other means, e.g. symmetry aspects leaving only one choice for combining $G_{\mu\nu}$ and the energy density tensor $T_{\mu\nu}$.

Here, the ansatz will be the action S, defined by the Lagrangian $\mathcal{L} = \mathcal{L}_G + \mathcal{L}_M$, that is, the gravitational part and the matter part. In terms of field theory, interactions are intermediated by $\mathcal{L}_G$, while $\mathcal{L}_M$ contains the source terms. Those two parts are guessed: Here we take basically taking the curvature scalar R and the trace of the energy density tensor $T = T_\lambda^\lambda$. The low energy matching is traditionally accomplished by a prefactor κ, so one ends up with the *Einstein-Hilbert action* including matter,

$$S = \int \sqrt{-g}\, \mathrm{d}^4 x \left(\frac{R}{2\kappa} + T \right). \tag{2.12}$$

Note that $\sqrt{-g}$, with g the determinant of the metric $g^{\mu\nu}$, is neccessary for the invariant volume element.

By splitting up the integral into two parts S_R and S_T and calculating the variation individually, one finds for S_R,

$$\delta S_R = \frac{1}{2\kappa} \delta \int \sqrt{-g}\, \mathrm{d}^4 x\, R_{\mu\nu} g^{\mu\nu} \tag{2.13}$$

$$= \frac{1}{2\kappa} \int \mathrm{d}^4 x\, R_{\mu\nu} \delta(\sqrt{-g} g^{\mu\nu}) + \frac{1}{2\kappa} \int \mathrm{d}^4 x\, \sqrt{-g} g^{\mu\nu} (\delta R_{\mu\nu}). \tag{2.14}$$

One can show that the integral over the variation of $\delta R_{\mu\nu}$ vanishes (surface integral) while the variation $\delta \sqrt{-g} g^{\mu\nu}$ contributes.

For a full discussion, one typically switches to *tensor densities* which are "salted" with $\sqrt{-g}$ and written in German gothic letters [50],

$$\mathfrak{T}_{\ldots}^{\ldots} = \sqrt{-g}\, A_{\ldots}^{\ldots}, \tag{2.15}$$

where $A_{\ldots}^{\ldots}$ represents a tensor in a local coordinate frame. By using the identity $\delta\sqrt{-g} = -\tfrac{1}{2}\sqrt{-g}g_{\mu\nu}\delta g^{\mu\nu}$, one finds

$$\delta S_R = \int \mathrm{d}^4 x\, R_{\mu\nu}(\delta\sqrt{-g}g^{\mu\nu}) = \int \mathrm{d}^4 x \sqrt{-g} \left(R_{\mu\nu} - \frac{1}{2}g_{\mu\nu}R \right)\delta g^{\mu\nu}. \tag{2.16}$$

Secondly, the variation of S_T reads

$$\delta S_T = \int \mathrm{d}^4 x\, \sqrt{-g}\,(\kappa T_{\mu\nu})\,\delta g^{\mu\nu}. \tag{2.17}$$

By requiring $\delta S = \delta S_R + \delta S_T = 0$ and collecting the terms under the integrals, one has

$$R_{\mu\nu} - \frac{1}{2}g_{\mu\nu}R = \kappa T_{\mu\nu}, \tag{2.18}$$

known as the *Einstein field equations* (EFE). The low energy matching with the Newtonian potential

$$\Phi(r) = -\frac{GM}{r} \tag{2.19}$$

allows determining $\kappa = -8\pi G$. The dimensionful constant G is the Newton's constant, not to be confused with the rarely used trace of the Einstein tensor G^μ_μ. The choice of prefactors 8π and the sign $-$ (Misner, Thorne and Wheeler call it the "Einstein sign" [50]) in κ is convention. This text follows the sign from Adler, Bazin, Schiffer.

An astonishing fact of the Einstein field equations is that they allow for deriving all classical predictions of mechanics. The energy conservation law $\nabla_\mu T^{\mu\nu} = 0$ is also intrinsically contained in the Einstein field equations. One can show that in $d = 3 + 1$ space-time dimensions, the EFE are 10 independent non-linear coupled equations which are only possible to solve analytically for highly symmetric problems.

2.1.6 The Planck Scale

The Planck scale is the name of the energy and length scales that one inevitably connected with the Einstein field equations (2.18). It can be found with the low energy limit, as from Newton's law (2.19) it follows for the unit of G that $[G] = \frac{1}{\mathrm{Mass}^2}$. It can also be found as follows:

- Recall that the metric is a dimensionless tensor.

- The curvature scalar R as second derivative of the metric must then have unit

$$[R] = \frac{1}{\mathrm{Length}^2} = \mathrm{Mass}^2.$$

- The energy momentum tensor $T_{\mu\nu}$ in 4 space-time dimensions has dimension

$$[\boldsymbol{T}] = \text{Mass}^4.$$

As a result, the Einstein field equations look like

$$R_{\mu\nu} - \frac{1}{2} g_{\mu\nu} R = -8\pi \frac{1}{M_{\text{Pl}}^2} T_{\mu\nu} \tag{2.20}$$

with a mass $M_{\text{Pl}} = \sqrt{1/G}$, the Planck mass. Reinserting units gives a numerical value of $M_{\text{Pl}} \sim 10^{16}$ TeV. Numerical values are often given in multiples of Planck mass M_{Pl}, Planck length L_{Pl}, Planck time $T_{\text{Pl}} = L_{\text{Pl}}/c$, etc. In SI units, the Planck units are given as

$$M_{\text{Pl}} = 2.1 \cdot 10^{-8} \text{ kg}, \tag{2.21}$$
$$L_{\text{Pl}} = 1.6 \cdot 10^{-35} \text{ m}, \tag{2.22}$$
$$T_{\text{Pl}} = 5.4 \cdot 10^{-44} \text{ s}. \tag{2.23}$$

Compared to the mass scales of particle physics, the Planck mass is incredibly big, while the time and length scales are incredibly small. For comparison, a typical scale in QCD is $\Lambda_{\overline{\text{MS}}} \sim 220$ MeV [66]. For the electroweak force, the scale is ~ 100 GeV. The large ratio of Planck mass over electroweak mass is called the *weak hierarchy problem* of the standard model of particle physics.

As a consequence, gravity can be neglected in particle collision center of mass energies accessible at ground based colliders like the Large Hadron Collider (LHC) at CERN (~ 10 TeV). As a thumb rule, gravity must be considered when the amount of energy of the order of Planck mass is compressed in a cube with edge length of the order of the Planck length $L_{\text{Pl}} = 1/M_{\text{Pl}} \sim 10^{-35}$ m.

In the next sections, a theory is proposed in order to avoid these circumstances, basically by *lowering* the Planck mass to some accessible range with the LHC.

2.2   Vacuum solutions of General Relativity

This section proposes three exact solutions of General Relativity which bother the issue of vacuum in General Relativity. Loosely speaking, vacuum is when $T_{\mu\nu} = 0$. This is only globally true for the Minkowski spacetime.

There are books collecting and classifying exact solutions (in contrast to numerical solutions or expansions) of Einstein gravity like Griffiths [34] and Stephani [73]. For an introductory overview about the spacetimes developed by Schwarzschild and DeSitter, see the book of Griffiths [34]. This section follows his reasoning.

2.2.1   Minkowski space-time

Minkowski spacetime is the Einstein solution of the empty and flat space $R_{\mu\nu} = 0$. Working in Cartesian coordinates with a $g_{\mu\nu} = \eta_{\mu\nu} = \text{diag}(-1, +1, +1, +1)$ signature, the Minkowski line

element can be given as

$$ds^2 = g_{\mu\nu}dx^\mu dx^\nu = -dt^2 + dx^2 + dy^2 + dz^2, \qquad (2.24)$$

with the coordinates $t, x, y, z \in (-\infty, \infty)$. It is convenient to switch to spherical coordinates when a spherical symmetric problem is given (as it is in this thesis). Spherical coordinates can be given by the transformation rules $x = r\sin\theta$, $y = r\sin\theta\sin\phi$ and $z = r\cos\theta$, with $r \in [0, \infty)$, $\theta \in [0, \pi]$ and $\phi \in [0, 2\pi)$. In these coordinates, the same line element reads

$$ds^2 = -dt^2 + dr^2 + r^2(d\theta^2 + \sin^2\theta d\phi^2) = -dt^2 + dr^2 + r^2 d\Omega_2^2. \qquad (2.25)$$

Considering spherical coordinates in flat Minkowski space is a good opportunity to learn about *coordinate singularities*: Apparently, the spherical line element (2.25) exhibits singularities at points where $r = 0$ or $\sin\theta = 0$. But the cartesian coordinate choice (2.24) tells that these singularities are not "real", because equation (2.24) shows coordinates without singularities, so the apparent singularities are no true singularities. In contrast, a *curvature singularity* is distinguished by a diverging curvature scalar $R = R^\mu_\mu$, and no choice of coordinates can avoid a coordinate singularity at points where a curvature singularity occurs. In the next section, the most simple space-time exposing a single curvature singularity point is encountered.

2.2.2 Schwarzschild metric

The Schwarzschild metric can be interpreted as the solution for the spherically symmetric static point mass distribution

$$\rho_\delta(r) := \frac{M}{4\pi r^2}\delta(r), \qquad (2.26)$$

which is — having the Coulomb potential of electrostatics in mind — probably the most basic non-empty matter distribution one can imagine. The Schwarzschild solution is frequently called a vacuum solution, because one excludes the region $r = 0$ in the derivation when solving the Laplace equation $\Delta\Phi(r) = 0$ for Newton's potential $\Phi(r)$ with boundary conditions [7]. As a matter of fact, it is a nonempty space solution, as at the origin, the energy-momentum tensor does not vanish ($T_{\mu\nu} \neq 0$). The Poisson equation $\Delta\Phi(r) = -\rho_\delta(r)$ confirms that fact. Properly speaking, the only vacuum solution of EFEs is the Minkowski spacetime.

The problem of finding a static, spherically symmetric solution, as can be found in text books [50, 80], is typically divided into the *outer* Schwarzschild metric, which describes the space outside a spherically symmetric static mass distribution, and the *interior* Schwarzschild metric, which describes the space-time inside the source (a perfect fluid).

It is worth mentioning that the outer Schwarzschild metric is derived from $\rho_\delta(r)$, as given in (2.26), but it will be assumed to be the solution outside of any spherical symmetric matter distribution $\rho(r)$. This even holds for non-static (*i.e.* time dependent) spherical symmetric distributions, e.g. monopole gravitational waves. This is a consequence of the *Birkhoff theorem* which states that any spherically symmetric solution of the vacuum Einstein field equations must be static and *asymptotically* flat (Minkowski for $r \to \infty$). Note that the Birkhoff theorem

only holds in $d = 4$ space-time dimensions (c.f. the next section about higher dimensional gravity).

The solution of (2.26) is given by the Schwarzschild metric

$$\mathrm{d}s^2 = -(1 + 2\Phi(r))\mathrm{d}t^2 + (1 + 2\Phi(r))^{-1}\mathrm{d}r^2 + r^2\mathrm{d}\theta^2 + r^2\sin^2(\theta)\mathrm{d}\phi^2 \qquad (2.27)$$

with the gravitational potential (Newton's potential) $\Phi(r)$ from eq. (2.19). Note that r is not the *distance* from the origin $r = 0$, as space time is deformed and r actually gets timelike for $r < 2GM$.

In contrast to (2.27), another form to display Schwarzschild metrics is conventionally used in this thesis, using the *gravitational function* $V(r) = -2\Phi(r)$ and displaying the same metric as

$$\mathrm{d}s^2 = -(1 - V(r))\mathrm{d}t^2 + (1 - V(r))^{-1}\mathrm{d}r^2 + r^2\mathrm{d}\theta^2 + r^2\sin^2(\theta)\mathrm{d}\phi^2. \qquad (2.28)$$

The radius $r_H = 2GM$ has a special meaning. At r_H, the metric (2.27) has a *coordinate* singularity which is not a curvature singularity, as one can see when switching e.g. to Eddington-Finkelstein coordinates (Tortoise coordinates). What physically happens at r_H is that light from the space time region enclosed by the $r = r_H$ cannot escape that surface, *i.e.* it is literally trapped (*trapping* surface). For this reason, one calls this a *black hole* with event horizon radius r_H, as no event that takes place inside the horizon can be seen by an outside observer.

Actually, the Schwarzschild space-time features a curvature singularity at $r = 0$, which was already "announced" by the Dirac delta function, $\rho_\delta(r) \xrightarrow{r \to 0} \infty$. The singularity is shielded by the event horizon, so whatever happens near it cannot be observed outside. In 1969, Roger Penrose formulated the *cosmic censorship hypothesis* which states that curvature singularities are always "hidden" behind an event horizon, so there are no *naked singularities*. In fact, there are solutions of the EFEs with naked singularities, like the hyper-extreme Reissner-Nordström space-time, discussed in section 6.1.6.

Many modifications of the Schwarzschild line element have been investigated, e.g. $g_{00} = 1 - 2GM/r \to \epsilon - 2GM/r$, with $\epsilon \in \mathbb{R}$, or by describing an extended object with mass distribution $M(\boldsymbol{x})$, or by including new physics (like electrical charge). Such approaches have been studied [34], and approximating the Dirac delta function $\delta(r)$ with a distribution $h(r)$ describes best the roadmap for this thesis. However, in any General Relativity text book, the Schwarzschild metric is alsmost always extended with angular momentum J and/or electric charge Q, as there exist the old and well-known solutions of the Reissner-Nordström (RN) metric ($Q \neq 0, J = 0$), the Kerr metric ($Q = 0, J > 0$) and the Kerr-Newman metric ($Q \neq 0, J > 0$). The *no-hair theorem*, formulated by John Wheeler, postulates that all black hole solutions resulting from the Einstein equations (including electromagnetism, so strictly spoken Einstein-Maxwell equations) are fully characterized by only mass M, electrical charge Q and angular momentum J. Actually, this theorem has not been proven and is therefore only a *conjecture*. The four black hole evaporation phases stated in section 2.4.2 are based on this conjecture.

While angular momentum is probably the most relevant parameter for astronomical purposes, in this thesis it turns out that the RN metric possesses analogies to the regular black hole solutions that will be derived (section 6.1.6). Note that in this thesis, spinning black holes are

not studied. This is not neccessarily bad, as here only the final evaporation phases of black holes are concerned.

2.2.3 De Sitter space-time

Considering the vacuum issue, the DeSitter space time also turns out to be of interest, as it is frequently discussed as vacuum solution of Einstein equations with cosmological constant.

The DeSitter space time can be found as one of the three unique solutions with constant curvature R. The other ones are flat Minkowski space time and anti-DeSitter space time. The class of DeSitter space times can be derived by the 10 isometries of space-time in four dimensional space-time by the local condition [34]

$$R_{\alpha\beta\gamma\delta} = \frac{R}{12}(g_{\alpha\gamma}g_{\beta\delta} - g_{\alpha\delta}g_{\beta\gamma}). \tag{2.29}$$

Using the Einstein equations with cosmological constant Λ,

$$G_{\mu\nu} + \Lambda g_{\mu\nu} = 8\pi G T_{\mu\nu}, \tag{2.30}$$

these two solutions *can be seen* as real vacuum solutions ($T_{\mu\nu} = 0$), and $R = 4\Lambda$, $R_{\alpha\beta} = \Lambda g_{\alpha\beta}$. Space with $R > 0$ is called *de Sitter* space-time (dS) while space with $R < 0$ is called *anti-de Sitter* space-time (AdS), after the Dutch physicist Willem de Sitter. The issue whether DeSitter space is vaccuum or not is connected to the dual theory concept of EFE without cosmological constant. This concept is discussed in the context of nonlocal gravity (section 3.3) and the deSitter core of a black hole (section 6.1.4).

There is a set of spherical coordinates that do not cover the complete deSitter space time, but is well enough for the considerations done in this thesis. Robert Mayers calls these the "static patch" coordinates [54], and the gravitational function—constructing a metric according to (2.28)—is given by

$$V(r) = \frac{\Lambda}{3}r^2 := \left(\frac{r}{\ell}\right)^2. \tag{2.31}$$

In de Sitter space, our coordinates $g_{00} = 1 - r^2/\ell^2$ have a singularity at $r = \ell := \sqrt{3/\Lambda}$. Of course, since $R = 4\Lambda$ everywhere, this is not a curvature singularity. Anyway the surface $r = \ell$ forms a horizon. One can show that this is a *cosmological horizon* [34] which reveals a universe expansion speed higher than the speed of light: Events beyond $r > \ell$ cannot reach the observer at $r = 0$ anymore. An exact discussion requires introduction of Friedmann-Lemaître-Robertson-Walker-like (FLRW) coordinates and "struggling" with cosmology, which is beyond the scope of this thesis.

2.3 Extra Dimensions

From the mathematical/geometrical viewpoint, in terms of tensor calculus, the generalization from 4 to d space-time dimensions is trivial: One can write the Einstein equations in d space-time dimensions as

$$R_{AB} - \frac{1}{2}g_{AB}R = -8\pi G T_{AB} \tag{2.32}$$

with capital latin indices (like A, B) running from $0, 1, \ldots, d-1$ while the lower Greek indices (like α, β, μ, ν) refer to the 4d submanifold and run from 0 to 3. Lower Latin indices (like a, b) indicate the 3d spatial submanifold as before. Without indices, bold vectors (like $\boldsymbol{x}$, $\boldsymbol{y}$) shall indicate d-dimensional vectors, while vectors with arrow (like $\vec{x}, \vec{y}$) indicate $(d-1)$-dimensional vectors (just the spatial part in a given metric).

2.3.1 The ADD model of large extra dimensions

In 1998, Nima Arkani-Hamed, Savas Dimopoulos and Gia Dvali (ADD) proposed a model with n large spatial extra dimensions (LXDs or LEDs). According to their proposal, the observable four-dimensional universe, called the *brane* (the term comes from membrane) is embedded in the higher-dimensional *bulk*. Together brane and bulk resemble the $d = 4 + n$ dimensional space-time.

The n extra dimensions are taken to be flat and compactified e.g in a torodial way with a large compactification radius R_c compared to the Planck length. A typical value is $R_c \approx 44\mu$m. This is small enough to agree with non-observed deviations from Newton's law. The idea of the ADD model is that all Standard Model fields *live* on the brane, *i.e.* they do not notice the existence of more than four dimensions. Only gravity [40] is allowed to propagate everywhere (bulk and brane). See figure 2.2a for a way to imagine brane and bulk space, while figure 2.2b displays a way to imagine compactified extra dimensions.

The large extra dimension scenario can solve the weak hierarchy problem of the Standard Model by imposing a new fundamental mass scale M_* in the order of 1 TeV. The model states that one can see on feasible scales only an "effective" weak coupling constant $G = 1/M_{\text{Pl}}^2$, because it is the result of the integrated out volume of the extra dimensions, where gravity also propagates. This ratio is defined as

$$M_{\text{Pl}}^2 = C_n V_n M_*^{n+2} \, , \tag{2.33}$$

with V_n the volume of the enrolled extra dimensions, with tori and compactification radii R_c e.g. $V_n = (2\pi R_c)^n$ and a dimensionless prefactor $C_n = \mathcal{O}(1)$.

Note that there are multiple conventions about the prefactor C_n in (2.33). Here it is chosen most like the Han-Lykken-Zhang notation (HLZ), as proposed in the appendix of [20]:

$$C_n = \left(\frac{\Omega_{n+2}}{\Omega_2} \right)^{\frac{1}{n+2}} \tag{2.34}$$

The prefactor C_n is used to compensate higher dimensional numerical contributions from volume integrals, *i.e.* the surfaces Ω_{d-1} of d-spheres S_d. For details about d-spheres, see appendix D. Without extra dimensions, $n = 0$ and $C_n = 1$, and therefore $M_{\text{Pl}} = M_*$.

The new fundamental scale M_* reaches the TeV scale, if n and R_c are big enough (c.f. figure 2.3). This opens the door for experimental tests [12, 13, 47, 58], as the center of mass energy of the Large Hadron Collider (LHC) at CERN is in the same order of magnitude (10 TeV).

(a) Brane world physics

(b) Compactified extra dimensions

(c) Hoop conjecture

(d) Quantum Black Hole
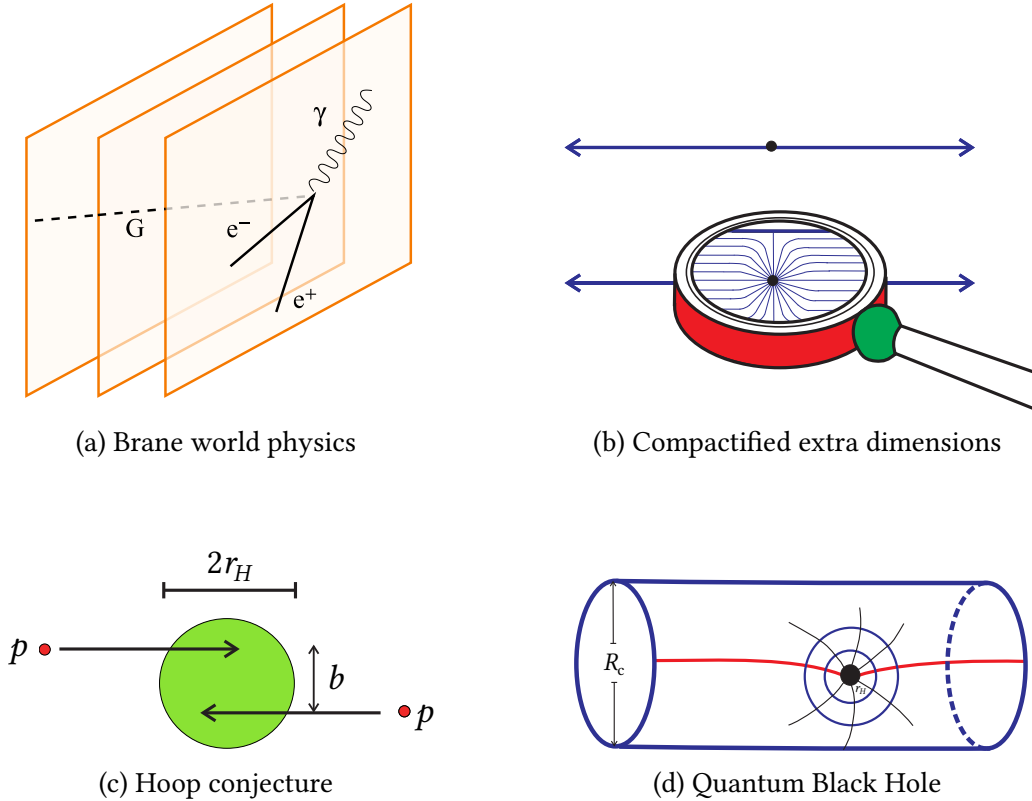
Figure 2.2: Illustrations on how to imagine large extra dimensions and brane world physics.
(a) The (orange) 4d branes are displayed as 2d surfaces, while one extra dimension is displayed horizontally. While the QED process takes place on the brane, and neither electron, positron and photon can escape the brane, the graviton is allowed to freely traverse the whole space-time.
(b) The compactification picture shows where one faces extra dimensions even in real life: When zooming in, the one dimensional horizontal line shows a vertical substructure. At big distances, the extra dimensions are not visible.
(c) The hoop conjecture illustration shows how to imagine a particle collision with impact parameter $b < 2r_H = 2L_*$ which produces a black hole with event horizon $2R_H$.
(d) A black hole with $r_H \ll R_c$, that is, the BH is much smaller than the compactification radius of the tori, does not notice the extra dimensional periodic boundary geometry.
Pictures taken and adapted from [20, 36, 47].

Figure 2.3: The ADD fundamental mass lowering mechanism. The lines show $M_*(R_c)$ from eq. (2.33) on a GeV scale. For comparison, the LHC energy scale (10 TeV) is shown, as well as the Planck scale ($n = 0$). The plot does not show real data, but illustrates the mechanism: By gravitational experiments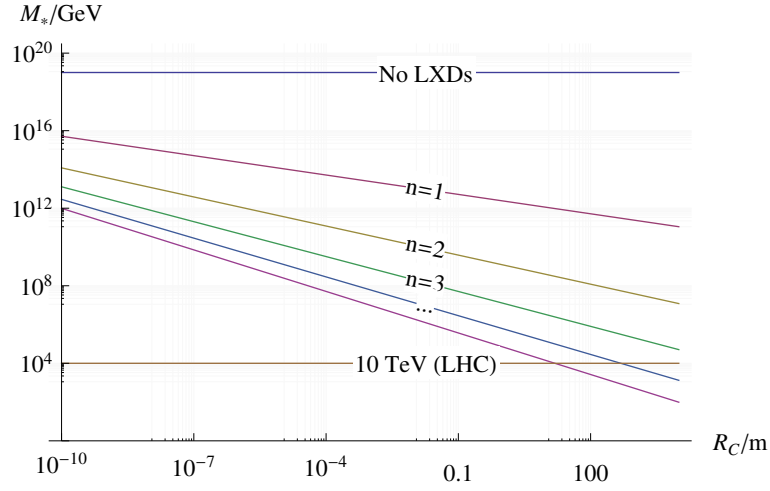, one can make upper bound constraints on R_C. Small number of extra dimensions, like $n = 1$, are ruled out because they reach the TeV scale only at very large distances.

2.3.2 The Schwarzschild-Tangherlini solution

Black holes in higher dimensions are more diverse than in 4d, since more topologies are possible [27], for example ring solutions ("black rings", like Doughnuts). The most simple generalization of the Schwarzschild solution to d dimensions is the *Schwarzschild-Tangherlini* metric (STM). It describes the spherical and static black hole produced by a point like matter source in higher dimensions and was found in 1963 by Tangherlini. The metric is displaye by the line element

$$\mathrm{d}s^2 = -(1 - V(r))\mathrm{d}t^2 + (1 - V(r))^{-1}\mathrm{d}r^2 + r^{d-2}\mathrm{d}\Omega_{d-2}^2. \tag{2.35}$$

This line element is a straightforward extension of the 4d Schwarzschild line element (2.27). The gravitational function is retrieved by replacing the $1/r$ Newtonian radial falloff by $1/r^{d-3}$, getting [27]

$$V(r) = \frac{2}{d-1}\frac{MG_d}{r^{d-3}} = \left(\frac{r_H}{r}\right)^{d-3}, r_H^{d-3} = \frac{d-1}{2}MG_*, \tag{2.36}$$

with the d-dimensional coupling constant G_d and mass parameter M. The modification of the coupling constant is a crucial reason why extradimensional gravity is done and subject to the following section. The d-dimensional coupling constant G_d will be refered to as G_*. The number of dimensions arises from the context. Writing the gravitational potential in terms of the horizon radius (2.36) uncovers the *no more* linear size-mass relation $r_H \propto M$, It is only linear in 4 dimensions.

2.4 Black Holes in Large Extra Dimensions

2.4.1 Production

There is no accelerator on Earth which can probe quantum gravity at the Planck scale $\sim 10^{16}$ TeV, as already mentioned in section 2.1.6. On the contrary, the ADD scenario allows black holes production in particle accelerators.

By means of the *hoop conjecture* (figure 2.2c), black holes are produced as soon as $M_{\text{center of mass}} \sim M_*$. As $L_* \ll R_c$, no problems arise with the special enrolled nature of the spatial extra dimensions (figure 2.2d): The black hole is very small compared to the extra dimensional tori, so it locally looks $3 + n$-spherically symmetric [36].

The production rate is governed by a geometrical cross section approximation

$$\sigma(M) \sim \pi r_H^2. \tag{2.37}$$

This experimental signature is the main motivation for investigating black holes in large extra dimensions [32].

2.4.2 Evaporation

Mini black holes produced in particle colliders evaporate by Hawking radiation, because their lifetime is very short, compared to their astronomical counterparts. The evaporation process is typically categorized in four phases [13, 36, 47]:

(a) **Balding phase**. In this phase the black hole looses *hair* which consist of asymetries (multipole moments and gauge fields, if applicable). It is expected that the BH goes throught the balding phase very rapidly [82]. At the end of this phase, the BH is axisymmetric and rotating. This kind of BH is described by the Kerr-Newman metric.

(b) **Spin down phase**. The black hole radiates away all of its angular momentum and some mass. The evaporation is understood in terms of Hawking and Unruh-Starobinsky radiation. At the end of this phase, the BH is spherical symmetric and nonrotating. This kind of BH is described by the Schwarzschild metric.
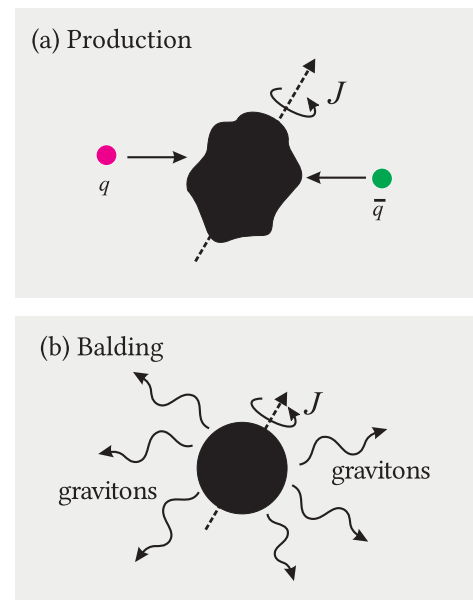
Figure 2.4: Sketch of the phases, modified from [36]
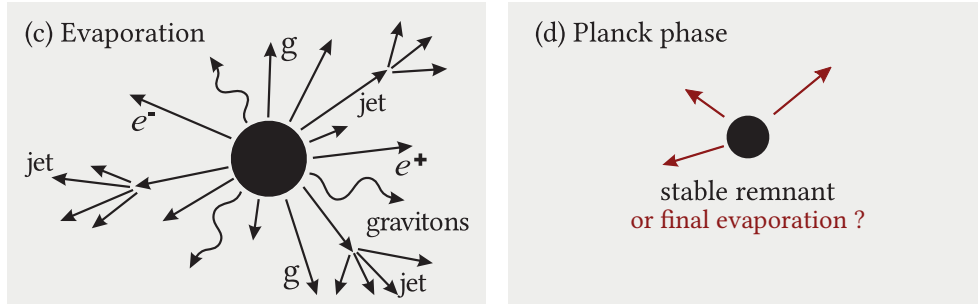
Figure 2.5: Sketch of the evaporation phases, modified from [36].

(c) **Schwarzschild phase**. The black hole is spherical and still radiates by Hawking radiation (monopole radiation).

At the end of this phase, the semiclassical thermodynamics, based on the Hawking temperature

$$T_H = \frac{\hbar}{8\pi GM},$$
(2.38)

get more and more *ill defined*. The evaporating black hole gets hotter and hotter and evventually emits particles with the same order of mass as the black hole mass. The thermodynamical canonical ensemble gets wrong because the Black hole cannot be in a stable equilibrium with its surrounding heat bath any more [30].

(d) **Planck phase**. The black hole mass reaches the Planck mass and quantum gravity effects get strong. In this phase, $r_H \sim L_*$ and the semiclassical picture breaks down. There are two widely acknowledged opportunities: The black hole completely evaporates away to particles of the Standard Model, or it gets a stable configuration, the *black hole remnant*.

Chapter 3

Minimal length in physics

One of the tenets of high energy physics is the association of the failure of a theory at scales where the theory predicts singularities. It is common belief that nature is nonsingular in the same way (classical) physics is supposed to be "smooth" everywhere. Accordingly, the problem of the Schwarzschild black hole is the curvature singularity in the origin which may be back-traced to the Dirac delta distribution composing the matter source $\delta(\boldsymbol{x})$. The dirac distribution is a good model (in the sense of a matter profile) as seen from far from the origin, while it fails at small distance to the origin.

Most quantum gravity approaches address this problem by *nonlocality*. The nonlocality is typically intermediated by a minimal length scale which serves as energy scale when nonlocal effects become strong [6, 19, 37].

3.1 The black hole—particle duality

At shortest scales there is a tangible particle-black hole *duality*, illustrated in figure 3.1a. On the quantum mechanical side, each particle with mass (=energy) m can be assigned to a length scale. From quantum mechanics, candidates are the *de Broglie wavelength* and the *Compton wavelength*. For particles with speed of light, the de Broglie wavelength $\lambda_B = h/p$ becomes the Compton wavelength $\lambda_C = \hbar/mc$. As we consider energy scales $pc \propto M_{\text{Pl}}$, the velocity limit $v \to c$ is justified.

The compton wavelength for quantum mechanical particles suggests $L_{\text{particle}} \sim 1/m$, as the red curve in figure 3.1a indicates (The mass m for a particle with $v = c$ is just $m = pc^2$). On the other hand, the black hole picture in four space-time dimensions assigns to each mass distribution a length by means of the Schwarzschild event horizon $r_H = 2GM/c^2$, so $L_{\text{black hole}} \sim m$, as the blue curve indicates. These two curves cross at the Planck scale $L_{\text{particle}} \sim L_{\text{black hole}} \sim \sqrt{\hbar c/G} := L_{\text{Pl}}$ (numerical factors are suppressed in this picture).

Trace as a gedankenexperiment a particle in an accelerator where its energy (velocity) is increased, resulting in a better length scale resolution (particle compression, red arrow). At the Planck scale M_{pl}, suddenly by the *hoop conjecture* one expects the particle to become a black hole, and further energy (i.e. acceleration) increases the size of the object (again). The resulting
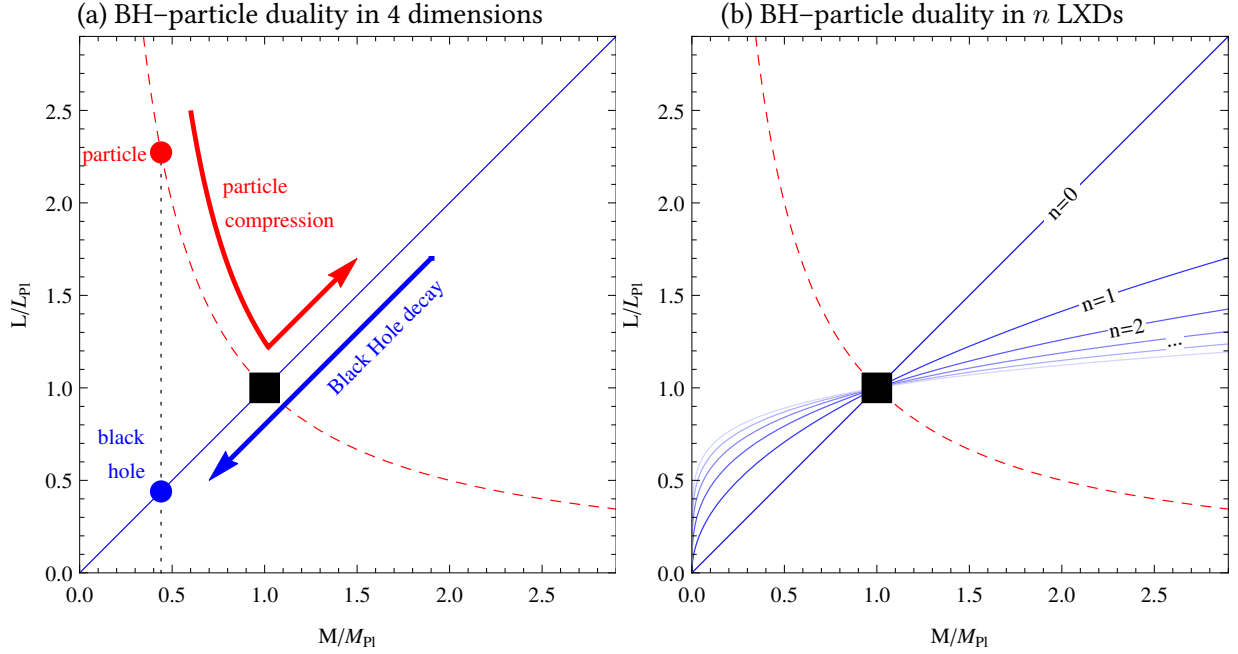
Figure 3.1: Length-vs-mass pictures for the Schwarzschild(-Tangherlini) space time (blue lines) vs the quantum mechanical picture (red dashed line)

black hole is quite unstable and decays by Hawking evaporation (blue arrow). As there is no *inverse hoop conjecture* in particle physics, nothing prevents the Schwarzschild black hole from evaporating at scales below the Planck scale. One ends up with a situation where two theories predict two different sizes for the same system.

Note that in the extra dimensional scenario, the black hole mass–length ratio is no more propertional, but $L_{\text{black hole}} \sim \sqrt[2+n]{m}$. The situation is displayed for different choices of n in figure 3.1b. The modified mass–length relation does not change the qualitative nature of the black hole–particle duality, for each number of extra dimensions the above statement holds.

3.2   Self-Completeness

There are two ways out of the black hole–particle ambiguity: Either General Relativity breaks down and must be replaced by a completely different theory, or it can be saved by some kind of *completeness*. In figure 3.2, a solution is sketched: By modifying the gravitational event horizon in a way that it smoothly merges into the particle picture, one gets a unique particle–black hole interpretation and a *minimum length scale* of physics L_{Pl}. In this theory, there is literally no way to probe distances below L_{Pl} as it is either circumvented by quantum mechanical uncertainty or black hole production.

Gravity is called *self complete* if the validity of the Einstein field equations (EFE) is recognized at any energy scale (i.e. mass scale M at figure 3.1), but it is *self protecting* against minimal length singularities [22]. This is imposed by completing the EFE by a nonlocal contribution.

It is motivated by fundamental principles like the generalized uncertainty principle, noncommuting geometry or theories like loop quantum gravity and string theory [71, 72]. Appendix B.2 gives a short overview about these theories.
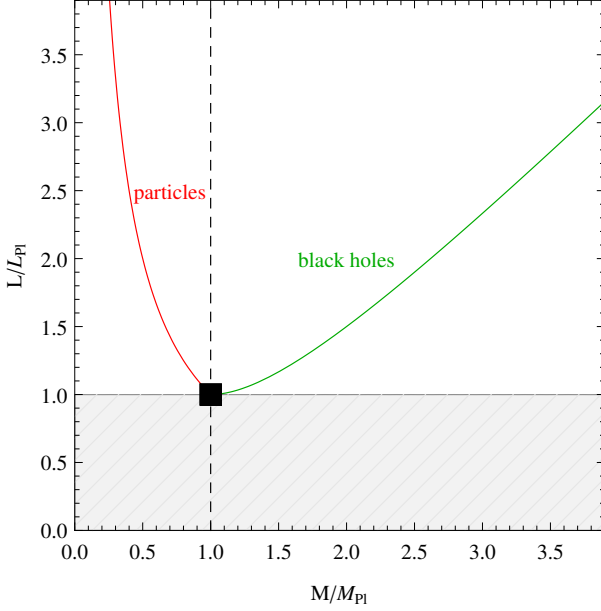

Figure 3.2: Self complete gravity: The red line displays the unaltered length scale associated with quantum particles, while the green line is an exemplary placeholder for a quantum gravity improved black hole horizon. The picture suggests a "smooth" transition at the Planck scale $M = M_{\mathrm{PL}}$, $L = L_{\mathrm{Pl}}$. In this way, the length scales $L < L_{\mathrm{Pl}}$ are no more physically accessible.

This picture shall be understood as the goal of the short scale improved black hole metrics which are subject of the following chapters.

3.3 Nonlocal gravity

The nonlocal contributions to the geometric part of the Einstein field equations are introduced with a bilocal operator $\mathcal{A}^2$ which mediates *nonlocal* effects in space-time. $\mathcal{A}^2$ is a function of the generally covariant D'Alambert operator $\Box = g^{\alpha\beta}\nabla_\alpha\nabla_\beta$ associated with an energy scale $1/l_0$ which is generated by the physical length scale l_0 at which short distance effects get important. $\mathcal{A}^2(\Box\, l_0^2)$ is a dimensionless and generally covariant operator. To shorten notation, it will frequently be abbreviated as $\mathcal{A}^2$. It enters the Einstein field equations on the right hand side of Einstein equations as the inverse $\mathcal{A}^{-2}$,

$$G_{\mu\nu} = 8\pi G\, \mathcal{A}^{-2}T_{\mu\nu} := 8\pi G\mathcal{T}_{\mu\nu}. \tag{3.1}$$

The non-classical matter distribution $\mathcal{T}_{\mu\nu} = \mathcal{A}^{-2}T_{\mu\nu}$ is described by the nonlocal operator. By multiplying the inverse $\mathcal{A}^2$ of $\mathcal{A}^{-2}$ from the left hand side, the *dual theory* is found:

$$\mathcal{A}^2\, G_{\mu\nu} := \mathcal{G}_{\mu\nu} = 8\pi G\, T_{\mu\nu}. \tag{3.2}$$

In the dual theory, the nonlocality is *shifted* to the geometrical part (the Einstein tensor) of the field equations, while the matter part remains purely classical.

Note the difference between equation (3.1) and (3.2): While the field equations (3.1) represents classical gravity coupled to a quantum mechanical source term $\mathcal{T}_{\mu\nu}$, the field equations

(3.2) describe equations for nonlocal spacetime $\mathcal{G}_{\mu\nu}$ coupled to a classical source term $T_{\mu\nu}$ after "modified rules" of general relativity. These two interpretations are (mathematically and physically) equivalent [53, 57].

The action of the nonlocal field theory is obtained by the modified Ricci scalar $\mathcal{R}$ in the modified Einstein tensor $\mathcal{G}_{\mu\nu} = \mathcal{R}_{\mu\nu} - \frac{1}{2}g_{\mu\nu}\mathcal{R}$. The nonlocal Ricci tensor defines the gravitational action and a variational derivation as in section 2.1.5 can be done just by replacing $R \rightarrow \mathcal{R}$.

3.4 The generalized uncertainty principle

The generalized uncertainty principle (GUP) is one way to find a minimal length scale in physics [2, 18]. It proposes a modification of the Heisenberg uncertainty principle

$$\Delta x \, \Delta p \geq \frac{\hbar}{2}. \tag{3.3}$$

As the Heisenberg uncertainty principle is a consequence of the quantum mechanical commutator relation $[\boldsymbol{x}, \boldsymbol{p}] = i\hbar$, the GUP is usually introduced by complementing this commutator relation for momentum and/or position dependent terms [42],

$$[\boldsymbol{x}, \boldsymbol{p}] = i\hbar(1 + \alpha\boldsymbol{x}^2 + \beta\boldsymbol{p}^2). \tag{3.4}$$

This yields a modified uncertainty relation of the form

$$\Delta x \, \Delta p \geq \frac{\hbar}{2} \left(1 + \alpha\boldsymbol{x}^2 + \beta\boldsymbol{p}^2 + \alpha\langle\boldsymbol{x}\rangle^2 + \beta\langle\boldsymbol{p}\rangle^2 \right). \tag{3.5}$$

Restricting to the case $\alpha = 0$ allows to find a Hilbert Space representation [42] in momentum space. Solving relation (3.5) for exact equality for Δp requires for exact momentum measurement $\langle p \rangle = 0$ a minimal position uncertainty

$$\Delta x \geq \hbar\sqrt{\beta}. \tag{3.6}$$

It is possible to derive a black hole solution based on this priniciple which implements a *smearing* of point-like mass distributions [38, 39, 45, 48]. The GUP can also be expressed as a nonlocal field theory. For further details, see appendix B.2.3, as a complete discussion is beyond the scope of this work.
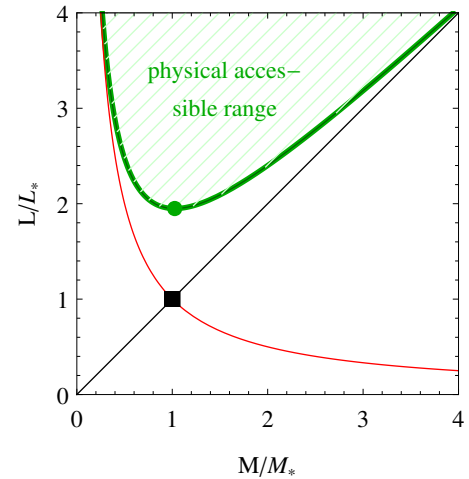

Figure 3.3: The GUP predicts a minimal length (green dot). Here, $\beta = 2$ and $\hbar = 1$.

Chapter 4

Quasi-classical black holes

In this chapter, a class of generic black hole solutions is introduced. This is done as a preparatory effort to derive the mathematical equations used to discuss two physically motivated subclasses of black holes in the next two chapters.

The class of black holes described in this chapter is constructed by a quasi-classical source term which models a *smeared* Dirac delta distribution. This is one way to introduce nonlocal gravity effects. Such effects turn out to be successful to encounter the problems of the Schwarzschild black hole, discussed in the previous chapters. The modifications from the ordinary Schwarzschild setup are supposed to be large only at short distances around the center, while at large distance, all metrics in the currently discussed class of generic *smeared* Schwarzschild black holes shall match the ordinary Schwarzschild black hole.

In the static radial symmetric setup, we can compute the modifications from the ordinary Schwarzschild setup. In this chapter, a concrete choice for the smearing will not be made. It is introduced only in a fashion $\Theta(r) \to H(r)$ with $\Theta(r)$ the Heaviside step function and $H(r)$ an approximation function, characterized by a regulator $\tilde{r}_0$ with dimension of length. As we will derive a nonlocal operator for this class of black holes in the end of the chapter, $1/\tilde{r}_0$ turns out to be the energy scale where modifications to General Relativity apply. These modifications are encoded in $H(r)$. According to $H(r)$, the modifications can improve the low distance regime of General Relativity.

(a) Heaviside step function $\Theta(r)$

(b) Dirac delta function $\delta(r)$

(c) Heaviside-approximation $H(r)$

(d) Dirac-approximation $H'(r)$
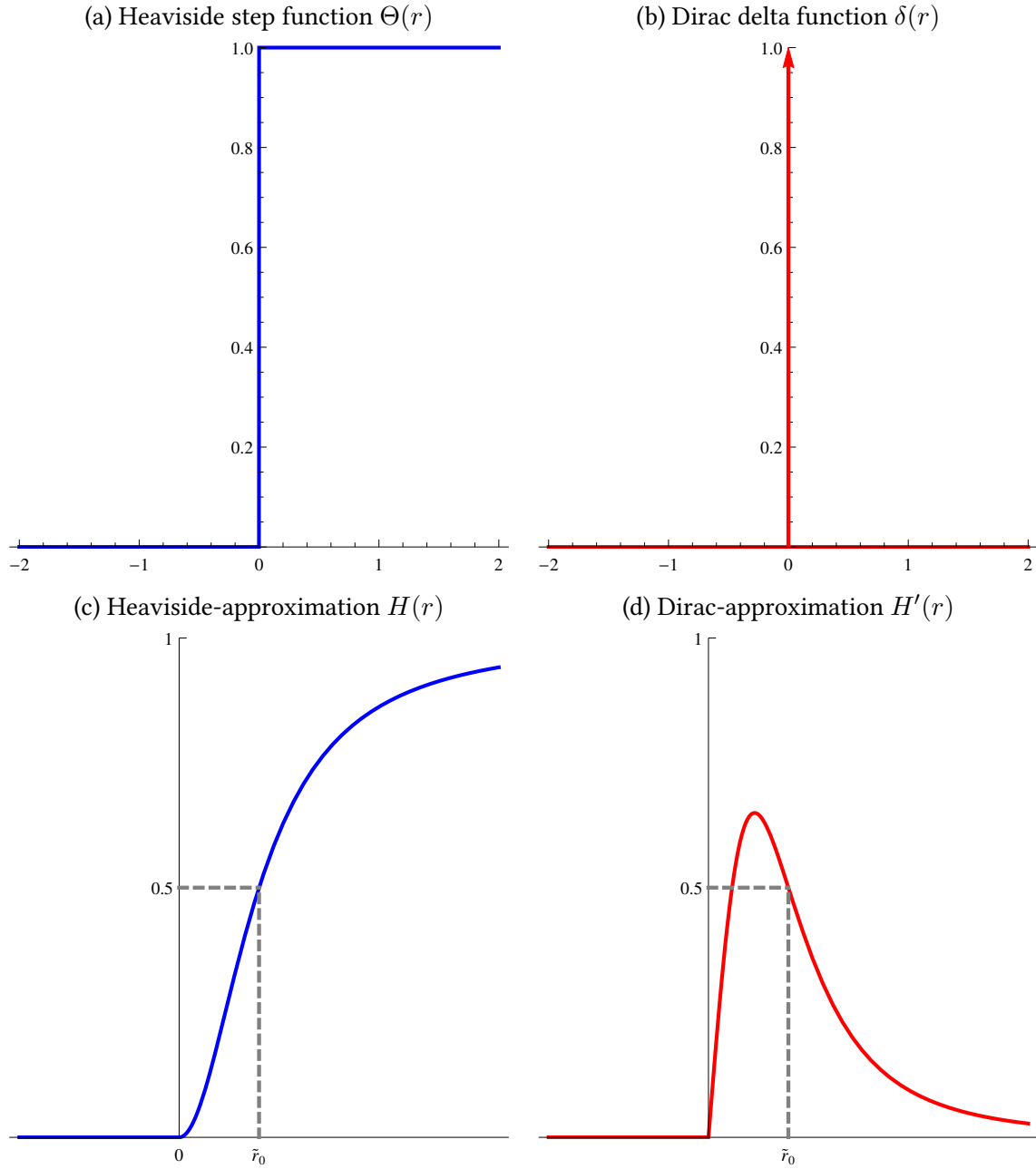
Figure 4.1: Illustrative plots to emphasize the impact of replacing $\delta(r) \rightarrow H'(r)$ or $\Theta(r) \rightarrow H(r)$, respectively, in the Schwarzschild matter distribution. The exact definition of the Heaviside step function 4.1a at the origin $r = 0$ is not important here. Note that the smearing is not performed around the origin $r = 0$, but in a manner that $H(0) = 0$ is ensured. Else, the physical interpretation of $H(r)$ as a matter distribution would be lost, as $r < 0$ is not a valid position in spherical coordinates. The *amount* of delocalization is supplied by the length scale $\tilde{r}_0$. For illustration purpose, here $H(\tilde{r}_0) = H'(\tilde{r}_0) = \text{1/2}$. Note that for $\tilde{r}_0 \rightarrow 0$, the approximation functions $H(r)$ and $H'(r)$ match their ideal $\Theta(r)$ or $\delta(r)$, respectively.

4.1 From a quasi-classical source term to the metric

In this section, the metric for any static spherical symmetric gravitational potential $V(r)$ in d space time dimensions will be derived. As the ADD model is used, the d dimensions are spanned by 1 timelike and $d - 1 = n + 3$ spacelike dimensions, where n indicates the number of extradimensions.

The only further requirement is large distance matching of the Netwon's potential (2.19). This is equivalent to starting with a static isotropic matter density $\rho(r)$ and requiring $\lim_{r \to \infty} \rho(r) = 0$.

The ansatz for the solution is the following $d = n + 4$ dimensional spherical symmetric and static metric, described by a line element

$$\mathrm{d}s^2 = -e^{\nu(r)}\mathrm{d}t^2 + e^{-\nu(r)}\mathrm{d}r^2 + r^2\mathrm{d}\Omega_{n+2}^2 \tag{4.1}$$

$$= -\left(1 - V(r)\right)\mathrm{d}t^2 + \left(1 - V(r)\right)^{-1}\mathrm{d}r^2 + r^2\mathrm{d}\Omega_{n+2}^2 \tag{4.2}$$

with Ω_{n+2} the surface line element of an $(n + 3)$ sphere (for details about the sphere, see appendix D). The spherical coordinates are given by $\boldsymbol{x} = (x_0, \vec{x}) = (x_0, r, \phi, \theta_1, \ldots, \theta_{n+2})$. To improve readability, it is written i instead of θ_i ($i = 1, \ldots, m$ and $m := n + 2$) when the angular coordinates appear in the indices of tensors. The diagonal coefficients in the metric are therefore refered to as

$$g_{AB} = \mathrm{diag}\left(g_{00}(r), -g_{00}^{-1}(r), g_{\phi\phi}(r, \phi), g_{11}(r, \theta_1), \ldots, g_{mm}(r, \theta_m)\right). \tag{4.3}$$

This notation is the same as in [68].

The argumentation follows the derivation of the inner Schwarzschild solution, as can be found in General Relativity textbooks: The property $-g_{00} = g_{11}^{-1}$ is required for flat space at large distances.

Given the matter density and the metric ansatz, the stress tensor T^{AB} can be determined. Due to the symmetry of the problem, it can already be stated as

$$T^{AB} = \mathrm{diag}\left(T^{00}, T^{rr}, T^{\phi\phi}, T^{11}, T^{22}, \ldots, T^{mm},\right) = \mathrm{diag}\left(-\rho, -\rho, p, p, \ldots, p\right), \tag{4.4}$$

following [59,68]. Now switching to a $(1, 1)$ type tensor for $\boldsymbol{T}$ yields the conservation of energy equation as $\nabla_A T_B^A = 0$ with

$$T_B^A = g_{BC}T^{AC} = g_{BB}T^{AB} = \mathrm{diag}(g_{00}T^{00}, g_{rr}T^{rr}, \ldots, g_{mm}T^{mm}). \tag{4.5}$$

The conservation equation $\nabla_A T_B^A = 0$ is now computed for all d possible values of the free index B. Starting with the index $B = r$ case gives the equation (no sum convention here)

$$0 = \nabla_0 T_r^0 + \nabla_r T_r^r + \sum_i \nabla_i T_r^i. \tag{4.6}$$

The covariant derivative ∇_A and the Christoffel symbol Γ_{AB}^C must be computed (see appendix F for the definitions). The summands of (4.6) are given by

$$\nabla_0 T_r^0 = \partial_0 T_r^0 + \Gamma_{0D}^0 T_r^D - \Gamma_{0r}^D T_D^0 = \frac{1}{2} g^{00} T_r^r \partial_r g_{tt} + \frac{1}{2} g^{00} T_0^0 \partial_r g_{tt} \tag{4.7a}$$

$$\nabla_r T_r^r = \partial_r T_r^r + \Gamma_{rD}^r T_r^D - \Gamma_{rr}^D T_D^r = \partial_r T_r^r \tag{4.7b}$$

$$\forall i: \quad \nabla_i T_r^i = \partial_i T_r^i + \Gamma_{iD}^i T_r^D - \Gamma_{0r}^D T_D^i = \frac{1}{2} g^{ii} T_r^r \partial_r g_{ii} + \frac{1}{2} g^{ii} T_0^0 \partial_r g_{ii} \tag{4.7c}$$

One ends up with the explicit equation

$$0 = \partial_r T_r^r + \frac{1}{2} g^{00} \left(T_r^r - T_0^0 \right) \partial_r g_{00} + \frac{1}{2} \sum_i g^{ii} \left(T_r^r - T_i^i \right) \partial_r g_{ii} \tag{4.8}$$

By construction of T_B^A, the term $T_r^r - T_0^0 \sim \rho - \rho = 0$ vanishes. The remaining contribution from each angle i is

$$g^{ii} \partial_r g_{ii} = \frac{1}{r^2 \sin^i(\theta_i)} \partial_r \left(r^2 \sin^i(\theta_i) \right) = \frac{2}{r}, \tag{4.9}$$

where $\sin^i(x) = (\sin(x))^i$ displays the ith power of $\sin(x)$. By summing up $d-2$ equal terms (4.9), all remaining energy momentum components are determined to

$$T_i^i = T_0^0 + \frac{r}{n+2} \partial_r T_0^0 = \rho + \frac{r}{n+2} \partial_r \rho. \tag{4.10}$$

As a result, the index $B = r$ case of the energy conservation law $\nabla_A T_B^A = 0$ already determined the energy momentum tensor. It is not shown here that the other $d-1$ energy conservation equations do not contribute any further information.

In order to solve the Einstein equation, in addition to the energy momentum tensor one needs the Ricci tensor as additional ingredient. It is given as the contraction of the Riemann tensor

$$R_{AB} = \partial_C \Gamma_{BA}^C - \partial_B \Gamma_{CA}^C + \Gamma_{AD}^C \Gamma_{BA}^D - \Gamma_{BD}^C \Gamma_{CA}^D \tag{4.11}$$

see Appendix F.1 for the values of all Christoffel symbols. The Ricci tensor is again diagonal, with the entries, as (1,1) type tensor,

$$R_0^0 = R_r^r = -\frac{e^\nu}{2} \left(\partial_r^2 \nu + (\partial_r \nu)^2 + (n+2) \frac{\partial_r \nu}{r} \right) = \frac{1}{2} V''(r) - \frac{n+2}{2} \frac{V'(r)}{r} \tag{4.12a}$$

$$\forall i: \quad R_i^i = \frac{1 + n - e^\nu \left(1 + n + r \partial_r \nu \right)}{r^2} = (1+n) \frac{V(r)}{r^2} + \frac{V'(r)}{r}. \tag{4.12b}$$

The Ricci scalar is then given by

$$R = R_A^A = \frac{(n+2)V(r)}{r^2} + V''(r). \tag{4.13}$$

Now one can write out the Einstein equations in a trace reversed form, in $(1,1)$ tensor notation for d dimensions:

$$R_A^B = \frac{1}{M_*^{n+2}} \left(T_A^B - \delta_A^B \frac{T_C^C}{n+2} \right) \tag{4.14}$$

Since $\boldsymbol{R}, \boldsymbol{T}, \boldsymbol{\delta}$ are diagonal, the Einstein equations reduce to d non-zero equations where only two equations differ from each other, identified by their indices $A, B = r, r$ and $A, B = i, i$. The latter gives the following first order differential equation for $V(r)$:

$$V'(r) + \frac{n+1}{r} V(r) = \frac{1}{M_*^{n+2}} \frac{r\rho(r)}{n+2} \tag{4.15}$$

The general solution of the metric for any $\rho(r)$ is given by the integral

$$V(r) = \frac{1}{r^{n+1}} \left(\frac{1}{(n+2)M_*^{n+2}} \int_{c_1}^{r} x^{n+2}\rho(x)\mathrm{d}x + c_2 \right) \quad \text{with} \quad c_1, c_2 = \text{const} \tag{4.16}$$

The boundary values $V(0)$ and $V'(0)$ give rise to the two integration contants c_1 and c_2. Physically, they allow for the low-energy matching of the theory. In the context of this thesis, c_1 is important for discussion about minimal lengths.

4.2 A smeared point-like matter density

The matter density choice to be inserted into (4.16) is based on the Schwarzschild-Tangherlini point-like static and spherically symmetric density

$$\rho(r) = \frac{M}{\Omega_{n+2} \, r^{n+2}} \delta(r) = \frac{M}{\Omega_{n+2} \, r^{n+2}} \frac{\mathrm{d}\Theta(r)}{\mathrm{d}r}, \tag{4.17}$$

with the Dirac delta distribution $\delta(r)$ and the Heaviside unit step function

$$\Theta(r) = \begin{cases} 0 & \text{when} \quad r < 0 \\ 1 & \quad r \geq 0 \end{cases}. \tag{4.18}$$

The occurence of the Heaviside function in the Schwarzschild source term (4.17) is now replaced by a *smeared* version we refer to as $H(r)$. By construction, the function $H(r)$ encodes all nonlocal effects of the theory. The generic *Schwarzschild-like* energy density is therefore

$$\rho(r) = \frac{M}{\Omega_{n+2} \, r^{n+2}} \frac{\mathrm{d}H(r)}{\mathrm{d}r}. \tag{4.19}$$

Inserting (4.19) into the integral 4.16 gives us the *gravitational function* $V(r)$ with n large extra dimensions as

$$V(r) = \frac{1}{2+n} \frac{M}{M_*^{n+2}} \frac{H(r)}{r^{n+1}}. \tag{4.20}$$

Here, M_* is the fundamental Planck mass, and M is a constant that will be identified as mass. $V(r)$ determines the metric according to

$$ds^2 = -(1 - V(r))\,dt^2 + (1 - V(r))^{-1}\,dr^2 + r^2 d\Omega_{n+2}^2. \qquad \text{(4.1 revisited)}$$

The gravitational function $V(r)$ replaces the Newton's potential (2.19) with a prefactor -2, because plugging $V(r) = -2\Phi(r)$ with $\Phi(r) = -GM/r$ into (4.1) resembles the Schwarzschild solution.

4.2.1 The Mass

The mass contained inside a $(3+n)$-sphere (the object will be referred to as $\mathcal{B}(r)$) with radius r is given by the integral

$$m(r) = \int_{\mathcal{B}(r)} \rho(x)\,d^{n+3}x = M \int_0^r \frac{dH}{dr}(r')\,dr' = MH(r). \qquad (4.21)$$

From the mathematical viewpoint, the mass M is just a constant that may be used to fulfill the horizon equation $V(r_H) = 1$ at an arbitrary event horizon r_H. Therefore I set

$$M := (n+2)M_*^{n+2}\frac{r_H^{n+1}}{H(r_H)}, \qquad (4.22)$$

so when plugging into the metric

$$V(r) = \frac{1}{n+2}\frac{M}{M_*^{n+2}}\frac{H(r)}{r^{n+1}} = \left(\frac{r_H}{r}\right)^{n+1}, \qquad \text{(4.20 revisited)}$$

the horizon equation $V(r) = 1$ is fulfilled at $r = r_H$. The physical meaing of M is the mass of a black hole of radius r_H [61]. When substituting $n+1$ powers of M_* by $M_* = 1/L_*$, one can easily relate

$$M = (n+2)\left(\frac{r_H}{L_*}\right)^{n+1}\frac{1}{H(r_H)}M_* . \qquad (4.23)$$

4.2.2 The regulator

The "spread" of *smearing* accomplished by the function $H(r)$ must be encoded in a constant of dimension length. For example, consider the Gaussian delta approximation

$$\delta_\sigma(r) = \frac{1}{\sqrt{2\pi\sigma}}\exp\left(-\frac{r^2}{2\sigma}\right), \qquad \delta(r) = \lim_{\sigma\to 0}\delta_\sigma(r). \qquad (4.24)$$

as a canidate for $H'(r) := \delta_\sigma(r)$. The variance σ, also refered to as the *width* of the Gaussian, is the regulator of the metric constructed when inserting the cumulative normal distribution function $H(r) := \propto \int_{-\infty}^r e^{-x^2/2\sigma}dx$ into (4.20).

In the physical models in the next chapters, the *width* (from now on the symbol $\tilde{r}_0$ will be generally used) will be linked to a physical length scale by imposing principles like self-encoding.

To take the limit $H(r) \to \Theta(r)$, one has to examine the limit of the regulator $\tilde{r}_0 \to 0$. The limit $\tilde{r}_0 \to 0$ is accomplished by the replacement rules

$$H(r) \to 1, H'(r) \to 0, H''(r) \to 0, \ldots. \tag{4.25}$$

Replacing occurences of $H(r)$ and derivatives according to (4.25) only holds when evaluating expressions containing $H(r)$ and derivatives for nonzero radius. This resembles the well-known finite values of $\Theta(r) = 1$ for $r > 0$ and $\delta(r) = 0$ for $r > 0$.

This of course also holds for products like $H(r)H'(r) \to 0$.

4.3 Geometry

The mass M and gravitational potential $V(r)$ have been determined for arbitrary $H(r)$. For specific choices of $H(r)$, one is able to do a discussion about event horizons ($g_{00} = 1 - V(r) \stackrel{!}{=} 0$) and evventually draw a conformal diagram. This is done for two models in sections 5.1 and 6.1. Here, the discussion will be a general one about special features of any metric described by $H(r)$.

4.3.1 Remnants

Nonlocal matter distributions described by $H(r)$ exhibit extremal configurations which can be identified with the two *remnant equations*, also known as *degenerate horizon conditions*:

$$\begin{cases} g_{00}(r_0) & = 0 & \text{(4.26a)} \\ \partial_r|_{r=r_0}\, g_{00}(r) & = 0 & \text{(4.26b)} \end{cases}$$

The first equation (4.26a) ensures the metric has a horizon at r_0. The second equation (4.26b) requires the metric to have an extremal value at r_0.

As will be shown in section 4.4.1, the second equation (4.26b) also states that the extremal configuration temperature, which is propertional to $\partial_r g_{00}(r)$, shall vanish at r_0. It will be shown in section 4.4 that, if condition (4.26b) is met, the extremal configuration is stable and decays no more. The situation motivates the name *black hole remnant* for the black hole with horizon radius $r_H = r_0$.

When inserting the generic potential (4.20), the remnant equations give

$$g_{00}(r_0) = 0 = 1 - \frac{1}{2+n}\frac{M}{M_*^{n+2}}\frac{H(r_0)}{r_0^{n+1}} \tag{4.27a}$$

$$\partial_r|_{r=r_0}\, g_{00}(r) = 0 = H'(r_0) - (n+1)\frac{H(r_0)}{r_0}. \tag{4.27b}$$

The shape of $H(r)$ determines if the second remnant equation (4.27b) is fulfilled, while the first remnant equation (4.27a) will always be fulfilled for $H(r) \neq \Theta(r)$.

4.3.2 Curvature finitness

According to (4.12), the Ricci scalar is given by

$$R(r) = R_N^N = \frac{(n+2)V(r)}{r^2} + V''(r) \tag{4.28a}$$

$$= \frac{2}{2+n} \frac{M}{M_*^{2+n}} \frac{(2+n)^2 H(r) - 2(1+n)rH'(r) + r^2 H''(r)}{r^{3+n}}. \tag{4.28b}$$

A profile $H(r)$ can produce a non-singular black hole origin if the nominator in (4.28b) has a taylor expansion at least of order r^{3+n}. When expanding $H(r)$ and its derivatives in a series expansion around $r = 0$ as

$$H(r) = \sum_{n=0}^{\infty} \frac{H^{(n)}(0)}{n!} r^n \approx H(0) + H'(0)r + \frac{1}{2}H''(0)r^2, \tag{4.29}$$

$$H'(r) = \sum_{n=0}^{\infty} \frac{H^{(n+1)}(0)}{n!} r^n \approx H'(0) + H''(0)r \tag{4.30}$$

$$H''(r) = \sum_{n=0}^{\infty} \frac{H^{(n+2)}(0)}{n!} r^n \approx H''(0) \tag{4.31}$$

one can determine the leading term (biggest power of r) from the nominator in (4.28b) as

$$(2+n)^2 H(r) - 2(1+n)rH'(r) + r^2 H''(r)$$
$$\sim (2+n)^2 H(0) + (3 + 2n + n^2)H'(0)r + (\frac{1}{4}n^2 - n)H''(0)r^2$$
$$\propto H(0). \tag{4.32}$$

A regular black hole therefore fulfills the condition

$$H(r) = \mathcal{O}(r^{3+n}) \quad \text{at origin } r = 0. \tag{4.33}$$

4.3.3 Energy conditions

Energy conditions in General Relativity are a tool to put constraints on matter distributions (that is, energy-momentum tensors) in a way how some expects them to behave. They are formulated from a classical viewpoint and *not* deduced from Einstein field equations or other first principles. Roughly speaking, they generalize the statement that one does not observe negative masses or regions of negative mass distribution.

Approaches to Quantum Gravity regularly violate energy conditions, and by examining how and where they violate these conditions, one understands about the quantum nature in General Relativity. For example, one expects energy conditions violate around the black hole center, e.g. violations occur in a region $r \lesssim l_0$ while they hold for $r \gtrsim l_0$, with l_0 a physical mass scale associated with the theory under discussion. As Ansoldi notes, this is cannot be taken for granted in a non linear theory as General Relativity is [3].

We check the following energy conditions (EC):

- **Null energy condition**, defined that for every (future) *null* vectors x^μ the observed matter density

$$\rho_{\text{obs}} = T_{AB} x^A x^B \tag{4.34}$$

is non negative, $\rho_{\text{obs}} \geq 0$. In words, this means a matter density ρ_{obs} observed by a *light ray* must be positive. A null vector fulfills $x_A x^A = -x_0^2 + x_1^2 + \sum_{i=2}^{3+n} x_i^2 = 0$, and if it is a *future* null vector, $x_A > 0\ \forall$ possible indices A. Since $T_{AB} \sim \text{diag}(-\rho, -\rho, p, \ldots, p)$ we get

$$\rho_{\text{obs}} \sim -\rho x_1^2 + \sum_{i=2}^{3+n} p x_i^2 = -\rho x_1^2 + p(x_0^2 - x_1^2) = -(\rho + p)x_1^2 + p x_0^2 \overset{!}{\geq} 0 \tag{4.35}$$

The negative contribution is governed by

$$f_{\text{weak}}(r) := \rho + p = 2\rho + \frac{r}{n+2}\partial_r \rho. \tag{4.36a}$$

$$= \frac{2M}{\Omega_{n+2}}\left(\frac{2H'(r)}{r^{n+2}} + \frac{1}{n+2}\frac{H''(r)}{r^{n+1}}\right) \tag{4.36b}$$

In regions where $f_{\text{weak}}(r) > 0$, it is violated. For $H \to \Theta$, (4.36b) is exactly 0 except at the origin. For any non-Dirac distribution, derivatives of H are nonzero near the origin, and therefore the null energy condition is violated.

- **Strong EC** requires basically the same for any (future) *timelike* vector x^μ. We find it violated when

$$f_{\text{strong}}(r) = (2+n)p > 0, \tag{4.37}$$

with the same comment as the Null EC.

- **Dominant EC** requires for any (future pointing) timelike or null vector x^μ that $-T_B^A x^B = -T_A^A x^A = y_A$ is a future timelike or null vector.

4.4 Thermodynamics

Law	Thermodynamics	black holes
0.	T constant on a body in thermal equilibrium	κ constant on horizon of (stationary) BH
1.	$dE = TdS - pdV + \mu dN$	$dM = \frac{\kappa}{8\pi}dA + \Omega_H dJ + \Phi dq$
2.	$\delta S \geq 0$	$\delta A \geq 0$
3.	$T = 0$ cannot be reached	$\kappa = 0$ cannot be reached

Table 4.1: The laws of thermodynamics correspond with black hole thermodynamics

4.4.1 Hawking Temperature

For spherical symmetric problems, the Hawking temperature $T_H = \kappa/2\pi$ is defined by means of the surface gravity $\kappa = \frac{1}{2}\,\partial_r g_{00}|_{r=r_H}$ at the black hole horizon r_H. One gets the temperature

$$T_H = \frac{1}{4\pi}\left(\frac{1+n}{r_H} - \frac{H'(r_H)}{H(r_H)}\right). \tag{4.38}$$

Taking the Schwarzschild limit $H \to \Theta$ means $H'/H \to 0$, so one evventually gets the well known Schwarzschild temperature $T = 1/(4\pi r_H)$. The H'/H term is the quantum correction which has to cure the diverging behaviour of the first addend $\sim 1/r_H$ in the temperature if the theory shall be a useful Quantum Gravity approach. In terms of the *remnant* which was proposed in the previous section, a remnant at extremal radius $r_H = r_0$ is called *cold* if $T_H = 0$. Setting (4.38) to zero equals the remnant equation (4.27b).

4.4.2 Heat capacity

The heat capacity is an extensiv thermodynamical property, defined as a measure of the heat ΔE added to an object resulting from a temperature change ΔT, in terms

$$C = \frac{\Delta E}{\Delta T}. \tag{4.39}$$

For black holes, the total black hole mass M equates the heat E, so $E = M$. The heat capacity can be computed by reusing $T(r_H)$ and $M(r_H)$. Inserting $1 = \partial r_H/\partial r_H$ yields

$$C = \frac{\partial M}{\partial T_H} = \frac{\partial M}{\partial r_H}\left(\frac{\partial T_H}{\partial r_H}\right)^{-1}. \tag{4.40}$$

Inserting temperature (4.38) and mass (4.23), one can do the elaborate computation and ends up with the compact expression

$$C = -\frac{4\pi r_H^{n+2}}{M_*^{n+2}}\frac{(n+1)H(r_H) - r_H H'(r_H)}{r_H^2 H(r_H)H''(r_H) - r_H^2 H'(r_H)^2 + (n+1)H(r_H)^2}. \tag{4.41}$$

By simply letting $H, H', H'' \to 0$ according to section 4.2.2, one ends up with the heat capacity of ordinary Schwarzschild black hole:

$$
\begin{array}{ccc}
C & \xrightarrow{\quad H \to \Theta \quad} & -4(1+n)\pi r_H^{2+n}/M_*^{2+n} \\[2mm]
{\scriptstyle n \to 0}\Big\downarrow & & \Big\downarrow{\scriptstyle n \to 0} \\[2mm]
-4\pi r_H^2 G \frac{H - r_H H'}{r_H^2 HH'' - r_H^2 H'^2 + H^2} & \xrightarrow{\quad H \to \Theta \quad} & -4\pi r_H^2 G
\end{array}
\tag{4.42}
$$

Depending on $H(r)$, the heat capacity possibly undertakes changes of sign, where a phase transition takes place ($C \to \pm\infty$). Radii here $C(r) \to \pm\infty$ are called critical radii and labeled r_C. At such a point, the black hole temperature $T_H(r_C)$ (eq. 4.38) is maximal:

$$\partial_{r_H} T_H\big|_{r_H=r_C} = 0 \Leftrightarrow r_C = \sqrt{\frac{1+n}{H'(r_C) - H''(r_C)H(r_C)}} H(r_C). \tag{4.43}$$

Hier fehlt Einheit für r_C.

As $H(z) \to \Theta(z)$, the critical point goes to zero. This corresponds to the fact that the Schwarzschild metric has no critical point.

4.4.3 Entropy

Entropy is a measure of information, and there are many definitions for it. In statistical mechanics, entropy is typically defined as the amount of ignorance of information of a physical state of a thermodynamical system. It therefore counts all micro states which define an emerging macroscopic state.

In the context of black holes, entropy is maybe the most interesting quantity, since it deals with the *information paradox* of black holes. It is the issue what happens with information (i.e. physical states) that crosses the event horizon.

The Hawking-Bekenstein entropy is defined via the Hawking Temperature T_H as

$$S = \int \frac{\mathrm{d}M}{T_H}. \tag{4.44}$$

The entropy defining integral can also be subsituted like in the heat capacity in the section before, giving for generic H a compact expression:

$$S(r) = \int \frac{\mathrm{d}M}{T} = \int \mathrm{d}r_H \left(\frac{1}{T}\frac{\mathrm{d}M}{\mathrm{d}r_H}\right) = \frac{\pi(n+2)}{2} M_*^{n+2} \int \mathrm{d}r_H \frac{r_H^{1+n}}{H(r_H)} \tag{4.45}$$

Approaching the limit $H \to \Theta$, one gets the Entropy of the Schwarzschild-Tangherlini black hole,

$$\frac{\pi(n+2)}{2} M_*^{n+2} \int \mathrm{d}r_H\, r_H^{1+n} = \frac{\pi(n+2)}{2(n+1)} M_*^{n+2} r_H^{2+n}. \tag{4.46}$$

Taking the limit $n \to 0$, one gets the Hawking-Bekenstein entropy for the four dimensional Schwarzschild black hole

$$\pi M_*^{n+2} r_H^2 = \frac{\Omega_2 r_H^2}{4G}, \quad \text{with } \Omega_2 = 4\pi \tag{4.47}$$

4.5 Nonlocal operator

In this chapter, I want to derive a nonlocal operator $\mathcal{A}^{-2}(\boldsymbol{x})$ for the given smearing models $H(r)$. In the long distance limit (where the fundamental length L_* can be considered zero: $L_*/r \to 0$),

this operator is supposed to vanish $\mathcal{A}^{-2} \to 1$. This section ties up with the introduction of nonlocal operators given in the previous chapter according to [53, 57].

The operator is linked to $H(r)$ with a Fourier transformation. Working in momentum space allows one to easily compute the inverse. The smeared energy-momentum tensor reads

$$\mathcal{T}_0^0 = M\mathcal{A}^{-2}(\square)\delta^{3+n}(\vec{x}). \tag{4.48}$$

It produces the matter density given in (4.19),

$$\mathcal{T}_0^0 = \frac{M}{\Omega_{n+2}\, r^{n+2}} \frac{\mathrm{d}H(r)}{\mathrm{d}r}. \tag{4.49}$$

Matching equations (4.48) and (4.49) means

$$\mathcal{A}^{-2}(\square)\delta^{3+n}(\vec{x}) = \frac{1}{\Omega_{n+2}r^{n+2}} \frac{\mathrm{d}H(r)}{\mathrm{d}r}. \tag{4.50a}$$

Writing the dirac delta by its plane wave momentum space representation $\delta(\vec{x}) = \int \mathrm{d}^{3+n}p\, e^{+ipx}$ on the left hand side and inserting a $1 = \mathcal{F}^{-1}\mathcal{F}$ by means of a double fourier transformation on the right hand side allows computing a solution for the operator in momentum space by means of a fourier transformation of the right hand side:

$$\Leftrightarrow \int \mathrm{d}p^{3+n}\, \mathcal{A}^{-2}(\square)\, e^{ipx} = \frac{1}{\Omega_{n+2}r^{n+2}} \frac{\mathrm{d}H(x)}{\mathrm{d}x} \tag{4.50b}$$

$$\Leftrightarrow \int \mathrm{d}^{3+n}p\, \mathcal{A}^{-2}(p^2)\, e^{ipx} = \int \mathrm{d}^{3+n}p\, \overbrace{\left(\frac{1}{(2\pi)^{2+n}} \int \mathrm{d}^{3+n}z \frac{1}{\Omega_{n+2}\|z\|^{n+2}} \frac{\mathrm{d}H(\|z\|)}{\mathrm{d}\|z\|} e^{-ipz} \right)}^{\tilde{T}_0^0(p)} e^{ipx} \tag{4.50c}$$

$$\Leftrightarrow \mathcal{A}^{-2}(p^2) = \frac{1}{(2\pi)^{2+n}\Omega_{n+2}} \int \mathrm{d}^{3+n}z \frac{1}{z^{n+2}} \frac{\mathrm{d}H(z)}{\mathrm{d}z} e^{-ipz} \tag{4.50d}$$

Note that, by concept, the operator $\mathcal{A}^{-2}$ is dimensionless. It is therefore valid to switch the coordinate system $(r, p) \to (z, q)$ without prefactors, where $z = r/L_*$, $q = pL_*$ are dimensionless coordinates with the fundamental length scale L_*.

4.5.1 Higher-dimensional Fourier Transformation

To solve (4.50d), one can integrate out all extra dimensional angles and effectively reduce the higher-dimensional fourier transformation of the radial symmetric function to a one dimensional one. Calling $V(r) := \frac{H'(r)}{r^{n+2}}$ the higher dimensional Fourier kernel, an effective one-dimensional Fourier transformation is be derived in this section. This is motivated by the well-known three dimensional procedure which is easier to read and given in appendix E.1.

Start with the $N = n + 3$-dimensional fourier transformation and rewrite it into conventional polar coordinates:

$$\hat{V}(p) = \frac{1}{(2\pi)^{3+n}} \int d^{3+n}r \; e^{-i\vec{r}\cdot\vec{p}} V(r) \tag{4.51a}$$

$$= \frac{1}{(2\pi)^{3+n}} \int_0^\infty dr \; r^{2+n} \int_0^{2\pi} d\varphi \prod_{i=1}^{n+1} \int_0^\pi d\theta_i \sin^i(\theta_i) \; e^{-i\vec{r}\cdot\vec{p}} V(r) \tag{4.51b}$$

Now use the angle θ_1 for identification with the inner scalar product angle $\vec{r}\cdot\vec{p} := rp\cos\theta_0$. Subsitute $\int_0^\pi d\theta_1 \sin(\theta_1) = -\int_{-1}^{+1} d\cos\theta := \int_{-1}^1 dx$. Integrating out *all other* n angles θ_i as well as the angle φ gives a $\Omega_{2+n}/2$ contribution, as the $n + 3$-sphere volume is given by $\int d^{3+n}r = \int dr \Omega_{n+2} r^{n+2}$. Divide it by the missing factor $\int_0^\pi d\theta \sin(\theta) = 2$, used for the scalar product substitution. One ends up with

$$= \frac{1}{(2\pi)^{3+n}} \frac{\Omega_{n+2}}{2} \int_{-1}^{+1} dx \int_0^\infty dr \; r^{2+n} V(r) \; e^{-irpx} \tag{4.51c}$$

$$= \frac{1}{(2\pi)^{3+n}} \frac{\Omega_{n+2}}{2} \int_0^\infty dr \; r^{2+n} V(r) \left[\frac{1}{-ipr} e^{-iprx} \right]_{-1}^{+1} \tag{4.51d}$$

$$= \frac{1}{(2\pi)^{3+n}} \frac{\Omega_{n+2}}{2} \frac{i}{p} \left(\int_0^\infty dr \; r^{1+n} V(r) e^{-ipr} - \int_0^\infty dr \; r^{1+n} V(r) e^{+ipr} \right) \tag{4.51e}$$

To write this line as an effective one dimensional Fourier transformation, transform the second integral in line (4.51e), first by switching the integral borders, $\int_0^\infty dr = -\int_\infty^o dr$, second by variable substitution $r := -r'$. This inserts an alternating minus, depending on n, as $r^{1+n}dr = (-1)^{1+n}(r')^{1+n}(-1)dr' = (-1)^n r'dr'$. Note the substitution also toggles the sign of the integral borders, allowing to combine both integrals to

$$= \frac{1}{(2\pi)^{3+n}} \frac{\Omega_{n+2}}{2} \frac{i}{p} \int_{-\infty}^\infty dr \; r^{1+n} \left[V(r)\Theta(r) + (-1)^n V(-r)\Theta(-r) \right] e^{-ipr} \tag{4.51f}$$

$$= \frac{1}{2\pi} \int_{-\infty}^\infty dr \; v(r) \; e^{-ipr}. \tag{4.51g}$$

One derives an effective one dimensional Fourier transformation of the effective function

$$v(r) := \frac{1}{(2\pi)^{2+n}} \frac{\Omega_{2+n}}{2} \frac{i}{p} r^{1+n} \left[V(r)\Theta(r) + (-1)^n V(-r)\Theta(-r) \right]. \tag{4.52}$$

Note that the Heaviside step function $\Theta(z)$, which was used to combine the integrals from line (4.51e) to one in (4.51f) is understood on the complex plane as

$$\Theta(z) = \Theta(Re\,z). \tag{4.53}$$

The requirement (4.53) must be only exactly fulfilled at the evaluation points of the integral, that is, the poles of $v(r)$. This is a weaker requirement for $\Theta(z)$ on the complex plane:

$$\Theta(z) = \begin{cases} \Theta(Re\,z) & \text{if } z \text{ is a pole of } v(r), \\ \text{arbitrary finite value} & \text{else.} \end{cases} \tag{4.54}$$

See appendix E for more details.

Issues may arise with holomorphy when Cauchy theorem is applied. This is discussed further in the appendix E, realizing that solving the integral on the complex plane works in three dimensions, so it shall work in any higher number of dimensions. Note that this approach was also successfully applied to a GUP-inspired nonlocal operator in an onging work [48].

4.5.2 Inverting the bilocal smearing operator

It is possible to solve the $\mathcal{A}^{-2}$ integral (4.50d) by rewriting it to an one-dimensional one. By inserting

$$V(r) = \frac{1}{\Omega_{n+2} r^{n+2}} \frac{\mathrm{d}H(r)}{\mathrm{d}r} \tag{4.55}$$

into equation (4.51f), a compact integral can be derived:

$$\mathcal{A}^{-2}(p^2) = \frac{1}{(2\pi)^{3+n}} \frac{i}{2p} \int_{-\infty}^{\infty} \mathrm{d}r \frac{H'(|r|)}{r} e^{-ipr}. \tag{4.56}$$

This equation can be solved with the residue theorem. Since in (4.56), $r \equiv \|\vec{r}\| \geq 0$ and $p \equiv \|\vec{p}\| \geq 0$, there is only one integration contour for Jordan's lemma. For the forward Fourier transformation $\mathcal{F}_1$, as seen in (4.56), the contour is determined by requiring (for some constant $\# > 0$ representing the momentum)

$$\lim_{r \to \pm i\infty} e^{-ipr} = 0 \;\Rightarrow\; e^{-i(+\#)(\pm i\infty)} = e^{\pm\infty\#} = 0 \;\Rightarrow\; r \to -i\infty, \tag{4.57}$$

i.e. it is closed on the lower half complex plane ($Im\, r < 0$). For the inverse Fourier transformation $\mathcal{F}_1^{-1}$, it is closed on the upper half complex plane ($p \to i\infty \Leftrightarrow Im\, p > 0$).

Concluding, equation (4.56) allows deriving the inverse bilocal operator by inserting a specific choice of $H(r)$.

Chapter 5

The holographic black hole in higher dimensions

In this chapter, a member of the black hole family discussed in the previous chapter is proposed. It is based on a black hole proposed in [61]. It tackles the problems of the Schwarzschild black hole presented in the previous chapters. It will be derived that the class of black holes proposed in this chapter features:

1. A modified short-distance behaviour which allows the physical system to arrive at a *cold evaporation endpoint* (black hole remnant), supported by regular thermodynamics.

2. A *classical low-energy limit*, that is, Schwarzschild behaviour of the metric for big distances, in terms

$$g_{00}(r) = 1 - \frac{2GM}{r} \quad \text{for} \quad r \gtrsim l_0. \tag{5.1}$$

3. *Self-encoding* of the characteristic minimal length scale l_0 in the radius of the *extremal* configuration r_0, that is,

$$l_0 = r_0. \tag{5.2}$$

4. *Logarithmic entropy corrections*, like most theories of quantum gravity propose.

5. Compatibility with *large extra dimensions*: All previous points can be implemented in the ADD scenario, and one may identify the length scale l_0 with the fundamental length L_*.

It will be shown that this class of black holes still possesses a curvature singularity at the origin ($\lim_{r \to 0} R = \infty$). Anyway the property of self-encoding is crucial: It enables l_0 being the only *universal scale*, as the theory requires no new length scale like $\sqrt{\beta}$ from GUP, θ from NCG or ℓ_0 from String Theory.

This class of black holes is implemented by a special choice of $H(r)$ that will be refered to as $h(r)$ for distinction. By inserting $H(r) = h(r)$ in any equation of chapter 4, a number of

physical properties will be derived in this chapter. $h(r)$ defines the *holographic black hole* in n large extra dimensions:

$$h(r) := \frac{r^{2+n}}{r^{2+n} + \tilde{r}_0^{2+n}}. \tag{5.3}$$

$\tilde{r}_0$ is a regulation constant of dimension length that is discussed in the next sections. For $n \to 0$, the profile (5.3) reduces to the four dimensional profile first studied by Nicolini and Spalluci in [61].

Inserting $h(r)$ into the generic gravitational potential (4.20) creates for a fixed n and $\tilde{r}_0$ a geometry, uniquely determined by its mass M:

$$V(r) = \frac{1}{2+n} \frac{M}{M_*^{n+2}} \frac{r}{r^{2+n} + \tilde{r}_0^{2+n}}. \tag{5.4}$$

The gravitational potential (5.4) spawns a class of black hole geometries which is subject of this chapter.

Note that this profile is an *ab-initio* proposal, and especially the higher dimensional continuation is "guessed". The special feature is that *there is no further ingredient than General Relativity*. There is no need to stress a more advanced theory like String Theory or loop quantum theory to generate the metric defined by (5.4).

Compared to [61], the holographic metric was extended to higher dimensions. The higher dimensional modification will be justified by yielding logarithmic corrections to the black hole entropy in any number of dimensions.
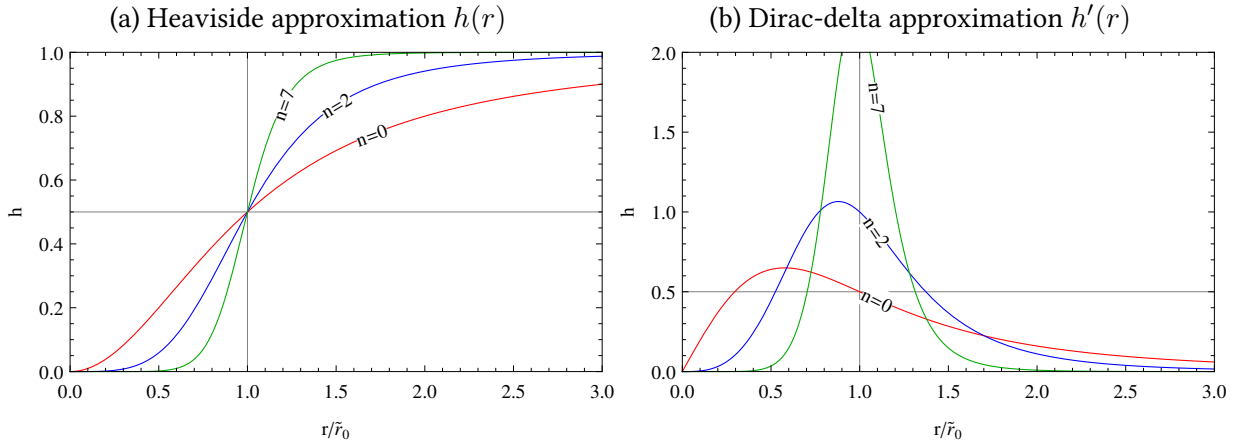

Figure 5.1: The Heaviside (a) and Dirac delta (b) approximation profile $h(r)$ against its built in length scale $\tilde{r}_0$ for a different number of large extra dimensions n. One sees that $\tilde{r}_0$ plays the role of the *width* of the profile. By choice, it is a kind of "half-life scale", as can be computed when computing $h(\tilde{r}_0) = 1/2$. Note also that increasing n create sharper distributions. For $n \to \infty$, the curve resembles a displaced step function $h_{n\to\infty}(r) = \Theta(r - \tilde{r}_0)$. This reflects the fact that all volume in a ∞-sphere lives on the surface.

5.1 Geometry

5.1.1 Horizons

The event horizon equation, considering r_H being the event horizon, requires

$$0 = g_{00}(r_H) \quad \Rightarrow \quad 0 = z^{2+n} - z\, m_n + 1, \quad \text{with } m_n = \frac{1}{n+2}\frac{M}{M_*^{n+2}} \tag{5.5}$$

and $z = r/\tilde{r}_0$. The number of (physically meaningful) solutions depends on m_n, that is, on the black hole mass M. For any n, there are three possible solutions, plotted in figure 5.2a. They are distinguished by the value of the ratio M/M_0, with the extremal mass M_0 that is found to be a special value:

$M < M_0$ The mass is too small to create a black hole. The physical object is a vacuum, self-gravitating particle-like structure which is stable.

$M > M_0$ There are two horizons with radii $r_\pm$. In figure 5.2a, they are indicated by red dots. Physically, one can argue that the outer horizon r_+ is the more relevant one, since it *shields* the black hole inner structure. Mathematically, r_- is a Cauchy horizon, and in the region $r_- < r < r_+$, where $g_{00} > 0$ and $g_{rr} < 0$, the coordinates r and t switch their meaning (cf. section 6.1.6).

There are no meaningful compact analytic expressions for the values of $r_\pm$, expcept for the holographic metric and without extra dimensions ($n = 0$), as already given in [61]:

$$r_\pm = GM \pm \sqrt{GM^2 - 4}. \tag{5.6}$$

For $n > 0$ and especially for the self-regular metric, the roots of (??) can simply be determined numerically.

Note that for $M \gg M_0$, r_+ approaches the Schwarzschild-Tangherlini horizon.

$M = M_0$ The two horizons merge to a single horizon which is called *extremal* or *degenerate* horizon $r_\pm = r_0$ and identified with the extremal mass $M = M_0$. In figure 5.2a, the green line displays the coefficient g_{00} with extremal mass, showing a single horizon, indicated by the green dot. Figure 5.2b displays the extremal configuration in higher dimensions.

(a) g_{00} in $n = 0$ for different masses M.

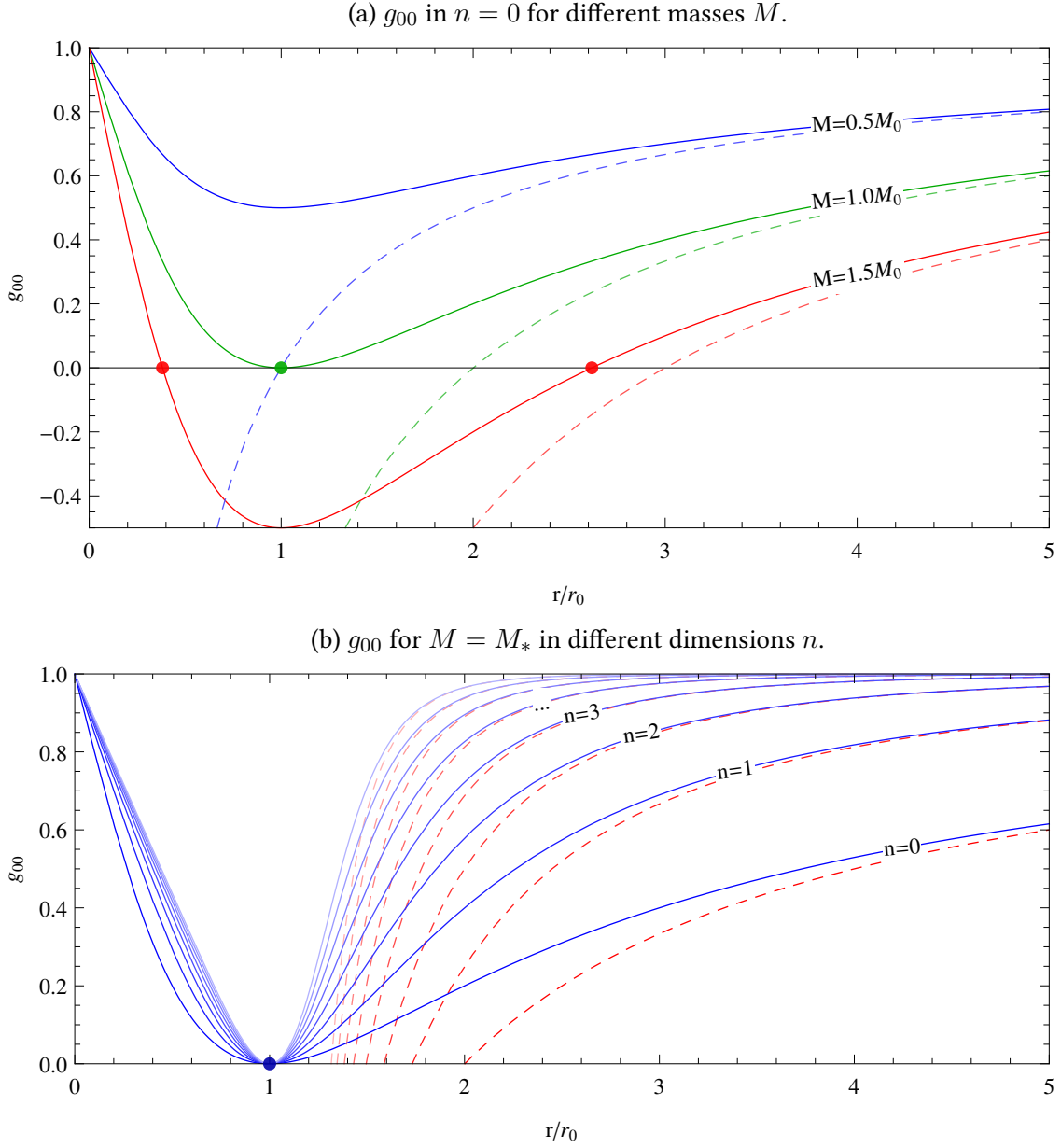(b) g_{00} for $M = M_*$ in different dimensions n.

Figure 5.2: The holographic gravitational potential. The upper panel 5.2a shows different geometries based on the black hole mass. The three curves represent a smaller than critical-mass (blue), critical mass (green) and heaviest mass (red).

The lower panel 5.2b shows the higher dimensional extension for the self-encoding masses $M_0 = M_*$. All curves are scaled for the individual L_* according to the numerical values given in table 6.2.

Compared to the fourdimensional metric (fig. 5.2a), one can see that the picture basically *stays the same*. In this figure, the curves qualitatively get "sharper" with increasing n, which corresponds to the increasing surface to volume ratio of n-spheres, which is a purely geometrical effect.

In any case, the dashed lines correspond to the equivalent Schwarzschild metric.

5.1.2 The self-encoding remnant

In the present class of black hole geometries, the extremal black hole configuration parameter $M = M_0$ or $r = r_0$ can be *self-encoded* with the built-in length scale $\tilde{r}_0$. The relation is found by inserting $h(r)$ into the second remnant equation (4.27b):

$$r_0 = \tilde{r}_0 \left(\frac{1}{1+n} \right)^{\frac{1}{2+n}} \tag{5.7}$$

Equation (5.7) allows to connect the length scale $\tilde{r}_0$ introduced as "built in" length scale in the holographic profile to a physical length scale r_0. This equation can be used to eliminate $\tilde{r}_0$ from the holographic profile (5.3) in favour of the physical meaningful r_0:

$$h(r) = \frac{r^{2+n}}{r^{2+n} + \tilde{r}_0^{2+n}} = \frac{r^{2+n}}{r^{2+n} + (1+n)r_0^{2+n}}. \tag{5.8}$$

Note that the *self-encoding* principle requires that the size of the remnant r_0 should be identical to the fundamental length scale of the physical theory l_0. For gravity in 4d space time, the only fundamental length scale is given by the coupling constant (Newtons constant) G which defines the Planck length $L_{\text{Pl}} = \sqrt{G} \approx 10^{-35}$ m. In 4d, (5.7) assures this is true, as already stated in [61]:

$$r_0 \overset{!}{=} l_0 = L_{\text{Pl}} = \tilde{r}_0. \tag{5.9}$$

With extra dimensions, there is the reduced Planck length L_* which is the actual fundamental length scale l_0, since the observable Planck length L_{Pl} is just a large-distance effective one. To express $h(r)$ only in terms of L_*, require $r_0 \overset{!}{=} l_0 \equiv L_*$ and find

$$\tilde{r}_0 = (1+n)^{\frac{1}{2+n}} L_* . \tag{5.10}$$

Implementing the self-encoding value for $\tilde{r}_0$ into the holographic profile (5.8) gives a profile which contains nothing more than the universal physical constant L_*:

$$h(r) = \frac{r^{2+n}}{r^{2+n} + (1+n)L_*^{2+n}} \tag{5.11}$$

When computing $M_0 = M(r_0)$, the self-encoding of the fundamental mass scale M_* is expected, that is, $M(r_0) = M_*$. It is $h(L_*) = 1/(2+n)$ and thus, by construction,

$$M(L_*) = \frac{1}{n+2} \left(\frac{L_*}{L_*} \right)^{1+n} \frac{1}{h(L_*)} M_* = M_*. \tag{5.12}$$

symbol	meaning
r	A placeholder for a radius.
r_H	The black hole horizon radius.
r_+	The outer Cauchy horizon of the holographic black hole, this is (if applicable) always accessible.
r_-	The inner Cauchy horizon of the holographic black hole, it is not visible from outside.
r_0	The extremal black hole horizon radius. When $r_+ = r_-$, the symbol r_0 is used.
r_C	The critical radius, at this radius the temperatures are maximal.
L_*	The fundamental length in the ADD scenario. In this chapter it is the fundamental physical length.
β	The fundamental length in the GUP scenario.
θ	The fundamental length in the NCBH scenario.
L_{Pl}	The Planck length (fundamental length in classical GR).
l_0	A placeholder for a fundamental physical length scale. Possible values are e.g. $l_0 \in \{L_*, L_{\mathrm{Pl}}, \beta, \theta, \dots\}$.

Table 5.1: Variables representing lengths used in this chapter. According to Mass=1/Length, each length scale represents also a mass scale.
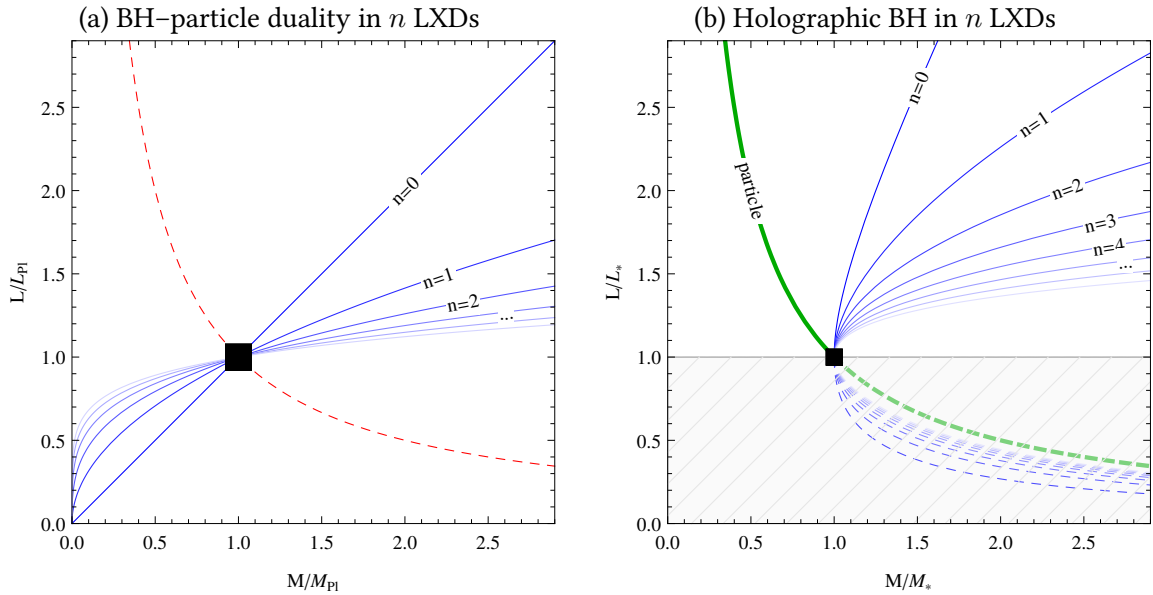

Figure 5.3: The holographic black hole (right panel) solves the BH–particle duality problem, shown in the left panel (it is figure 3.1 from section 3.1).

5.1.3 Minimal length

Figure 5.3 shows how the holographic black hole prohibits physics below the Planck scale by implementing the self-completeness principle. The quantum mechanics regime ($M < M_*$) and the general relativity regime ($M > M_*$) are clearly separated, and the holographic black hole never accesses the sub-Planckian regime but instead builds out a remnant (black dot).

Considering the right panel, the two horizons of the holographic black hole stand out as the upper and lower branches of the blue curves. While the upper branches display $r_+ > L_*$, the "visible" event horizons, the lower branches display the cauchy horizons $r_- < L_*$ that are shielded by r_+ for big masses $M > M_*$ and non-accessible by the remnant at $M = M_*$.

5.1.4 Curvature singularity

According to the curvature considerations for general profiles $H(r)$ in section 4.3.2, the holographic metric is still diverging. One can give an estimation for $R(0)$ based on the taylor expansions of the holographic profile $h(r)$ at $r = 0$:

$$h(r) = (r/L_*)^{2+n} + \mathcal{O}\left((r/L_*)^{2(2+n)}\right), h'(r) \approx (r/L_*)^{1+n}, h''(r) \approx (r/L_*)^{n} \qquad (5.13)$$

Inserting this into $R(r)$ for $H(r)$, equation (4.28b), gives $H(0) \approx L_*/r$. The holographic black hole has therefore still a curvature singularity at the origin.

n	0	1	2	3	4	5	6	7
$\tilde{r}_0$	1.00	0.79	0.76	0.76	0.76	0.77	0.78	0.79
r_C	2.060	1.600	1.480	1.410	1.360	1.330	1.300	1.280
$T(r_C)$	0.024	0.070	0.124	0.183	0.245	0.309	0.375	0.443

Table 5.2: Numerical properties of the holographic black hole. All values are given in nd Planck units (as multiples of L_*). $\tilde{r}_0$ is the initial length scale of $h(r)$ that was used to fix the self-encoding of the theory, according to eq. (5.7). Going from eq. (5.3) to (5.11), $\tilde{r}_0$ could be eliminated in favour of the fundamental L_*.
r_C is the critical radius according to eq. (5.16). $T(r_C)$ is the Hawking temperature for a black hole with extend r_C, it is the maximum temperature, also indicated in figure 5.4.

5.2 Thermodynamics

The thermodynamics of the holographic black hole arise from the equations given in section 4.4. By inserting the holographic profile $h(r)$ in the equations derived for general $H(r)$, the quantities in this section are derived.

Note that in this section, r_H always represents the outer horizon $r_+ > L_*$ which is the physical meaningful horizon for calculating thermodynamics of the holographic black hole.

5.2.1 Hawking Temperature

The Hawking Temperature of a holographic black hole with radius r_H in n LXDs is determined by (4.38) to

$$T_H = \frac{1}{4\pi r_H}\left(1 + n - (2+n)\frac{(L_*/r)^{(2+n)}}{1 + (L_*/r)^{(2+n)}}\right).\tag{5.14}$$

Figure 5.4 shows the temperature of the black holes. Comparing with the appropriate Schwarzschild black hole in n dimensions, the first thing to be noticed is the difference of the two curves which becomes large below $r \lesssim 3L_*$ or $r \lesssim {}^3\!/{}_2 r_C$, with the critical temperature r_C as defined in the next section. There is a maximum temperature at the critical radius r_C (indicated by the dots in fig. 5.4, numerical values are given in table 6.2), and for smaller radius the black hole cools down until it reaches zero temperature at r_0. One therefore speaks of a *cold remnant*.
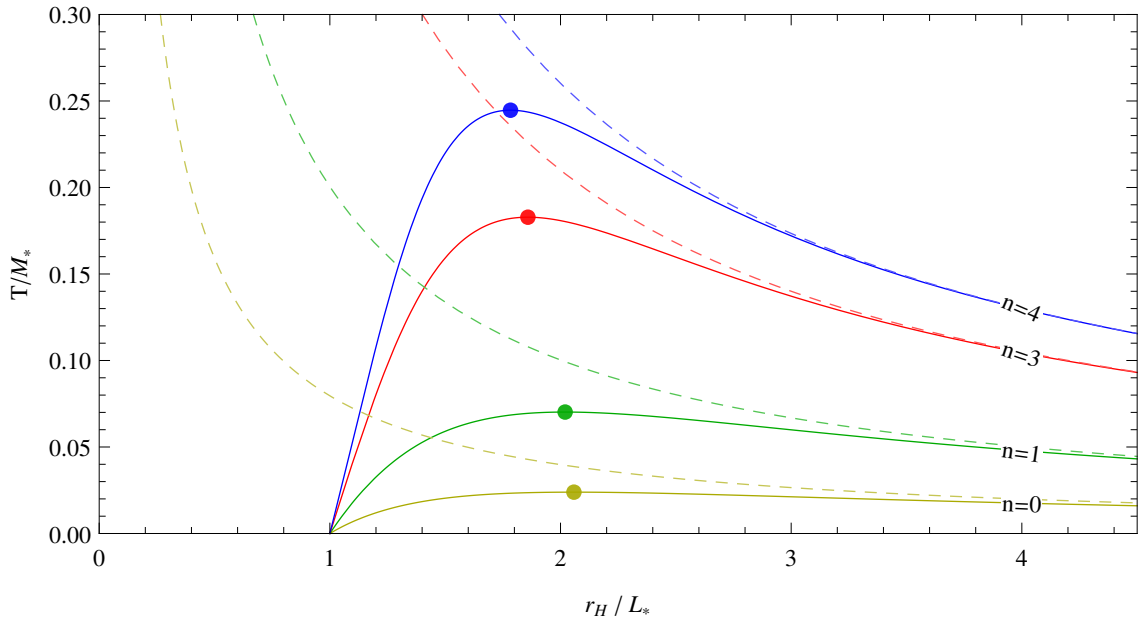

Figure 5.4: Temperature of the holographic black hole, compared to the dashed-line Schwarzschild-Tangherlini black hole temperature, in a different number of dimensions. The circles indicate the critical radii (eq. 5.16) where maximal temperatures occur.

5.2.2 Heat capacity

The heat capacity of a holographic black hole with radius r_H in n LXDs is determined by 4.41 to

$$C = -\frac{4\pi r_H^{2+n}}{M_*^{n+2}} \frac{\left(r_H^{-n} + r_H^2\right)^2 \left((1+n)r_H^2 - r_H^{-n}\right)}{(4 + 3n + n^2)\, r_H^{n-4} + r_H^{2n-2} - (1+n)r_H^6} \,. \tag{5.15}$$

The critical radius can be determined by evaluating the extremal temperature condition and inserting the current black hole model into (4.43):

$$r_C = 2^{\frac{1}{n+2}} \left((2+n)\sqrt{n^2 + 2n + 5} - n^2 + 3n - 4\right)^{-\frac{1}{n+2}} L_* \tag{5.16}$$

5.2.3 A phase transition

Eventually, having computed g_{00}, T and C, one is able to compare those quantities for black hole stability discussion. Figure 5.6 illustrates the curves and different phases, exemplary for the holographic black hole. Considering the sign of the heat capacity, three phases can be distinguished:

$r > r_C$ **.** The heat capacity is negative, the system is instable: Losing mass by radiation makes it hotter and hotter. This behaviour is well described by the Schwarzschild metric.

When reaching $r \to^+ r_C$, in the modified metrics this process stagnates, the temperature no longer rises. Now a phase transition takes place at r_C, the system gets stable.

$r_0 < r < r_C$ **.** The heat capacity is positive and the black hole system is stable. Losing mass now results in losing temperature. The system heavily deviates from the classical Schwarzschild solution. The Temperature decreases until it evventually reaches zero.

$r < r_0$ **.** This phase is physically never accessed, as the system got stable at r_0. The self-complete paradigm also ensures that no black holes cannot be generated at these distances, as smaller length scales then r_0 are not accessible.

Thermodynamics in this area is not physically meaningful. Mathematically, there is a negative temperature $T < 0$ and the system is basically instable again, since $C < 0$.

5.2.4 Entropy

Inserting the holographic profile $h(r)$ into the entropy integral (4.45) gives the entropy of the holographic black hole,

$$S_h(r_H) = \frac{4\pi}{L_*^{n+2}} \left(r_H^{n+2} - L_*^{n+2}\right) + 4\pi(n+2) \log\left(\frac{r_H}{L_*}\right) \tag{5.17}$$

Note the *logarithmic quantum corrections*. They motivate the label *holographic* for the metric. Since $\log(1) = 0$, the entropy goes to exactly to zero for $r_H \to r_0$. The remnant therefore has zero entropy.
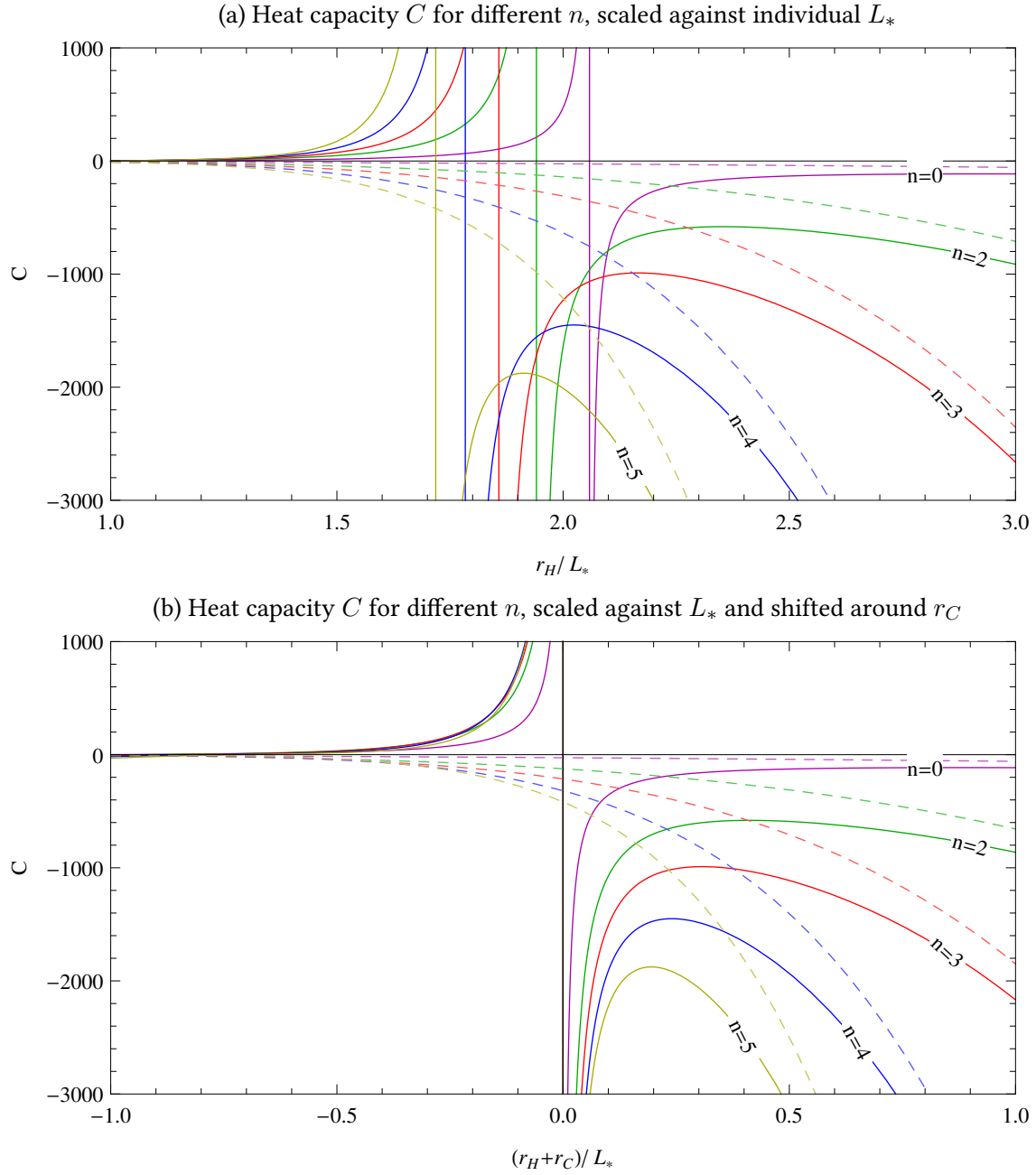
Figure 5.5: The heat capacity of the holographic black hole for different extra dimensions n, as a function of the black hole size r_H. The dashed line corresponds to the heat capacity of the classical Hawking-Beckenstein black hole in n extra dimensions.
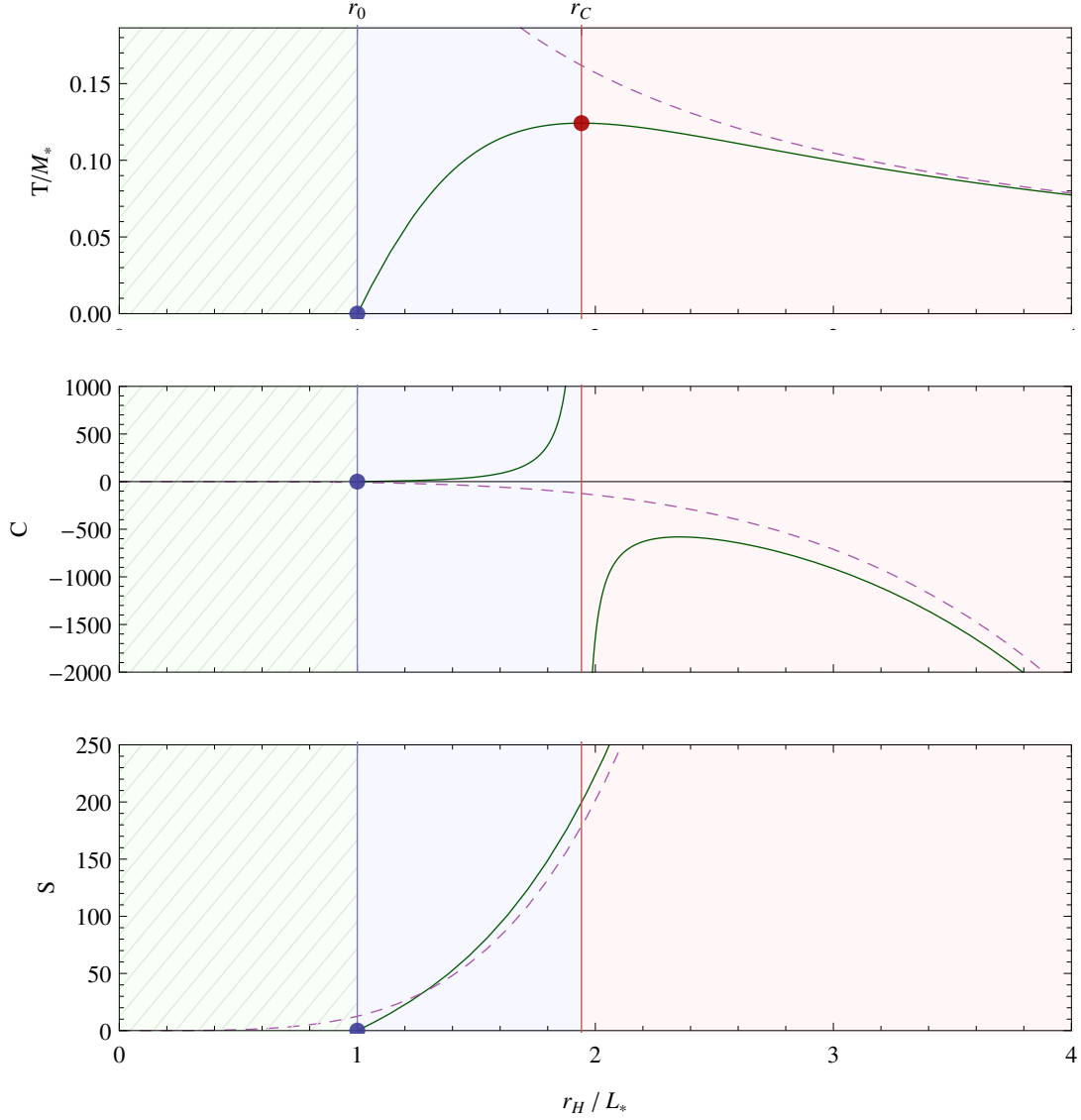
Figure 5.6: Comparison of temperature (top panel), heat capacity (middle panel) and entropy (bottom panel) on the same scale (Planck units everywhere). Here, $n = 2$, but the plot looks systematically the same in all dimensions. The dashed curves are the corresponding Schwarzschild behaviour.

Regarding the sign of the heat capacity (Sign $C = \pm 1$), there are three different states, indicated by colors and seperated by r_0 (blue line) and r_C (red line). Blue circles indicate the final, cold and stable evaporation state. The red circle indicates the position of the critical radius. Note that the shaded region $r_H < L_*$ is physically not accessible and in the self-complete paradigm of general relativity, thermodynamics are not defined there.

5.2.5 The area quantization picture

The black hole area theorem dates back to Wheeler 1973 and is a recasting of the Schwarzschild black hole entropy in terms of the horizon area $A = 4\pi r_H^2$, and therewith

$$S = 2\pi \frac{A}{A_0} \quad \text{with } A_0 = 4\pi L_P^2. \tag{5.18}$$

In the same spirit, we can recast the holographic metric black hole (5.17) as

$$S_h(A_+) = \frac{\pi}{A_0}(A_+ - A_0) + \pi \log(A_+/A_0), \tag{5.19}$$

with $A_+ = \Omega_{n+2} r_+^{2+n}$ and $A_0 = \Omega_{n+2} L_*^{2+n}$.

By means of a taylor expansion $\log(x) \approx (x-1) + \mathcal{O}\left((x-1)^2\right)$ around $x = 1$, one sees the entropy vanishes for $A_+ \to A_0$, which encodes the physical fact that the Planck size remnant can be only realized in one configuration [61]. We therefore interpret it as an *ground state* for a quantized area spectrum

$$A_+ = A_{n-1} = nA_0 = 4\pi n L_*^2, \tag{5.20}$$

to express A_+ (literally) stores n basic units of information. Wheeler created a new term for this concept of *bits* and *bytes*: One byte consists of 4π bits. This is also shown in figure 5.7.

The area quantization also motivates to a discrete mass spectrum and the analysis of a transition from a (semi-)classical regime to a quantum regime with different kinds of decay: thermal decay vs. quantum decay with discrete quanta emission. The higher dimensional extension does not change the picture drawn in [61].

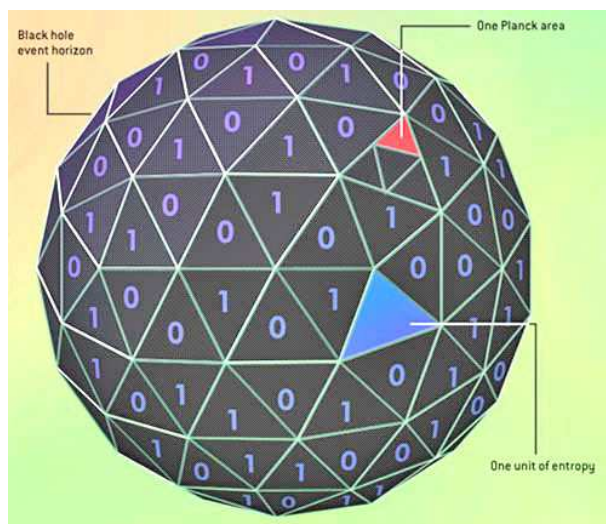The area quantization concept was also studied by Dvali [23, 24].

Figure 5.7: An artistic interpretation of the holographic principle, as it illustrated an science magazine article by Jacob Bekenstein [11]. The black hole entropy is quantizied in terms of Planck units. A Planck area (blue) has $A/4$ units of entropy (red).

5.3 Modified field equations

In the holographic model, insert $h(r)$ to derive from (4.56) the expression (note there is no need for powers of L when switching to dimensionless coordinates)

$$\mathcal{A}^{-2}(q^2) = \underbrace{\frac{2+n}{(2\pi)^{3+n}}\frac{i}{2q}}_{f_0}\int_{-\infty}^{\infty}\mathrm{d}z\left[\underbrace{\frac{z^n}{(1+z^{2+n})^2}}_{f_+}\Theta(z) + \underbrace{\frac{(-1)(-z)^n}{(1+(-z)^{2+n})^2}}_{f_-}\Theta(-z)\right]e^{-iqz}. \quad (5.21)$$

The poles of f_+ are the same as for f_-, just mirrored at the imaginary axis $Re(z) = 0$, in symbols $f_+(z) = -f_-(-z)$. The poles of f_+ are given by

$$\left(1 + z^{2+n}\right)^2 = 0 \quad \Leftrightarrow \quad z = (-1)^{\frac{1}{2+n}} = \exp\left\{\frac{i\pi + 2\pi ik}{n+2}\right\} \quad \forall k \in \mathbb{N}_0. \quad (5.22)$$

There are $n+1$ unique poles, each to be counted twice due to the power of 2 in the denominator of f_+. Due to the integration contour (4.57), only the $\frac{n+1}{2}$ unique poles in the region $Im(z_0) \leq 0$ are taken into account. For f_+, only the $\frac{n+1}{4}$ poles in the region $Re(z_0) \geq 0$ are visible. Identify these poles by their set of angles in the complex phase,

$$\Phi_n = \left\{\varphi = \arg(z) \: : \: 1 + z^{n+2} = 0 \wedge Im(z) \leq 0 \wedge Re(z) \geq 0\right\} \quad (5.23)$$

$$= \left\{\varphi = \pi\frac{1-2k}{n+2} \: : \: k \in \mathbb{N}_0 \wedge k \leq \frac{n}{4}\right\}, \quad (5.24)$$

and write $e^{i\Phi_n} = \{z = e^{i\varphi} : \varphi \in \Phi_n\}$ to denote the set of complex numbers associated with Φ_n. Note the number of angles $|\Phi_n| = \lfloor\frac{n+1}{4}\rfloor$ is a step function, so it is unlikely that a more compact expression than the subsequent one can be derived for general n.

All poles $z_0 \in e^{i\Phi_n}$ are of 2nd order, the residues are therefore given by

$$\operatorname*{Res}_{z\to z_0} f_+(z)e^{iqz} = \lim_{z\to z_0}\frac{\mathrm{d}}{\mathrm{d}z}(z-z_0)^2 f_+(z)e^{iqz} = \frac{\operatorname{sign}(z_0)\bar{z}_0}{(n+2)}e^{iz_0q}(1-iz_0q) \quad (5.25)$$

and enter the holographic $\mathcal{A}^{-2}$ integral from (5.21) in a way that

$$\int \mathrm{d}z\left(f_+(z)\Theta(z) + f_-(z)\Theta(-z)\right)e^{iqz} = (2\pi i)(-1)\cdot$$

$$\cdot\left(2\sum_{z_0\in e^{i\Phi_n}}\operatorname*{Res}_{z\to z_0} f_+(z) + 2\sum_{z_0\in e^{\Phi_n}}\operatorname*{Res}_{z\to z_0} f_-(z)\right). \quad (5.26)$$

Note that due to symmetry of the poles, there are either poles z_0 (produced by f_+) and $-z_0$ (produced by f_-) which residues sum to the expression

$$\operatorname*{Res}_{z_0} f_+ e^{izq} + \operatorname*{Res}_{-z_0} f_- e^{izq} = \operatorname*{Res}_{z_0} f_+ e^{izq} - \operatorname*{Res}_{z_0} f_+ e^{-izq} = \frac{2i\bar{z}_0}{(2+n)^2}\sin(z_0q), \quad (5.27)$$

or the f_+ and f_- share a common pole at $z_0 = -i$, then

$$\operatorname*{Res}_{-i} f_+ e^{izq} = \frac{i}{n+2} e^{+q}(1-q). \tag{5.28}$$

Note that poles at $z_0 = -i$ only occur at integer $n/4$, that is $n = 0, 4, 8, \ldots$. In favour to give a closed form result, one therefore cannot always apply the simplification rules (5.27) and (5.28). The overall result is given by

$$\mathcal{A}^{-2} = \frac{(2\pi)^{2+n}}{q} \sum_{\varphi \in \Phi_n} \operatorname{sign}(z_0) \bar{z}_0 e^{iz_0 q} (1 - iz_0 q) \tag{5.29}$$

with $z_0 = e^{i\varphi}$. Without extra dimensions ($n = 0$) is the only case where a purely real result can be given, for $n > 0$ complex phases always survive in (5.29). For $n = 0$ we get (with $q = pL$):

$$\mathcal{A}^{-2} = \frac{1}{4\pi} \left(\frac{e^{-q}}{q} + e^{-q} \right). \tag{5.30}$$

Reinserting L and sending $L \to 0$ gives $\mathcal{A}^{-2} \to 1/4\pi$. (There is missing some 4π here to ensure $\mathcal{A}^{-2} \to 1$).

Chapter 6

The self-regular black hole in higher dimensions

This chapter is devoted to another member of the black hole family discussed in chapter 4. It was first proposed in four dimensions in [60]. It engages the problems of the Schwarzschild black hole, presented in chapters 2 and 3. It will be proven that the class of black holes proposed in this chapter features:

1. A *regular black hole center* that has no more curvature (Ricci scalar) singularity at the origin, in terms

$$R(0) < \infty. \tag{6.1}$$

2. A modified short-distance behaviour which allows the physical system to arrive at a *cold evaporation endpoint* (black hole remnant), supported by regular thermodynamics.

3. A *classical low-energy limit*, that is, Schwarzschild behaviour of the metric for big distances, in terms

$$g_{00}(r) = 1 - \frac{2GM}{r} \quad \text{for} \quad r \gtrsim l_0. \tag{6.2}$$

4. *Self-encoding* of the characteristic minimal length scale l_0 in the radius of the *extremal* configuration r_0, that is,

$$l_0 = r_0. \tag{6.3}$$

5. Compatibility with *large extra dimensions*: All previous points can be implemented in the ADD scenario, and one may identify the length scale l_0 with the fundamental length L_*.

The self-regular black hole shares some features with the holographic black hole (sect. 5). Therefore, the discussion will always make a comparison with the holographic black hole.

Again, the property of self-encoding is crucial: It enables l_0 being the only *universal scale*, as the theory requires no new length scale like $\sqrt{\beta}$ from GUP, θ from NCG or ℓ_0 from String Theory. To implement both self-encoding and regularity (therefore the name *self-regular*), the theory is equipped with an additional degree of freedom $\alpha \in \mathbb{R}$. To distinct the special choice

of $H(r)$ for the self-regular black hole, it will be refered to as $h_\alpha(r)$. By inserting $H(r) = h(r)$ in any equation of chapter 4, a number of physical properties will be derived in this chapter. $h_\alpha(r)$ defines the *self-regular black hole* in n large extra dimensions:

$$h_\alpha(r) := \frac{r^{3+n}}{\left(r^\alpha + \tilde{r}_0^\alpha/2\right)^{\frac{3+n}{\alpha}}}. \tag{6.4}$$

$\tilde{r}_0$ is a regulation constant of dimension length and plays the same role as for the holographic model. The dimensionless α couples, as it turns out, together the two fundamental theories encoded in this black hole model. n counts the number of extra dimensions, and for $n \to 0$, the profile (6.4) reduces to the four dimensional profile first studied by Nicolini and Spalluci in [60].

Note that also the self-regular profile, as the holographic profile, is an *ab-initio* proposal, and especially the higher dimensional continuation is "guessed". It is a special feature that *there is no further ingredient than General Relativity*. There is no need to stress a more advanced theory like string theory or loop quantum theory to generate the self-regular metric, given by plugging (6.4) into (4.20),

$$V(r) = \frac{1}{2+n} \frac{M}{M_*^{n+2}} \frac{r^2}{\left(r^\alpha + \tilde{r}_0^\alpha/2\right)^{\frac{3+n}{\alpha}}}. \tag{6.5}$$

The class of black holes spanned by (6.5) is a quite big one, as it turns out that e.g. the Bardeen black hole [8] is a part of the class, with a special choice of α.
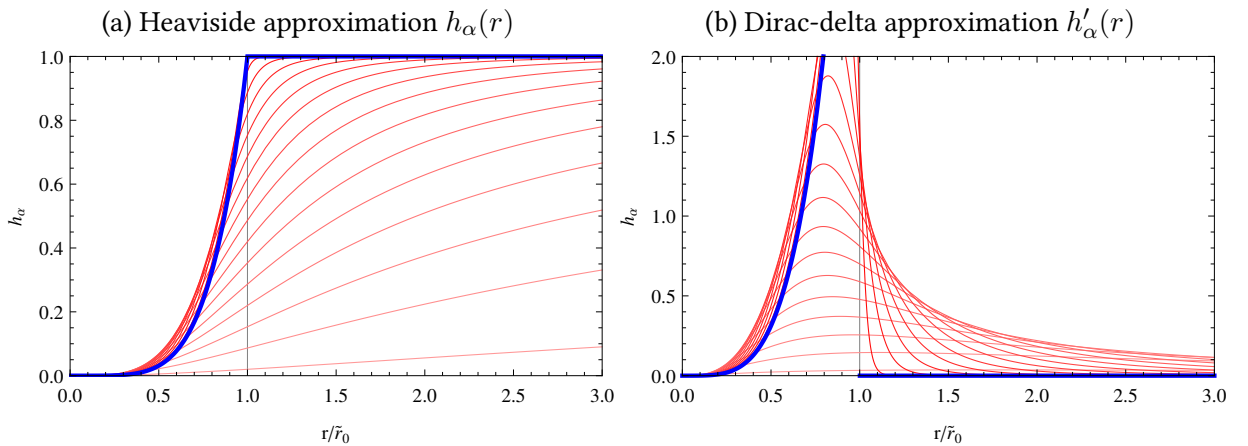

Figure 6.1: The Heaviside (a) and Dirac delta (b) approximation profile $h_\alpha(r)$ against it's built in length scale $\tilde{r}_0$ for different choices of α and fixed n. Red color saturation indicates increasing α, while the thick blue curve represents $\alpha = \infty$. See appendix C for details of the graph.

6.1 Geometry

Compared to the holographic black hole, the self-regular black hole excells in its outstanding geometric features, while it does not possess the thermodynamic features one expects from a quantum gravity.
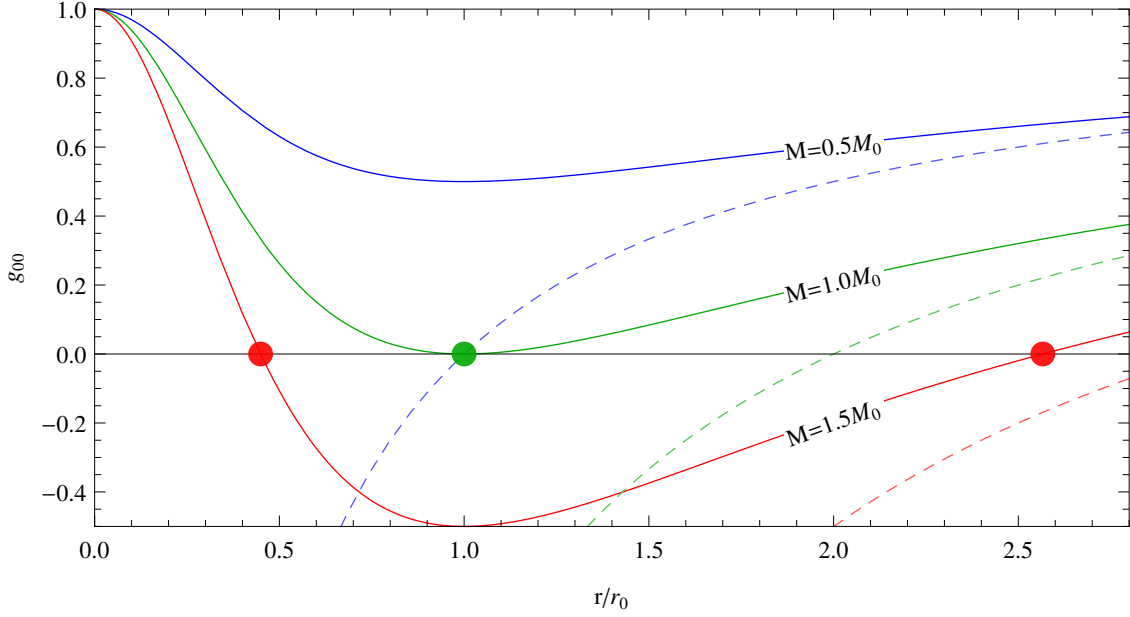

Figure 6.2: g_{00} for the self-regular, self-encoding ($\alpha = \alpha_0$) black hole in 4d ($n = 0$). The three curves represent a smaller than critical-mass (blue), critical mass (green) and a too heavy mass (red). In any case the dashed line corresponds to the equivalent Schwarzschild metric. Note the different behaviour as $z = r/r_0 \to 0$ compared to the holographic figure 5.2a.

6.1.1 Horizons

The event horizon equation, considering r_H being the event horizon, requires $0 = g_{00}(r_H)$. For the self-regular black hole, the horizons r_H are given by the root of the polynomial

$$0 = z^2(z^\alpha + 1/2)^{(3+n)/\alpha} - m_n, \quad \text{with } m_n = \frac{1}{n+2}\frac{M}{M_*^{n+2}} \tag{6.6}$$

and $z = r/\tilde{r}_0$. The number of (physically meaningful) solutions depends on m_n, that is, on the black hole mass M. For any n, there are three possible solutions, plotted in figure 6.2. They can be distinguished by the extremal mass M_0:

$M < M_0$ The mass is too small to create a black hole. The physical object is called a *G-lump* after Dymnikova [25] and represents a vacuum, self-gravitating, regular, particle-like structure [3].

n	0	1	2	3	4	5	6	7
α_0	1.755	4.285	7.081	9.333	10.642	11.128	11.098	10.805
$\tilde{r}_0/L_*$	1.	0.851	0.856	0.862	0.86	0.851	0.839	0.825

Table 6.1: Numerical results for the self-encoding choice of α, given from eq. (6.7), as well as the ratio $\tilde{r}_0/L_*$ that was found in eq. (6.9) to make the currently discussed class of black holes self-encoding. This replacement allows to remove the nonphysical parameter $\tilde{r}_0$ from the initial profile (6.4) to a profile containing only the fundamental length scale L_*, displayed in eqref...

$M > M_0$ There are two horizons with radii $r_\pm$. In figure 6.2, they are indicated by red dots. Physically, one can argue that the outer horizon r_+ is the more relevant one, since it *shields* the black hole inner structure. Mathematically, r_- is a Cauchy horizon, and in the region $r_- < r < r_+$, where $g_{00} > 0$ and $g_{rr} < 0$, the coordinates r and t switch their meaning (cf. section 6.1.6).

There are no meaningful compact analytic expressions for the values of $r_\pm$, but the roots of (6.6) can simply be determined numerically.

Note that for $M \gg M_0$, r_+ approaches the Schwarzschild-Tangherlini horizon.

$M = M_0$ The two horizons merge to a single horizon which are called $r_\pm = r_0$. This is the *extremal* radius, identified with the extremal mass M_0. In figure 6.2, the green line displays the gravitational potential with extremal mass, showing a single horizon, indicated by the green dot.

6.1.2 The self-regular self-encoding remnant

As the holographic model, the self-regular black hole exhibits an extremal configuration $M = M_0$. Using the remnant equation (4.27b), one can relate the extremal radius r_0 to the self-regular "width" paramter r_0:

$$r_{0,\alpha} = \tilde{r}_0 \left(\frac{1}{1+n} \right)^{\frac{1}{\alpha}}. \tag{6.7}$$

Equation (6.7) allows to connect the length scale $\tilde{r}_0$ introduced for self-regular model to a physical length scale r_0. Note that the *self-encoding* principle requires that the size of the remnant r_0 should be identical to the fundamental length scale of the physical theory l_0. For gravity in 4d space time, the only fundamental length scale is given by the coupling constant (Newtons constant) G which defines the Planck length $L_{\text{Pl}} = \sqrt{G} \approx 10^{-35}$ m. In 4d, (??) assures this is true, as already stated in [61]:

$$r_0 \overset{!}{=} l_0 = L_{\text{Pl}} = \tilde{r}_0. \tag{6.8}$$

With extra dimensions, there is the reduced Planck length L_* which is the actual fundamental length scale l_0, since the observable Planck length L_{Pl} is just an effective one. To express the

profile $h_\alpha(r)$ only in terms of L_*, one requires $r_0 \overset{!}{=} l_0 = L_*$ and finds

$$\tilde{r}_0 = (1+n)^{\frac{1}{\alpha}} L_* .\tag{6.9}$$

Implementing the self-encoding value for $\tilde{r}_0$ into the self-regular profile (6.4) gives a profile which contains only the universal physical constant L_*:

$$h_\alpha(r) = \frac{r^{3+n}}{\left(r^\alpha + \frac{1+n}{2}L_*^\alpha\right)^{\frac{3+n}{\alpha}}}\tag{6.10}$$

When computing $M_0 = M(r_0)$, the self-encoding of the fundamental mass scale M_* is expected, that is, $M(r_0) = M_*$. This allows fixing α. Using the mass (4.23), it reads

$$M(r_0) = \underbrace{\frac{1}{n+2}\left(\frac{3+n}{2}\right)^{\frac{3+n}{\alpha}}}_{\overset{!}{=}1}\left(\frac{r_0}{L_*}\right)^{n+1} M_* = M_* \quad \text{with } \alpha = \alpha_0 \tag{6.11}$$

This gives the self-encoding value for the α parameter:

$$\alpha_0 = \frac{3+n}{\ln(2+n)} \ln \frac{3+n}{2}.\tag{6.12}$$

Henceforward, the self-regular black hole with $\alpha = \alpha_0$ will be refered to as the *self-encoding and self-regular* black hole.

6.1.3 Minimal length

The self-regular black hole solves the BH–particle duality problem, proposed in section 3.1. While there is qualitatively no difference for fixed α in different numbers of dimensions n to the holographic mass-length figure 5.3, one can display the effects of the choice of α. Figure 6.3 shows this exemplary in four dimensions. For increasing α, the outer horizon approaches the blue Schwarzschild radius $M\tilde{L}$. Again, the inner cauchy horizon $r_- < L_*$ is physically not relevant. Self-completeness of gravity is fulfilled.
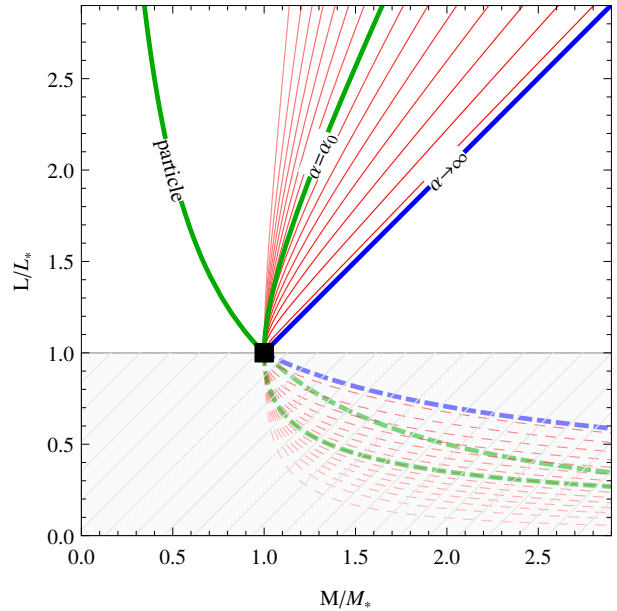

Figure 6.3: The self-regular black hole in $n = 0$ with different choices of α.

6.1.4 The regular core

According to the curvature considerations for general profiles $H(r)$ in section 4.3.2, the self-regular metric offers a non-diverging curvature at the origin. One can give an estimation for $R(0)$ based on the taylor expansions of the self-regular profile $h_\alpha(r)$ at $r = 0$:

$$h_\alpha(r) = (r/L_*)^{3+n} + \mathcal{O}\left((r/L_*)^{2(3+n)}\right), \; h'_\alpha(r) \approx (r/L_*)^{2+n}, \; h''_\alpha(r) \approx (r/L_*)^{1+n} \tag{6.13}$$

Inserting this into $R(r)$ for $H(r)$, equation (4.28b) gives a finite value for $R(0)$ as soon as $\alpha > 0$, c.f. figure 6.4. This is the reason for the name of the "self-regular metric". In general, black holes with no curvature singularity at the origin are called "regular" [?, 3].
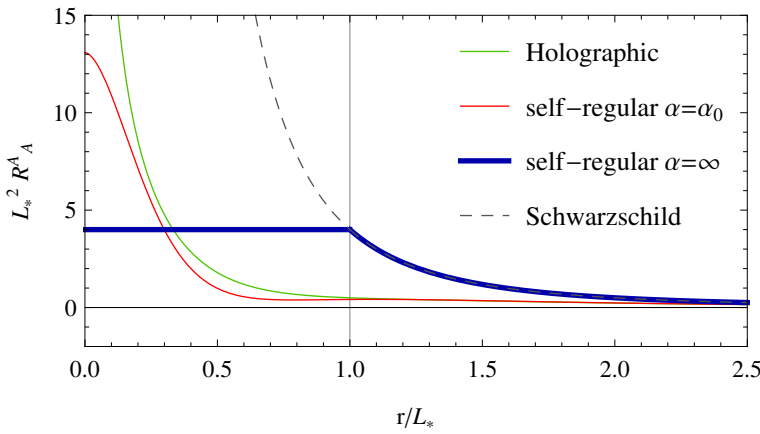
Figure 6.4: The curvature scalar R with $n = 0$ and $GM = 1$ for the holographic (red) and self-regular model (blue and black). While the curvature diverges for the holographic black hole, any value of the self-regular black hole archieves a finite value $R(0)$.

To learn more about the origin of the regularity, one can investigate the limit $\alpha \to \infty$, plotted in figure 6.5. At $\alpha \to \infty$, the two constituent metrics of the black hole clearly stand out. For simplicity, one should discuss the case in $n = 0$ and $M = M_*$. It is

$$\lim_{\alpha \to \infty} g_{00} = \begin{cases} 1 - 2GMr^2 & , r < L \\ 1 - \frac{2GM}{r} & , r > L. \end{cases} \tag{6.14}$$

Recognize the de Sitter space gravitational potential from section 2.2.3,

$$g_{00} = 1 - \frac{\Lambda}{3}r^2, \tag{2.31 revisited}$$

with positive cosmological constant $\Lambda = {}^{2}\!/\!{}_{3}\,GM$ and positive constant curvature $R = 4$ (cf. figure 6.4). This is called the de Sitter *core* since for physical meaningful theories, $r < \infty$.

What is the meaning of the cosmological vacuum solution like de Sitter in the context of quantum black holes? EFE relate the space-time encoding Einstein tensor $G_{\mu\nu}$ to the matter encoding Stress-energy tensor $T_{\mu\nu}$. In this thesis, the term *dual theory* is frequently encountered, which means shifting contributions between $G_{\mu\nu}$ and $T_{\mu\nu}$. In this context, the dual theory to de Sitter space-time as a solution of EFEs with cosmological constant and zero energy momentum tensor $T_{\mu\nu}$ is EFE without cosmological constant but shifted contributions inside the energy
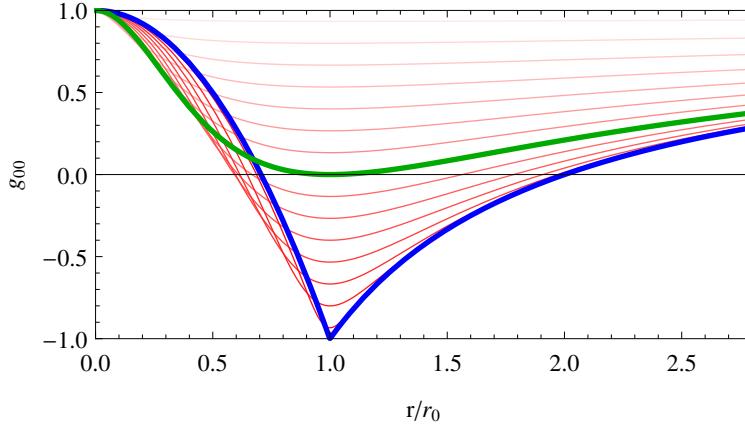
Figure 6.5: g_{00} for $M = 1$ and different choices of $\alpha \in \{0, 20\}$. The blue curve shows the limit $\alpha \to \infty$. Color saturation encodes the α scale. The special self-encoding choice $\alpha = \alpha_0$ is highlighted as green line (as in fig. 6.2). For details of the α choice, see Apx. C.

momentum tensor. This idea goes back to Dymnikova [25], but is also already discussed in text books as vacuum polarisation [50, p. 411]. In the quantum picture, this is interpreted as the *Quantum Vacuum* and is characterized by its *outward pressure* we were encountered with already at the time of the derivation of the black hole, equation (4.10) that defines the tangential pressure as

$$p = \rho + \frac{r}{n+2}\partial_r\rho > 0. \tag{6.15}$$

One can imagine this type of pressure as the one driving a Fermi gas and refer to it as degeneracy pressure. This kind of pressure also prevents the G-lump from collapsing in its own gravitational inward pressure. For a review about regular interiors of Schwarzschild-like black holes with $T_0^0 = T_1^1$, see also [26].

6.1.5   The Bardeen black hole

The Bardeen black hole (reviewed e.g. in [3]) was one of the first regular black hole solutions examined in literature. It is described by the gravitational potential

$$V(r) = \frac{2Mr^2}{(r^2 + e^2)^{3/2}} = 2\frac{M}{e}\frac{1}{(1 + e^2/r^2)^{3/2}}. \tag{6.16}$$

The Bardeen metric is a special case of the self-regular black hole with parameters

$$n = 0, \ \alpha = 2 \quad \text{and} \quad \tilde{r}_0 = 2^{1/\alpha}e, \tag{6.17}$$

where e is an electric charge (with the Coulomb constant $(4\pi\epsilon_0)^{-1} \equiv 1$). Apparently, the Bardeen black hole is not self-encoding, as $\alpha_0 \neq 2$.

The Bardeen black hole was found to cure the nacked singularities of the Reissner Nordström (RN) black hole. While this thesis does not cover charged black holes, the geometry of the RN black hole is tightly connected to the self-regular black hole. The RN metric describes a static nonrotating black hole with electrical charge e in $d = 4$ (with $G = 4\pi\epsilon_0 = c = 1$) and its gravitational potential is given by

$$V(r) = \frac{2M}{r} - \frac{e^2}{r^2} = 2\frac{M}{e}\frac{z-1}{z^2} \quad \text{with } z = r/e. \tag{6.18}$$

Figure 6.6 compares the RN black hole with the Bardeen black hole. In this figure, one sees that the hyper-extreme case $M < e$ is replaced by G-lumps, giving flat space for $M/e \to 0$. Therefore, the Bardeen black hole cures both the naked singularity as well as the repulsive gravity regime ($g_{00} > 1$).
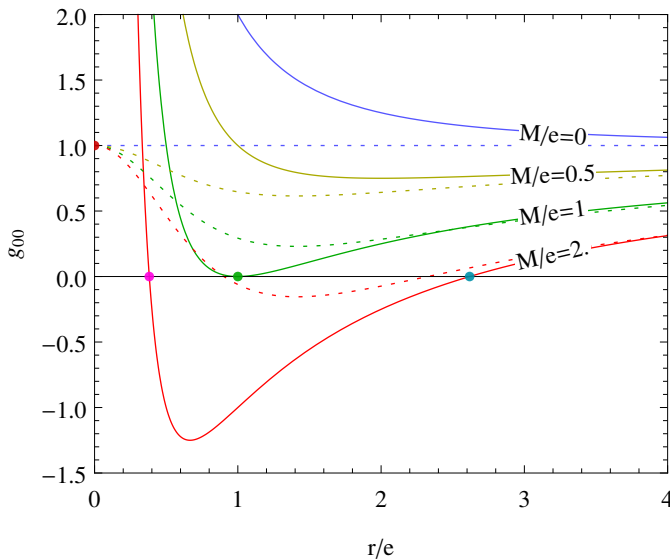

Figure 6.6: The Reissner-Nordström gravitational potential for different mass-charge ratios M/e, compared with the Bardeen solution for the same mass-charge ratios (dashed lines).

Further details and analogies are discussed in the next section about the conformal structure of the self-regular black hole.

6.1.6 Conformal Structure

It is often helpful to transform coordinates in a way that the global structure of space-time is mapped on a finite diagram. If this mapping is conformal (preserving angles locally) and two-dimensional, such diagrams are called *(Carter-)Penrose diagrams* [34, 50, 80].

The three Penrose diagrams that represent the three possible space-times presented in section 6.1.1 are displayed in figure 6.7. It is the diagram of a *regular black hole* which resembles the structure of the *Reissner Nordström* (RN) black hole.

One can discuss the Penrose diagrams shortly without going into detail how to find the maximally extended space-time that describes space-time everywhere, taking up the distinction of cases in section 6.1.1. Figure 6.7 contains three panels:

(a) The G-lump is probably the biggest archievement for the description of a charged black hole (RN), as it cures the naked singularity. In the context of phyics at the Planck scale, the G-lump is the candidate for representing particles that only interact gravitationally.

(b) The conformal diagram for the maximally extended black hole is periodic on the vertical axis on infinite extend ("isometric" regions). There are three classes of regions: the untrapped and asymptotically flat space time region **I**. The timelike region of trapped surfaces **II**, characterized by $r_- < r < r_+$, connects outer **I** and core **III** regions. The again space-like and untrapped region **III** is hyperbolic, as dominated by de Sitter behaviour. Note that in this space-time, it is possible to *wrap around the universe* by starting from **I**, travelling **II** and **III** and leaving the black hole near zone again over **II** to **I**, all inside a causal light-cone with $45°$ angles.

(c) The extremal situation also made the singularity accessible from outside by travelling from region **I** to **III**. This is cured with a regular origin.
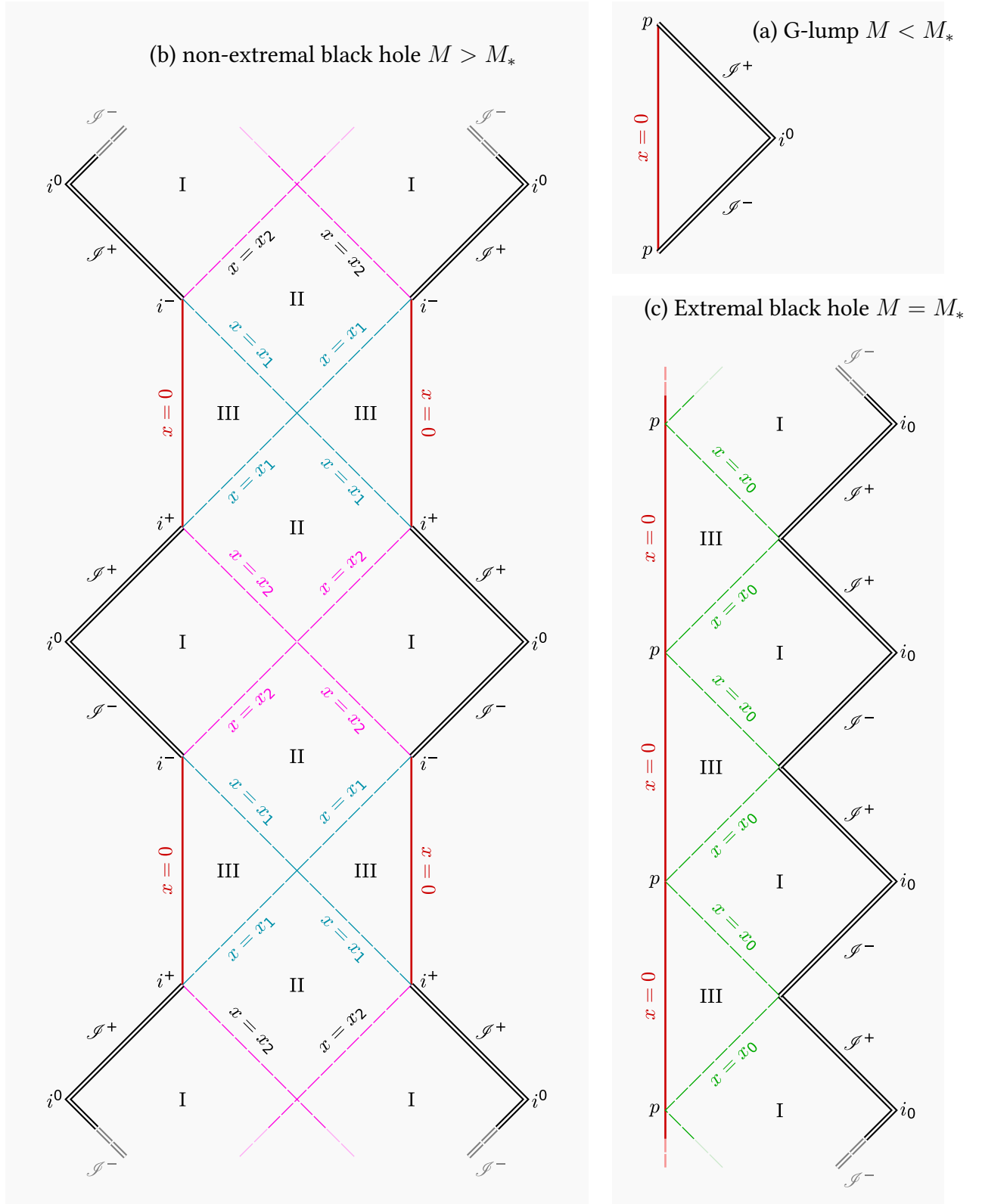
Figure 6.7: The penrose diagrams of the regular black holes, after [3,35,53]. x is a dimensionless coordinate $x = r/\tilde{r}_0$ and $x_2 = r_+/\tilde{r}_0$ is the outer horizon, while $x_1 = r_-/\tilde{r}_0$ is the inner horizon. $x_0 = r_1/\tilde{r}_0$ is the extremal horizon.

6.2 Thermodynamics

The thermodynamics of the self-regular black hole arise from the equations given in section 4.4. All quantities are derived by inserting the self-regular profile $h_\alpha(r)$ in the equations derived in section 4.4 for general $H(r)$. As in the sections before, a close comparison to the holographic black hole thermodynamics from section 5.2 will be made.

Note that in this section, r_H always represents the outer horizon $r_+ > L_*$ which is the physical meaningful horizon for calculating thermodynamics of the self-regular black hole.

n	0	1	2	3	4	5	6	7
r_C	1.970	1.460	1.340	1.290	1.260	1.250	1.230	1.220
$T(r_C)$	0.024	0.074	0.131	0.191	0.254	0.319	0.386	0.454

Table 6.2: Numerical values for the critical radii r_C and maximum temperature $T(r_C)$ for different extra dimensions n, according to eq. (6.21) and (6.19). Values are given for the self-encoding ($\alpha = \alpha_0$) self-regular black hole in nd Planck units (as multiples L_*).

6.2.1 Hawking Temperature

The Hawking Temperature of a self-regular black hole with radius r_H in n LXDs is determined by (4.38) to

$$T_H = \frac{1}{4\pi r_H}\left(1 + n - \frac{(L_*/r)^{4+n}}{1 + \frac{1}{\alpha}(L_*/r)^{3+n}}\right). \tag{6.19}$$

Below $r \lesssim 3L_*$, the temperature differs significantly from the Schwarzschild temperature. There is a maximum temperature at a critical radius r_C (indicated by the dots in fig. 6.8, numerical values are given in table 6.2), and for smaller radius the black hole cools down until it reaches zero temperature at r_0. The self-holographic metric produces therefore *cold* remnants.

6.2.2 Heat capacity

The heat capacity of a self-regular black hole with radius r_H in n LXDs is determined by 4.41 to

$$C = -\frac{4\pi r_H^{2+n}}{M_*^{n+2}}\frac{2^{-\frac{3+n}{\alpha}}\left(2 + r^{-\alpha}\right)^{\frac{3+n}{\alpha}+1}\left(r^{-\alpha} - (1+n)\right)}{r^{-2\alpha} - 2(1+n) + r^{-\alpha}(1 + 3\alpha + n\alpha - 1)}. \tag{6.20}$$

The critical radius can be determined by evaluating the extremal temperature condition (4.43):

$$r_C = 2^{\frac{1}{\alpha}}\left(\sqrt{(3+n)(3+n+\alpha(2+3\alpha+(\alpha-2)n))} + (n-1) - \alpha(3+n)\right)^{-\frac{1}{\alpha}}L_*. \tag{6.21}$$

The critical radius was used to rescale the abscissa in figure 6.9, so $(r_H - r_C)r_0$ is displayed. Thus it is easier to compare C for a different number of dimensions. Numerical values for r_C are given in table 6.2.
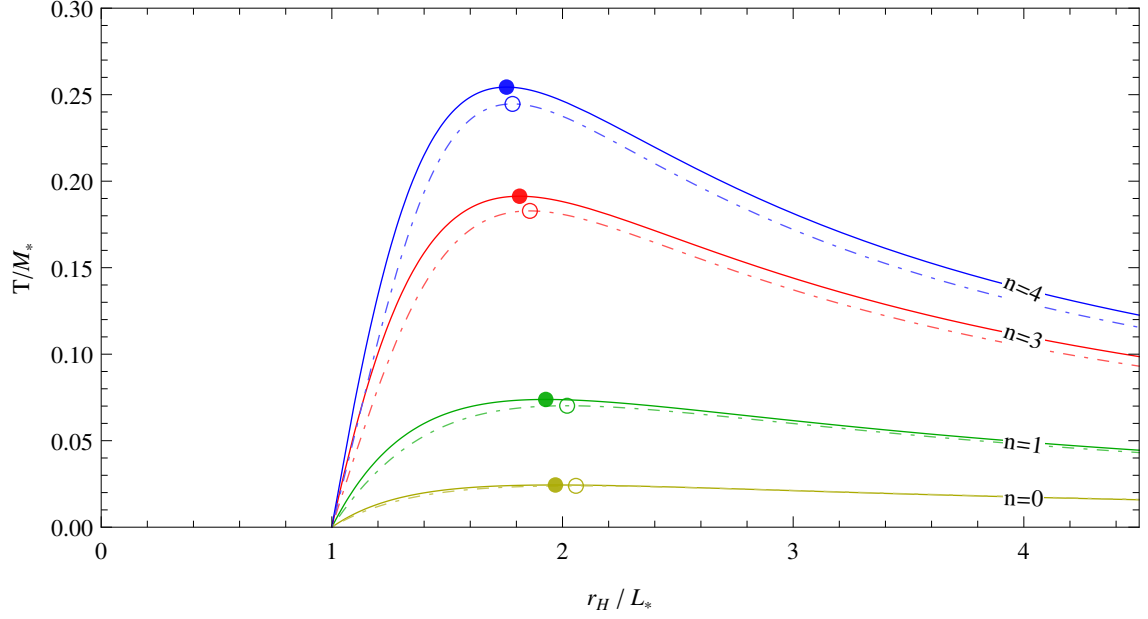
Figure 6.8: Temperature of the self-encoding self-regular black hole for different extra dimensions n (solid curves) in comparison to the holographic black hole temperatures (dot-dashed curve).
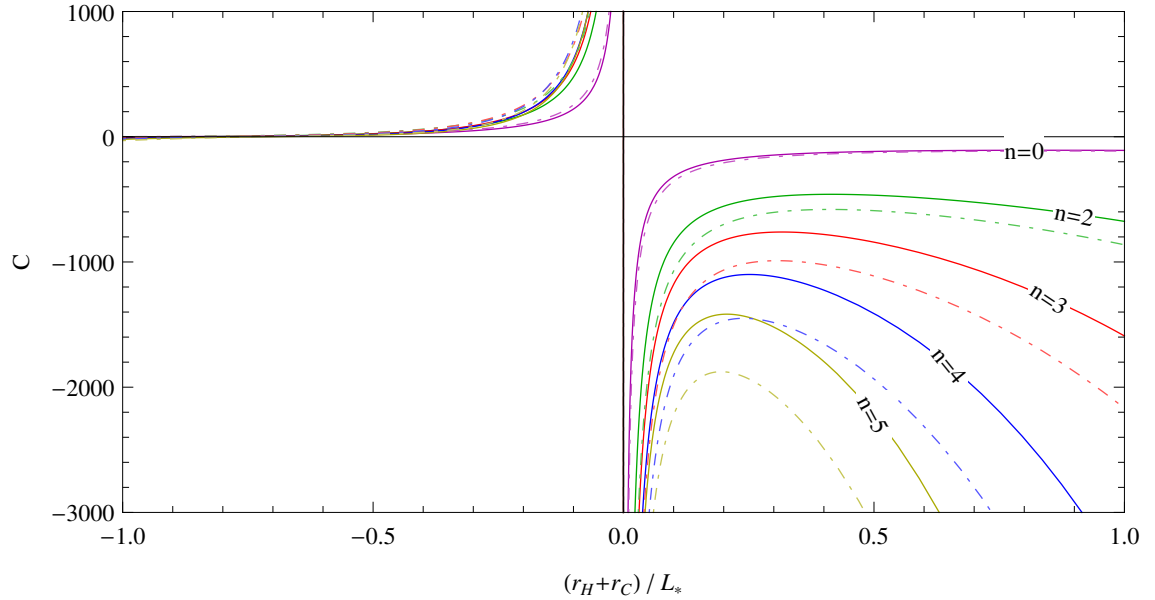

Figure 6.9: Heat capacity of the self-encoding ($\alpha = \alpha_0$), self-regular black hole (solid lines) compared with the holographic black holes (dot dashed lines), in different extra dimensions n. For each curve, the x-axis is shifted to the corresponding critical radius r_C (given by eq. 6.21) and scaled by the horizon length r_0 (given by eq. 6.7).

6.2.3 Entropy

The self-regular metric also does not possess a logarithmic entropy correction like the holographic metric (section 5.2.4), but a hypergeometrical one,

$$S = 4\pi M_*^{n+2}\left(r^2 + {}_2F_1\left(-\frac{2+n}{\alpha}, -\frac{3+n}{\alpha}, 1 - \frac{2+n}{\alpha}; -\frac{1}{2r^\alpha}\right)\right).\tag{6.22}$$

6.3 Modified field equations

For sef-encoding model, insert $h_\alpha(r)$ into the integral for $\mathcal{A}^{-2}$ as given in (4.56). For convenience, switch to a new dimensionless notation, $L' := L/2^{1/\alpha}$ and $z = r/L'$, $q = pL'$. With that notation, all poles will have radius 1. The integral reads:

$$\mathcal{A}^{-2}(q^2) = \underbrace{\frac{3+n}{(2\pi)^{3+n}}\frac{i}{2q}}_{f_0}\int_{-\infty}^{\infty}\mathrm{d}z\left[\underbrace{\frac{z^{1+n}}{(1+z^\alpha)^{\frac{3+n}{\alpha}+1}}\Theta(z)}_{f_+} + \underbrace{\frac{(-1)(-z)^{1+n}}{(1+(-z)^\alpha)^{\frac{3+n}{\alpha}+1}}\Theta(-z)}_{f_-}\right]e^{-iqz}.$$

$$\tag{6.23}$$

As with the holographic model, I chose $f_+(z) = -f_-(-z)$ and will therefore discuss only f_+. Its poles are given by

$$(1+z^\alpha)^{\frac{3+n}{\alpha}+1} = 0 \quad\Leftrightarrow\quad z = (-1)^{1/\alpha} = \exp\left\{\frac{i\pi + 2\pi ik}{\alpha}\right\} \quad \forall k \in \mathbb{N}_0.\tag{6.24}$$

For arbitrary choices of $\alpha \in \mathbb{R}_{\geq 0}$, as they were physically discussed in section **??**, the poles multiplicity in (6.24) is not an integral number. For the poles determination, this is not a problem, but for calculating residues it is.

Equation for nth order singularities of a function $g(z)$:

$$\operatorname*{Res}_{z\to a} g(z) = \frac{1}{(n+1)!}\lim_{z\to a}\frac{\partial^{n-1}}{\partial z^{n-1}}\left((z-a)^n g(z)\right)\tag{6.25}$$

Ways to solve that for $n := \frac{3+n}{\alpha}$: Fractional calculus...

> I will **remove** this section, as I was not able to compute the nonlocal operator for the self-regular black hole. **I am still free for hints how to solve the integral**.

Chapter 7

Discussion and Conclusion

In this thesis, two self-encoding black hole geometries with their extra dimensional generalization are presented. The discussion was preceded by an introducion about several topics, *i.e.* General Relativity, exact solutions, higher dimensional gravity scenarios and nonlocal gravity.

Considering the geometry of the two self-encoding black holes, the concept of the black hole *remnant* is introduced and the parallelism to the charged Reissner-Nordström black hole is showed. The de Sitter core as quantum vacuum source of outward pressure, stemming against the gravitational collapse, is introduced. For the self-encoding non-regular black hole, in this work refered to as the holographic black hole, the curvature singularity is hidden behind a horizon. This provides a fundamental minimal length in the sense that distances smaller than the remnant size L_* at energies bigger than the reduced Planck mass M_* can not be probed. As a result, the black hole center as well as sub-Planckian lenghts turn out to be permanently un-accessible. In addition, the trans-Planckian regime is dominated by neo-classical physics, described in terms of GR and/or QFTCS.

Regarding the thermodynamics of the self-encoding black holes, the remnants are found to be *cold* and *stable* in terms of a vanishing temperature and non-negative heat capacity. One finds logarithmic quantum corrections for the self-encoding holographic black hole in agreement with Loop Quantum Gravity and String Theory. The holographic picture leads to area quantization and finally gives rise to an emergent gravity interpretation that explains the gravity as an entropic force.

As a last step, the *dual* theory to the self-encoding black holes is constructed. By means of finding the nonlocal operator that, applied on a Dirac delta distribution, produces just the desired smeared distribution. This is a doorway of bringing the theory on a more fundamental level.

An appealing property of the geometries in this work is that one can do "paper and pen physics" without relying on numerical computations from the beginning. With the distinct feature of extra dimensions, this work pushes our tryings forward on the "route to testable predictions" [61].

Appendix A

Embedding diagrams

An embedding diagram displays a 4d spacetime as a three-dimensional diagram. For a spherical symmetric metric like the Schwarzschild metric, this is straightforward and the result is the well-known funnel-shaped surface. This surface is not gained by plotting the gravitational potential, but solving by the following steps.

The starting point is a (modified) Schwarzschild metric,

$$ds^2 = -(1 - V(r))dt^2 + (1 - V(r))^{-1}dr^2 + r^2 d\theta^2 + r^2 \sin^2(\theta)d\phi^2 \qquad \text{(2.28 revisited)}$$

with gravitational function $V(r)$. Now setting the constraints $dt = d\theta = 0$ and $\theta = \pi/2$ yields the two dimensional metric

$$ds^2 = \left(1 - V(r)\right)^{-1}dr^2 + r^2 d\phi^2 \qquad \text{(A.1)}$$

In order to display a plot in flat 3d cylindrical coordinates (r, ϕ, z), the metric (A.1) shall match

$$ds^2_{\text{flat}} = dz^2 + dr^2 + r^2 d\phi^2. \qquad \text{(A.2)}$$

The transformation function $z(r)$ is gained by requiring $ds \overset{!}{=} ds_{\text{flat}}$. One gets

$$dz^2 = \left(\frac{1}{1 - V(r)} - 1\right)dr^2. \qquad \text{(A.3)}$$

Now assuming that $z(r)$ is at least a C^2 function allows to compute $\frac{dz}{dr} = \sqrt{\frac{dz^2}{dr^2}}$ and therefore

$$\int_0^z dz' = \int_0^r dr' \sqrt{\frac{1}{1 - V(r')} - 1} \qquad \text{(A.4a)}$$

$$\Leftrightarrow z(r) = \int_0^r dr' \sqrt{\frac{V(r')}{1 - V(r')}} \qquad \text{(A.4b)}$$

The final integration (A.4b) determines the function $z(r)$ up to an integration constant. For example, for Newton's gravitational function $V(r) = 2GM/r$, the embedding diagram ordinate $z(r)$ is given by

$$z(r) = 2\sqrt{2GM}\sqrt{r - 2GM}. \tag{A.5}$$

It can therefore be plotted in the range $r \in (r_H, \infty)$. Below the Schwarzschild horizon $r_H = 2GM$, the ordinate z gets complex. Therefore the choice of coordinates (A.2) does not cover the complete space. In contrast, for the short scale modified black holes from chapters 5 and 6, $z(r)$ can be computed for $\mathbb{R}$.

Appendix B

Adjacent physical theories

This annexed chapter contains brief section about theories which did not make it in the main text.

B.1 Alternative extradimensional gravity approaches

In section 2.3, the large extra dimension scenario was proposed. While this term is usually used synonymously for the ADD model, another model with a large extra dimension was proposed at the same time, the Randall-Sundrum model. The historical predecessor for the extradimensional idea was Kaluza Klein theory, which proposes extra dimensions at the Planck scale (thus not *large*). A brief overview about these two theories is given at this point for completeness.

B.1.1 Kaluza Klein theory

Extending gravity to higher dimensions has a long history. First suggestions go back to Nord-ström and Kaluza [33] that proposed extra dimensions to unify gravity and electromagnetism. In 1921, they published a formulation today known as *Kaluza Klein theory* (KK theory), where Kaluza introduced one space-like extradimension and a scalar field ϕ (corresponding to a new particle). KK theory is capable of be producing both Einstein field equations and Maxwell equations at once. This works with any four dimensional metric $g_{\mu\nu}$ which is put in the five dimensional extension according to

$$ g_{MN} = \begin{bmatrix} g_{\mu\nu}e^{\phi/\sqrt{3}} + e^{-\phi^2}A_\mu A_\nu & e^{-\phi^2}A_\nu \\ e^{-\phi^2}A_\mu & e^{-\phi^2} \end{bmatrix}. \tag{B.1}$$

To clarify the notation: In equation (B.1), a block matrix notation was used to build up the 5×5 "matrix" g_{MN} by means of the 4×4 matrix $g_{\mu\nu}$. The fifth colum is spanned by four entries $e^{-\phi^2}A_0, \ldots, e^{-\phi^2}A_3$ and $e^{-\phi^2}$, while the fifth row is spanned by four entries $e^{-\phi^2}A_0, \ldots, e^{-\phi^2}A_3$ and $e^{-\phi^2}$.

The Einstein field equations (2.32) for $d = 5$ are a system of 25 equations that decouple to three independent field equations: The ordinary 4d Einstein equations with a modified (effec-

tive) 4d energy momentum tensor $\tilde{T}_{\mu\nu}$,

$$R_{\mu\nu} - \frac{1}{2}g_{\mu\nu}R = -8\pi G\tilde{T}_{\mu\nu}, \quad \text{with } \tilde{T}_{\mu\nu} = \frac{1}{4}e^{-\sqrt{3}\phi}F_{\mu\sigma}F_{\nu}^{\sigma} + \frac{\partial_{\mu}\phi\partial_{\nu}\phi}{2}. \tag{B.2}$$

The Maxwell's equations for the field A_{μ}, which read

$$\partial_{\mu}\partial^{\nu}A^{\mu} - \partial_{\mu}\partial^{\mu}A^{\nu} = 0. \tag{B.3}$$

And a relativistic equation for the scalar field ϕ:

$$\partial_{\mu}\partial^{\mu}\phi = \frac{-\sqrt{3}}{4}e^{-\sqrt{\phi}}F_{\mu\nu}F^{\mu\nu}. \tag{B.4}$$

Note that in this theory, the gravitational coupling constant G remained untouched ($G_d := G_4$). The fifth dimension is supposed to be compactified on *microscopic* scales (cf. figure 2.2).

B.1.2 Randall-Sundrum scenario

The Randall-Sundrum (RS) model was proposed in 1999 and also implies the existence of one large spatial extra dimension. In contrast to KK, the fifth dimension has constant negative curvature (AdS). The five dimensional line element is given by [41]

$$\mathrm{d}s^2 = e^{-2kr_c|y|}g_{\mu\nu}\mathrm{d}x^{\mu}\mathrm{d}x^{\nu} + r_c^2\mathrm{d}y \tag{B.5}$$

with $g_{\mu\nu}$ the 4d space time, $k \sim 1/L_*^2$ a parameter of the order of the fundamental Planck scale L_*, y the extra coordinate and r_c the compactification radius of the extra dimension. The RS metric can be derived like KK from the 5d EFEs with negative cosmological constant.

The RS (and KK) scenario are mentioned only for the sake of completeness and to show alternatives to the following ADD model which is the first one proposing *large* extra dimensions. Historically, the RS model is one year younger than the ADD model and also addresses the Hierarchy Problem by giving rise to an effective 4d Planck mass

$$M_{\mathrm{Pl}}^2 = (1 - e^{-2kr_c})M_*^3/k. \tag{B.6}$$

A review of the RS model in the context of micro black holes is given in [41].

B.2 Quantum Gravity black holes

This section gives a two-page overview about black holes in different Quantum Gravity approaches and their relationship to this work. It primarily follows the "six families of black holes" proposed in [62] and closes with *String theory*, which is certainly the most popular candidate for QG.

B.2.1 Non-local gravity black holes

These approaches are based on a nonlocal field theory by means of a nonlocal contribution to the geometric part of the Einstein field equations. In [53, 56], this is done with a derivation operator $\mathcal{F}^{-2}(\Box)$ acting on the Einstein tensor in a way that

$$\mathcal{F}^{-2}(\Box_{\mathbf{x}}/\Lambda_G^2)\left(R_{\mu\nu} - \frac{1}{2}g_{\mu\nu}R\right) = 8\pi G_N T_{\mu\nu}, \tag{B.7}$$

with a function $\mathcal{F}^{-2}$ of the generally covariant D'Alambert operator $\Box_{\mathbf{x}}$ acting on space-time vectors $\mathbf{x}$ which is scaled by the energy scale Λ_G of that theory, resulting in a dimensionless operator $\Box_{\mathbf{x}}/\Lambda_G^2$.

This goes back to nonlocal action modifications in gravity proposed by Barvinsky [9, 10]. Actually, such an approach is also used for curing divergences and formulating a pertubative super-renormalizable theory of Quantum Gravity [52].

Section 3.3 discusses nonlocal gravity in detail.

B.2.2 Noncommutative black holes

Noncommutative geometry (NCG) suggests a "fuzzy" spacetime by imposing a commutation relation on the quantum-mechanical position operator $\boldsymbol{x}^\mu$. In terms, this reads

$$[\boldsymbol{x}^\mu, \boldsymbol{x}^\nu] = i\theta^{\mu\nu} \tag{B.8}$$

with the matrix $\theta^{\mu\nu} > 0$ imposing the "discretization" of space-time. This idea leads to a space-time uncertainty and finally to a gaussian energy density approach as dirac replacement in the noncommutative inspired Schwarzschild solution,

$$\rho_\theta(r) = \frac{M}{(4\pi\theta)^{3/2}}e^{-r^2/4\theta}. \tag{B.9}$$

From this equation one can read that $r \sim \sqrt{\theta}$ corresponds to the length scale where noncommutative effects get strong. Funny enough, the metric produced by (B.9) possesses a regular core [59] like the one contrieved in chapter 6.

A in-depth review about Noncommutative black holes is [55]. The first extradimensional extension from Rizzo 2005 [68] actually determines the syntax and conventions in this thesis, considering extra dimensions.

B.2.3 Generalized Uncertainty Principle black holes

The generalized uncertainty principle (GUP) is perhaps the closest approach to create a "matching" picture 3.2. It can be formulated by suggesting as well a modified Compton scale as a generalized event horizon [15, 16] and states, in the simplest form

$$\Delta x \Delta p \geq \frac{\hbar}{2} \left(1 + \alpha x^2 + \beta p^2 \right).$$ (B.10)

Note that for $\alpha = \beta = 0$, this is the Heisenberg uncertainty principle. By means of a Hilbert space representation [42], for $\alpha = 0$ on can deduce a modified momentum integration measure where $p \sim \sqrt{\beta}$ plays the role of a high energy regulator, it is [42]

$$1 = \int_{-\infty}^{+\infty} \frac{\mathrm{d}p}{1 + \beta p^2} |p\rangle\langle p|.$$ (B.11)

This enables computing the Schwarzschild black hole in the GUP scenario. To do so, the GUP must be stated for vector operators. It follows that (B.11) basically holds for any number $m \in \mathbb{N}$ of spatial dimensions [38, 42]

$$1 = \int_{-\infty}^{+\infty} \frac{\mathrm{d}^m p}{1 + \beta p^2} |p\rangle\langle p| \quad \text{with } p = \|p\|.$$ (B.12)

The modified position space integration measure defines the nonlocal operator $\mathcal{A}^{-2}$ for the (quantum-modified) matter part of the GUP Schwarzschild black hole. It is introduced by means of the momentum representation of the Dirac delta distribution which constructs the Schwarzschild black hole:

$$\mathcal{T}_{\mu\nu} = -M\mathcal{A}^{-2}(\Box)\delta^3(\vec{r}) \overset{!}{=} -\frac{M}{(2\pi)^3} \int \frac{d^3p}{1 + \beta p^2} e^{i\vec{x}\cdot\vec{p}}$$ (B.13)

The nonlocal GUP operator in 4d spacetime therefore reads

$$\mathcal{A}(\Box) = (1 - \Box)^{1/2}$$ (B.14)

and fulfills $\mathcal{A} \to 1$ when $\Box \to 0$. The GUP effect (B.13) on a point-like mass distribution creates smeared energy densities [38, 39]

$$\rho_\beta(r) = \frac{M}{(2\pi)^3} \int \frac{\mathrm{d}^3p}{1 + \beta p^2} e^{i\boldsymbol{x}\cdot\boldsymbol{p}}.$$ (B.15)

Suprisingly, there also is a link to this thesis: Densities like (B.15) have been extended to higher dimensions [48], and the integration technique to solve nonlocal operators introduced in chapter 5.3 turned out to be successful to compute fourier transformations of GUP operators.

B.2.4 Loop Quantum black holes

Loop Quantum Gravity (LQG) is the competitor for String Theory that has the major advantage of preserving *background-independence*, as this is a major pillar of General Relativity. Therefore, LQG cannot be a pertubative expansion of Quantum GR by means of $\tilde{g}_{\mu\nu} = g_{\mu\nu} + h_{\mu\nu}$, since this would distinguish a special fixed classical background metric $g_{\mu\nu}$. The main principle in LQG is general covariance paired with quantum principles. Contemporary formulations use a graph as basic principe, a network (the "foam") with spacetime points as vertices and a discrete minimal length distance as edges and therefore refined the building word *loop* QG. According to Asthekar, "loops play no essential role in the theory now, for historical reasons, this name is widely used"; there lies the close relationship to lattice gauge theories, as closed loops resemble Wilson plaquettes [69, 79].

It is a long way from Loop Quantum Gravity to Loop Quantum black holes (LQBHs), and contemporary research about LQBHs is fairly less "descriptive" than the black holes modified by the principled mentioned before. See e.g. Modesto [51] who, amongst other things, finds out after a lengthy calculation that the Schwarzschild curvature singularity is no more present in LQBH.

Note that a particularly significant result is a fundamental explanation of the black hole logarithmic entropy correction that was predicted by Wilson. The logarithmic black hole entropy term is discussed section 5.2.4.

See the texts of Thiemann [77, 78] and Ashtekar [4] for an pedagogical review about LQG. For a pedagocigal introduction with focus on spin foams, see [65].

B.2.5 Asymptotically safe gravity black holes

Asymptotically safe gravity is built on a running coupling $G(k)$ which is the result of renormalization group treatments; general covariance is maintained with this approach. The basic idea is to make gravity an effective theory at momentum scale k and therefore be safely able to do physics with momenta $k' \gg k$.

Applied to black holes, $G(r)$ takes the place of Newton's contant in the Schwarzschild metric [28]. Thus it is possible to get black hole remnants that resemble the holographic profile we encounter in the next sections.

For introductory papers, see e.g. Reuter [14, 67] and the review [63] by the same author.

B.2.6 Black holes in String Theory

String Theory is the theory of quantum-mechanical relativistic one-dimensional "vibring strings" (like waves), and according to the popular picture, different excitation energies correspond to different point-like particles postulated by the standard model of particle physics. The term "String Theory" is usually used similary to superString Theory, that is, String Theory including supersymmetry (SUSY, a symmetry that relates each boson to its superpartner, the fermion, and vice versa). The existence of extra dimensions, as introduced in section ??, is actually predicted by String Theory. String Theory is most criticised because its large number of solutions and

especially because the dependence on a background spacetime which explicitly breaks general covariance. On the other hand, String Theory only needs one fundamental minimal length scale ℓ_0 and may be treated pertubatively.

Considering black holes, String Theory is especially able to make statements about extremal black hole situations, as we will encounter in the next chapter. The enticing recast of an extremal black hole as a *particle* is unique to String Theory. String Theory also predicts a logarithmic entropy correction as LQG does.

String Theory is handled e.g. in the book of Kiefer [44], black holes in String Theory are discussed in [49]. Probably a good closing overview over all approaches gives the review article [43].

Appendix C

Distribution profiles at a glance

The choice $H(r) = h(r)$ is called *holographic model* and the choice $H(r) = h_\alpha(r)$ is called *self-encoding model* in this thesis. They are distinguished by the index α on the h. Of course, one could also introduce a symbol like $h_n(r)$ to account the fact that the models scale with n, so eventually the symbol is arbitrary.

In this appendix, the full forms in the dimensionless notation $z = r/L$ are given. Since the models $H(r)$ represent a smeared Theta function, they are dimensionless, and the identity $H(r) = H(r/L)$ shall represent the fact that $H(r)$ is actually a function of r/L and can be expressed in the dimensionless coordinate $H(z)$:

$$h(r) = \frac{r^{2+n}}{r^{2+n} + L^{2+n}} \qquad\qquad h(z) = \frac{1}{1 + \left(\frac{1}{z}\right)^{2+n}} = \frac{z^{2+n}}{z^{2+n} + 1} \qquad (C.1)$$

$$h_\alpha(r) = \frac{r^{3+n}}{\left(r^\alpha + L^\alpha/2\right)^{\frac{3+n}{\alpha}}} \qquad\qquad h_\alpha(z) = \frac{1}{\left(1 + \left(\frac{1}{z}\right)^\alpha /2\right)^{\frac{3+n}{\alpha}}} \qquad (C.2)$$

The derivatives appear in many places and are therefore denoted here. Since $\frac{\mathrm{d}f}{\mathrm{d}r} = \frac{\mathrm{d}f}{\mathrm{d}z}\frac{\mathrm{d}z}{\mathrm{d}r} = \frac{1}{L}\frac{\mathrm{d}f}{\mathrm{d}z}$, one can always substitute $H'(r) = H'(z)/L$. It is important to remember this fact: $H'(r) \neq H'(z)$. In the end, this is because the Lagrange differential operation notation H' is not unique.

$$h'(r) = \frac{(2+n)\,r^{1+n}L^{2+n}}{(r^{2+n} + L^{2+n})^2} \qquad h'(z) = \frac{(2+n)\left(\frac{1}{z}\right)^{3+n}}{\left(1 + \left(\frac{1}{z}\right)^{2+n}\right)^2} = (2+n)\frac{h^2(z)}{z^{3+n}} \qquad (C.3)$$

$$h_\alpha'(r) = \frac{(3+n)L^\alpha r^{n+2}\left(\frac{L^\alpha}{2} + r^\alpha\right)^{-\frac{n+3}{\alpha}}}{L^\alpha + 2r^\alpha} \qquad h_\alpha'(z) = \frac{\frac{3+n}{2}\left(\frac{1}{z}\right)^{\alpha+1}}{\left(1 + \left(\frac{1}{z}\right)^\alpha /2\right)^{\frac{3+n}{\alpha}+1}} \qquad (C.4)$$

The dimensional analysis allows to resemble the powers of L in any expression written in terms of z. For example, the quantity $H'(z)/z$ has the unit $1/L^2$ and therefore $H'(z)/(zL^2) = H'(r)/(rL)$.
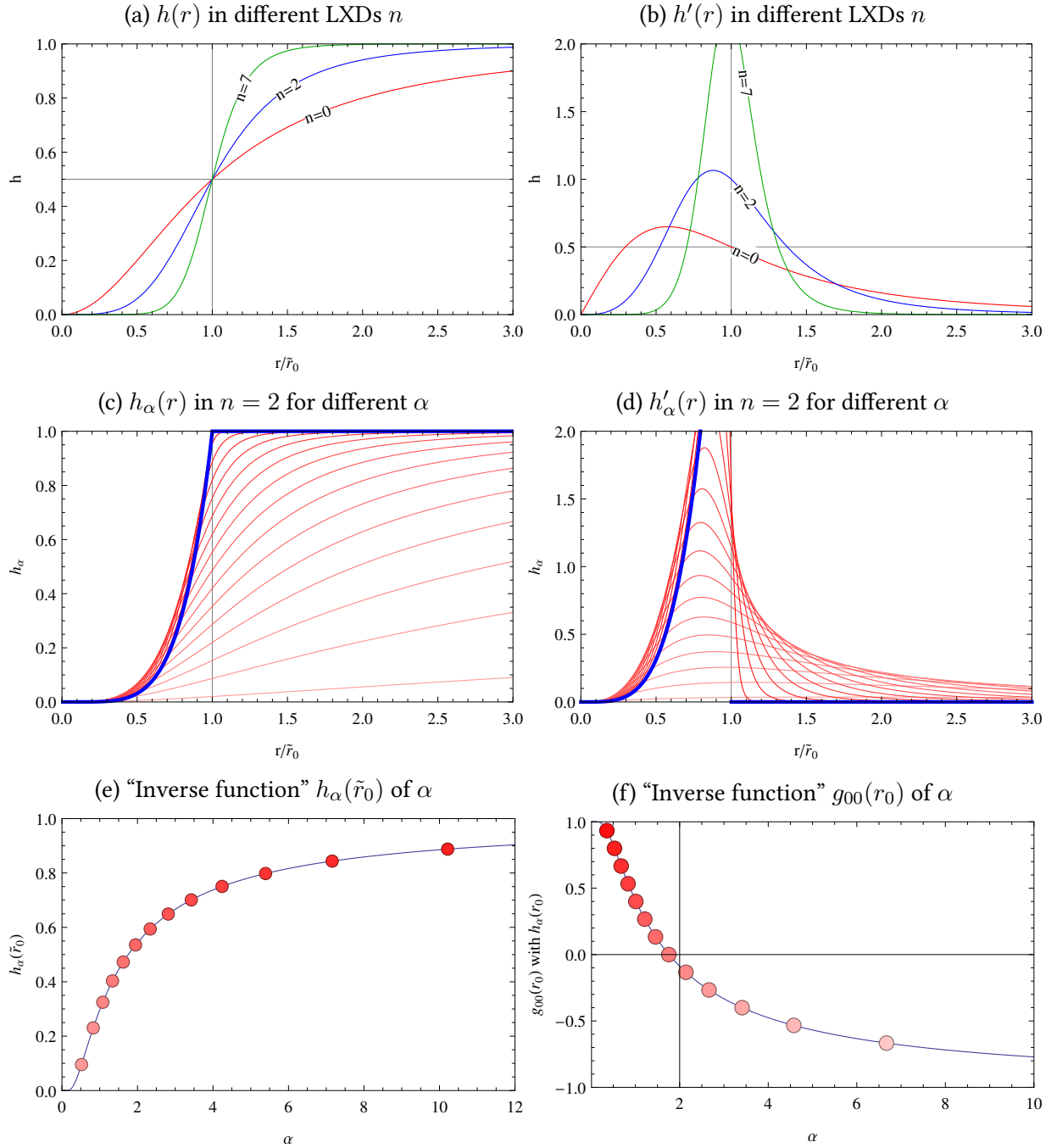
Figure C.1: Plots of the profiles $h(r)$ and $h_\alpha(r)$ as well as their derivatives. The panels C.1e and C.1f show the choices of α that result in uniformly spaced curves when choosing a set of α values for plotting $h_\alpha(\tilde{r}_0)$ or $g_{00}(r_0)$.

Appendix D

n-spheres

n-sphere is the common name for spheres in higher dimensions. To avoid confusion with the rest of the thesis, in this appendix instead of n, the letter d will be used to indicate the number of dimensions under discussion.

To point the emergence of d-spheres in this thesis, the d-dimensional volume integral in eucledian space is evaluated in spherical coordinates $k_i = (r, \phi, \theta_1, \ldots, \theta_{d-2})$, following Wagner [79]:

$$\int d^d r = \int_0^\infty dr\; r^{d-1} \underbrace{\int_0^{2\pi} d\phi \prod_{j=1}^{d-2} \int_0^\pi d\theta_j\; \sin^j(\theta_j)}_{=a_{n-2},\, \text{since } (n-2)-\text{Surface}} = \frac{2\pi^{d/2}}{\Gamma\left(\frac{d}{2}\right)} \int_0^r dr\; r^{d-1} := \Omega_{d-1} r^d := V_d$$

(D.1)

where $\Gamma(x)$ is the Euler Gamma function, either given by the integral

$$\Gamma(x) = \int_0^\infty dt\; t^{x-1} e^{-t} \quad; \text{incomplete version:} \quad \gamma(s,x) = \int_0^x t^{s-1} e^t dt.$$

(D.2)

or as the extension of the factorial function $x!$ to $\mathbb{C}$, using the recursion relations

$$\Gamma(x) = (x-1)!$$
$$\Gamma(x+1) = x\Gamma(x).$$

(D.3)

A notable special value of the Gamma function is $\Gamma(1/2) = \sqrt{\pi}$. The integration of the $d-2$ angles is done with the help of the identities

$$B(x,y) = \int_0^1 dt\; t^{x-1}(1-t)^{y-1} = \frac{\Gamma(x)\Gamma(y)}{\Gamma(x+y)}$$

(D.4)

$$\int_0^\pi \theta_j\; \sin^j(\theta_j) = \frac{\sqrt{\pi}\, \Gamma\left(\frac{j+1}{2}\right)}{\Gamma\left(\frac{j+2}{2}\right)}.$$

(D.5)

The d-sphere S_d with radius r is defined in an d-dimensional manifold (in this work always the eucledian space) by the set

$$S_d = \{\; \|\boldsymbol{x}\| = r \;\mid\; \boldsymbol{x} \in \mathbb{R} \;\}$$

(D.6)

d	0	1	2	3	4	5	6
$\mathcal{V}_d$	0	2	π	$\frac{4}{3}\pi$	$\frac{1}{2}\pi^2$	$\frac{8}{15}\pi^2$	$\frac{1}{6}\pi^3$
Ω_d	0	2	2π	4π	$2\pi^2$	$\frac{8}{3}\pi^2$	π^3

Table D.1: Volume and surface area prefactors of d-Spheres. The numerical factors can be computed by evaluating eq. (D.7).

The d-sphere is important for integration in spherical coordinates without angular dependence (isotropy or spherical symmetry). Integrating out the angles in a d-dimensional volume integration results in the surface area of the $(d-1)$-sphere, embedded in the d-dimensional space. The value of the d-ball and its corresponding $(d-1)$-sphere can be given as a closed formm expression

$$V_d = r^d \frac{\pi^{n/2}}{\Gamma\left(\frac{d}{2}+1\right)} \quad \text{and} \quad A_{(d-1)} = \frac{\mathrm{d}V_d}{\mathrm{d}r} = \frac{\pi^{d/2}}{\Gamma\left(\frac{d}{2}+1\right)} d\, r^{d-1} = 2\frac{\pi^{d/2}}{\Gamma\left(\frac{d}{2}\right)} r^{d-1} \tag{D.7}$$

There also exists recursion relations for determining V_d and A_d by their lower dimensional values:

$$\text{Prefactors:} \quad \begin{array}{l} V_d = v_d r^n \\ A_d = a_d r^n \end{array} \quad \text{Recursion:} \quad \begin{array}{l} v_0 = 1, \quad v_{d+1} = a_d/(d+1) \\ a_0 = 2, \quad a_{d+1} = 2\pi v_d \end{array} \tag{D.8}$$

In the main text, the r-dependence of the spheres is typically split up in favour to dimensionless constants Ω. by

$$A_d := \Omega_d r^d \quad \text{and} \quad V_d = \mathcal{V}_d r^d. \tag{D.9}$$

For numerical values of Ω_d and V_d, see table D.1.

As an example, consider the three dimensional space $d = 3$. Integrations in 3 dimensions can be performed in spherical coordinates, making use of a 3 ball with radius r. Acccording to (D.9), the surface element of the 2-sphere then is $2\pi r^2$.

Appendix E

Details of the spherical symmetric d-dimensional FT

This appendix ties up with section 4.5.1, where the d-dimensional Fourier Transformation is reduced to a one dimensional one for functions $V(\vec{x})$ which fulfill $V(\vec{x}) = V(|\vec{x}|)$.

The 3d case is actually well known in literature and is given here just for completeness and simpler readability in section E.1. In section E.2, we discuss about entire function aspects of $\Theta(z)$.

E.1   Review of the 3d Fourier transformation

We start the derivation in $d = 3$ total spatial dimensions ($\vec{r} \in \mathbb{R}^3$). Let $V = V(r)$ with $r = |\vec{r}|$ be a radially symmetric potential. Then it's fourier transformation is given by:

$$\hat{V}(p) = \frac{1}{(2\pi)^3} \int \mathrm{d}^3 r \; e^{-i\vec{r}\cdot\vec{p}} \, V(r) \tag{E.1a}$$

$$= \frac{1}{(2\pi)^3} \int_0^\infty \mathrm{d}r \int_0^\pi r^2 \sin\theta \, \mathrm{d}\theta \int_0^{2\pi} \mathrm{d}\varphi \, V(r) \, e^{-ipr\cos\theta_2} \tag{E.1b}$$

In line (E.1b) we already wrote the scalar product with an inner angle θ_2. We now substitute the radial angle θ (the θ which is part of $\vec{r} = (r, \theta, \varphi)$) integration with a $\cos\theta$ integration. This can be done because $\frac{\mathrm{d}\cos\theta}{\mathrm{d}\theta} = -\sin\theta$ and so $\int_0^\pi \sin\theta \mathrm{d}\theta = -\int_{-1}^1 \mathrm{d}\cos\theta := \int_{-1}^1 \mathrm{d}x$. We now identify $\cos\theta := x$ with $\cos\theta_1$ because they share the same domain, actually $\theta, \theta_1 \in \{0, \pi\}$ (this is a standard procedure, one can also argue with rotating the coordinate systems). Integrating out $\int_0^{2\pi} \mathrm{d}\varphi = 2\pi$ in mind, we continue with:

$$= \frac{2\pi}{(2\pi)^3} \int_{-1}^{+1} \mathrm{d}x \int_0^\infty \mathrm{d}r \, r^2 \, e^{-irpx} V(r) \tag{E.1c}$$

$$= \frac{1}{(2\pi)^2} \int_0^\infty r^2 \, \mathrm{d}r \, V(r) \left[\frac{1}{-ipr} e^{-iprx} \right]_{-1}^{+1} \tag{E.1d}$$

$$= \frac{1}{(2\pi)^2} \frac{i}{p} \int_0^\infty r \, \mathrm{d}r \, V(r) \left\{ e^{-ipr} - e^{+ipr} \right\} \tag{E.1e}$$

$$= \frac{1}{(2\pi)^2} \frac{i}{p} \left\{ \int_0^\infty r \, \mathrm{d}r \, V(r) e^{-ipr} - \int_0^\infty r \, \mathrm{d}r \, V(r) e^{+ipr} \right\} \tag{E.1f}$$

In line (E.1f), we splitted the integral, and we now make two recastings: At first, switching the integral borders, which inserts one minus: $\int_a^b = - \int_b^a$ in (E.1g). Second, another substitution of the integration parameter $r := -r'$ and therefore $\mathrm{d}r = -\mathrm{d}r'$. The two minus signs kill each other in (E.1h), so $r \mathrm{d}r = r' \mathrm{d}r'$. After substitution, we will call r' again r, which is totally valid.

$$= \frac{1}{(2\pi)^2} \frac{i}{p} \left\{ \int_0^\infty r \, \mathrm{d}r \, V(r) e^{-ipr} + \int_\infty^0 r \, \mathrm{d}r \, V(r) e^{+ipr} \right\} \tag{E.1g}$$

$$= \frac{1}{(2\pi)^2} \frac{i}{p} \left\{ \int_0^\infty r \, \mathrm{d}r \, V(r) e^{-ipr} + \int_{-\infty}^0 r' \, \mathrm{d}r' \, V(-r') e^{-ipr'} \right\} \tag{E.1h}$$

$$= \frac{1}{(2\pi)^2} \frac{i}{p} \int_{-\infty}^\infty r \, \mathrm{d}r \, e^{-ipr} \left\{ V(r)\Theta(r) + V(-r)\Theta(-r) \right\} \tag{E.1i}$$

$$= \frac{1}{(2\pi)^2} \frac{i}{p} \int_{-\infty}^\infty \mathrm{d}r \, \left\{ rV(|r|) \right\} \, e^{-ipr} \tag{E.1j}$$

$$= \frac{1}{2\pi} \int_{-\infty}^\infty \mathrm{d}r \, v(r) \, e^{-ipr} \tag{E.1k}$$

We derived an effective one dimensional fourier transformation of the new function ("kernel")

$$v(r) := \frac{i}{2\pi} \frac{r}{p} V(|r|) \tag{E.2}$$

For shortness, my usual definition of $v(r)$ differs from the one given in (E.2) in terms of non-complex prefactors. For the discussion, equation (E.1i) is the best starting point, as it contains the Heaviside step functions $\Theta(\pm r)$.

The most important issue with this calculation is the question of holomorphy. In these lines, $\Theta(z)$ must be understood as

$$\Theta(z) = \Theta(\mathrm{Re}\, z). \tag{E.3}$$

This definition is intrinsically nonholomorphic. On the other hand, as soon as Θ is implemented as a smeared distribution, like continuing the integral of a Dirac delta approximation like the Cauchy distribution, this might be cured. Anyway, there is no ordering relation $\leq_\mathbb{C}$ in the complex numbers, so the theta is likely to behave differently on the complex plane. In three dimensions this approach is well known and works.

Whats about the real and complex parts of this fourier transformation? By construction, $V(|r|)$ is an even function (definition: $f(x) = f(-x)$ is even, $-f(x) = f(-x)$ is odd). Therefore $r \, V(|r|)$ is an odd function. By Eulers formula $e^{i\varphi} = \cos\varphi + i\sin\varphi$, one quickly finds that the Fourier Transform of an even function includes only (also even) $\cos$ terms and the complex part vanishes, while the FT of an odd function only contains $\sin$ terms and the real part vanishes.

The integral in (E.1j) is therefore ony complex, $\int \mathrm{d}r \; rV(|r|)e^{-ipr} \in \mathbb{C} \setminus \mathbb{R}$. But the prefactor makes the final result in (E.1j) completely real again. This can help as a quick check wether the computed result of the integral is correct.

E.2 Analytic continuation of the Heaviside step function

The step function $\Theta : \mathbb{R} \to \mathbb{R}$, as given in

$$\Theta(x) = \begin{cases} 0 & \text{when} & x < 0 \\ 1 & & x \geq 0 \end{cases}, \qquad \text{(4.18 revisited)}$$

obviously cannot be simply extended on the complex plane. Anyway, in section 4.5.1, we already formulated *weaker constraints* instead of $\Theta(z) = \Theta(Re\,z)$, namely

- Step function behaviour only on the poles which are laid on the unit ring $|z| = 1$

- Approximate step function behaviour.

- Freedom of poles for $\Theta(z)$, so it does not contribute with poles to $v(z)$.

Freedom of poles means, we cannot have a rational function, so all theta approximations introduced in this thesis leave the stage. Such a theta approximation may be given by

$$\Theta_k(z) = \frac{1}{1 + \exp(-2kz)}, \quad \text{and} \;\; \Theta(x) = \lim_{k \to \infty} \Theta_k(x) \;\; \text{for}\; x \in \mathbb{R} \qquad \text{(E.4)}$$

Inserting $z = e^{i\phi}$ gives...

okay this is not true.

Appendix F

General Relativity formulary

In this section, I use greek lowercase letters ($\alpha\beta \ldots \mu\nu \ldots$) for all indices which may in general be running in 4 or $4 + n$ dimensions. Einstein sum convention is used, but summation symbols are given when special emphazise on the summation is intended.

1. Christoffels for Tensor

$$\Gamma^k_{ij} = \frac{g^{kl}}{2} \left(\partial_i g_{jl} + \partial_j g_{il} - \partial_l g_{ij} \right) \tag{F.1}$$

2. Christoffel symmetry:

$$\Gamma^\alpha_{\beta\gamma} = \Gamma^\alpha_{\gamma\beta} \tag{F.2}$$

3. Symmetric and antisymmetric part of tensors, exemplary for a $(0, 2)$ tensor:

$$\text{symmetric part} \quad T_{(ab)} = \frac{1}{2}(T_{ab} + T_{ba}) \tag{F.3}$$

$$\text{antisymmetric part} \quad T_{[ab]} = \frac{1}{2}(T_{ab} - T_{ba}) \tag{F.4}$$

The general definition for the (anti)symmetric part of a tensor is the sum over all permutations, e.g. using the Levi-Civita symbol, see e.g. [80].

4. Covariant derivative for covariant vector t:

$$\nabla_a t^\nu = \partial_a t^\nu + \Gamma^\nu_{ac} t^c \tag{F.5}$$

5. Covariant derivative for a $(2, 0)$ tensor A:

$$\nabla_\lambda A^{\mu\nu} = \sum_\delta \partial_\lambda A^{\mu\nu} + \Gamma^\mu_{\delta\lambda} A^{\delta\mu} + \Gamma^\nu_{\delta\lambda} A^{\mu\delta} \tag{F.6}$$

6. Covariant derivative for a $(1, 1)$ tensor A:

$$\nabla_a T^b_c = \partial_a T^b_c + \Gamma^b_{ad} T^d_c - \Gamma^d_{ac} T^a_d \tag{F.7}$$

7. Energy conservation equation with sums

$$\sum_{\mu} \nabla_{\mu} T^{\mu\nu} = \sum_{\mu,\rho} \partial_{\mu} T^{\mu\nu} + \Gamma^{\mu}_{\rho\mu} T^{\rho\mu} + \Gamma^{\nu}_{\rho\mu} T^{\mu\rho} \tag{F.8}$$

8. Lowering and raising indices

$$g_{\beta\gamma} A^{\alpha\gamma} = A^{\alpha}_{\beta} \tag{F.9}$$

9. Metric identity

$$g^{\alpha\beta} g_{\beta\gamma} = g_{\gamma\beta} g^{\beta\alpha} = \delta^{\alpha}_{\gamma} \tag{F.10}$$

10. Riemann Tensor

$$R^{\delta}_{\sigma\mu\nu} = \partial_{\mu}\Gamma^{\delta}_{\nu\sigma} - \partial_{\nu}\Gamma^{\delta}_{\mu\sigma} + \Gamma^{\delta}_{\mu\gamma}\Gamma^{\gamma}_{\nu\sigma} - \Gamma^{\delta}_{\nu\gamma}\Gamma^{\gamma}_{\mu\sigma} \tag{F.11}$$

11. Ricci tensor (sign is convention)

$$R_{\mu\nu} = \pm R^{\gamma}_{\mu\gamma\nu} \tag{F.12}$$

12. $(1,1)$-form of Ricci tensor

$$R^{a}_{b} = g^{ca} R_{cb} \tag{F.13}$$

F.1   Christoffel symbols for spherical symmetric spacetimes

The Christoffel symbols for a general d-dimensional spherical symmetric static metric, the parametrization $g_{tt} = -(1 - A(r))$, $g_{rr} = 1/(1 - A(r))$ and the alternative parametrization $g_{tt} = -e^{\nu(r)}$, $g_{rr} = g^{-\nu(r)}$. The index naming convention follows section 3. f' indicates the derivation $\partial_r f(r)$.

$$\Gamma^{t}_{tr} = \Gamma^{t}_{rt} = \frac{1}{2} g^{tt} \partial_r g_{tt} \quad = \frac{1}{2} \frac{A'}{A-1} \qquad = \frac{\nu'}{2} \tag{F.14}$$

$$\Gamma^{r}_{tt} = \frac{1}{2} g^{rr} \partial_r g_{tt} \quad = \frac{1}{2}(A-1)A' \qquad = \frac{1}{2} e^{2\nu} \nu' \tag{F.15}$$

$$\Gamma^{r}_{rr} = \frac{1}{2} g^{rr} \partial_r g_{rr} \quad = \frac{1}{2} \frac{A'}{1-A} \qquad = -\frac{1}{2} \nu' \tag{F.16}$$

$$\Gamma^{i}_{r}i = \Gamma^{i}_{ir} = \frac{1}{2} g^{ii} \partial_r g_{ii} \quad = \frac{1}{r} \tag{F.17}$$

$$\Gamma^{i}_{\phi\phi} = \frac{1}{2} g^{ii} \partial_i g_{ii} \quad = -\cos(\theta_i)\sin(\theta_i) \tag{F.18}$$

$$\Gamma^{\phi}_{r\phi} = \Gamma^{\phi}_{\phi r} = \frac{1}{2} g^{\phi\phi} \partial_r g_{\phi\phi} = \frac{1}{r} \tag{F.19}$$

$$\Gamma^{\phi}_{\phi i} = \Gamma^{\phi}_{i\phi} = \frac{1}{2} g^{\phi\phi} \partial_i g_{\phi\phi} = \frac{1}{\tan(\theta_i)} \tag{F.20}$$

List of figures and tables

This list helps to find and identify figures; they are labeled by their size and type (illustration or plots) and marked if they were not self-made.

List of figures

List of tables

Bibliography

[1] Adler, Ronald J., "Six easy roads to the Planck scale", *Am.J.Phys.*, **78**, 925–932 (2010). [DOI], [arXiv:1001.1205 [gr-qc]]. (Not cited.)

[2] Adler, Ronald J., Chen, Pisin and Santiago, David I., "The Generalized uncertainty principle and black hole remnants", *Gen.Rel.Grav.*, **33**, 2101–2108 (2001). [DOI], [arXiv:gr-qc/0106080 [gr-qc]]. (Cited on page 27.)

[3] Ansoldi, Stefano, "Spherical black holes with regular center: A Review of existing models including a recent realization with Gaussian sources", *arXiv*, e-print, (2008). [arXiv:0802.0330 [gr-qc]]. (Cited on pages 35, 58, 61, 63, 65, and 88.)

[4] Ashtekar, Abhay and Lewandowski, Jerzy, "Background independent quantum gravity: A Status report", *Class.Quant.Grav.*, **21**, R53 (2004). [DOI], [arXiv:gr-qc/0404018 [gr-qc]]. (Cited on page 76.)

[5] Aurilia, A. and spallucci, E., "Planck's uncertainty principle and the saturation of Lorentz boosts by Planckian black holes", *arXiv*, e-print, (2013). [arXiv:1309.7186 [gr-qc]]. (Not cited.)

[6] Aurilia, Antonio and Spallucci, Euro, "Why the length of a quantum string cannot be Lorentz contracted", *Adv.High Energy Phys.*, **2013**, 531696 (2013). [DOI], [arXiv:1309.7741 [hep-th]]. (Cited on page 24.)

[7] Balasin, Herbert and Nachbagauer, Herbert, "The energy-momentum tensor of a black hole, or what curves the Schwarzschild geometry?", *Class.Quant.Grav.*, **10**, 2271 (1993). [DOI], [arXiv:gr-qc/9305009 [gr-qc]]. (Cited on page 16.)

[8] Bardeen, James Maxwell, "Non-singular general-relativistic gravitational collapse. Proceedings of the International Conference GR5, Tbilisi, USSR", conference, (1968). (Cited on page 57.)

[9] Barvinsky, A.O., "Nonlocal action for long distance modifications of gravity theory", *Phys.Lett.*, **B572**, 109–116 (2003). [DOI], [arXiv:hep-th/0304229 [hep-th]]. (Cited on page 74.)

[10] Barvinsky, A.O., "Aspects of Nonlocality in Quantum Field Theory, Quantum Gravity and Cosmology", *arXiv*, e-print, (2014). [arXiv:1408.6112 [hep-th]]. (Cited on page 74.)

[11] Bekenstein, Jacob D. and Kamajian, Alfred T., "Information in the Holographic Universe", *Scientific American*, (December 17, 2005), p. ... (Cited on pages 53 and 88.)

[12] Bleicher, Marcus and Nicolini, Piero, "Large Extra Dimensions and Small Black Holes at the LHC", *J.Phys.Conf.Ser.*, **237**, 012008 (2010). [DOI], [arXiv:1001.2211 [hep-ph]]. (Cited on page 20.)

[13] Bleicher, Marcus and Nicolini, Piero, "Mini-review on mini-black holes from the mini-Big Bang", *Astron. Nachr.*, **335**, 605–611 (2014). [DOI], [arXiv:1403.0944 [hep-th]]. (Cited on pages 20 and 22.)

[14] Bonanno, A. and Reuter, M., "Spacetime structure of an evaporating black hole in quantum gravity", *Phys.Rev.*, **D73**, 083005 (2006). [DOI], [arXiv:hep-th/0602159 [hep-th]]. (Cited on page 76.)

[15] Carr, B.J., "The Black Hole Uncertainty Principle Correspondence", *arXiv*, e-print, (2014). [arXiv:1402.1427 [gr-qc]]. (Cited on page 75.)

[16] Carr, Bernard, Modesto, Leonardo and Premont-Schwarz, Isabeau, "Generalized Uncertainty Principle and Self-dual Black Holes", *arXiv*, e-print, (2011). [arXiv:1107.0708 [gr-qc]]. (Cited on page 75.)

[17] Carroll, Sean M., *Spacetime and geometry: An introduction to general relativity*, (Addison Wesley, San Francisco, 2004). (Cited on pages 10 and 12.)

[18] Casadio, R., "What is the Schwarzschild radius of a quantum mechanical particle?", *arXiv*, e-print, (2013). [arXiv:1310.5452 [gr-qc]]. (Cited on page 27.)

[19] Casadio, Roberto, Micu, Octavian and Nicolini, Piero, "Minimum length effects in black hole physics", *arXiv*, e-print, (2014). [arXiv:1405.1692 [hep-th]]. (Cited on page 24.)

[20] Cavaglia, Marco, "Black hole and brane production in TeV gravity: A Review", *Int.J.Mod.Phys.*, **A18**, 1843–1882 (2003). [DOI], [arXiv:hep-ph/0210296 [hep-ph]]. (Cited on pages 19, 20, and 87.)

[21] Dirkes, Alain R. P., Maziashvili, Michael and Silagadze, Zurab K., "Black hole remnants due to Planck-length deformed QFT", *arXiv*, e-print, (2013). [arXiv:1309.7427 [gr-qc]]. (Not cited.)

[22] Dvali, Gia and Gomez, Cesar, "Self-Completeness of Einstein Gravity", *arXiv*, e-print, (2010). [arXiv:1005.3497 [hep-th]]. (Cited on page 25.)

[23] Dvali, G. and Gomez, C., "Minimal length and black hole area quantization", *Fortsch.Phys.*, **59**, 579–585 (2011). [DOI]. (Cited on page 53.)

[24] Dvali, Gia and Gomez, Cesar, "Black Hole's Quantum N-Portrait", *Fortsch.Phys.*, **61**, 742–767 (2013). [DOI], [arXiv:1112.3359 [hep-th]]. (Cited on page 53.)

[25] Dymnikova, Irina, "Cosmological term as a source of mass", *Class.Quant.Grav.*, **19**, 725–740 (2002). [DOI], [arXiv:gr-qc/0112052 [gr-qc]]. (Cited on pages 58 and 62.)

[26] Elizalde, Emilio and Hildebrandt, Sergi R., "The Family of regular interiors for nonrotating black holes with T0(0)=T1(1)", *Phys.Rev.*, **D65**, 124024 (2002). [DOI], [arXiv:gr-qc/0202102 [gr-qc]]. (Cited on page 62.)

[27] Emparan, Roberto and Reall, Harvey S., "Black Holes in Higher Dimensions", *Living Rev.Rel.*, **11**, 6 (2008). [arXiv:0801.3471 [hep-th]]. (Cited on page 21.)

[28] Falls, Kevin, Litim, Daniel F. and Raghuraman, Aarti, "Black Holes and Asymptotically Safe Gravity", *Int.J.Mod.Phys.*, **A27**, 1250019 (2012). [DOI], [arXiv:1002.0260 [hep-th]]. (Cited on page 76.)

[29] Fließbach, T., *Allgemeine Relativitätstheorie*, Spektrum Lehrbuch, 5. Auflage, (Spektrum-Akademischer Vlg, Heidelberg, 2006). (Cited on page 10.)

[30] Frolov, V. and Novikov, I.D., *Black Hole Physics: Basic Concepts and New Developments*, Fundamental Theories of Physics, (Springer Netherlands, 1998). (Cited on page 23.)

[31] Giddings, Steven B., "Possible observational windows for quantum effects from black holes", *arXiv*, e-print, (2014). [arXiv:1406.7001 [hep-th]]. (Not cited.)

[32] Gingrich, Douglas M., "Noncommutative geometry inspired black holes in higher dimensions at the LHC", *JHEP*, **1005**, 022 (2010). [DOI], [arXiv:1003.1798 [hep-ph]]. (Cited on page 22.)

[33] Goenner, Hubert F. M., "On the History of Unified Field Theories", *Living Reviews in Relativity*, **7**(2) (2004). [DOI]. URL (accessed September 2014): http://www.livingreviews.org/lrr-2004-2. (Cited on page 72.)

[34] Griffiths, J.B. and Podolský, J., *Exact Space-Times in Einstein's General Relativity*, Cambridge Monographs on Mathematical Physics, (Cambridge University Press, Cambridge, 2009). (Cited on pages 15, 17, 18, and 64.)

[35] Hayward, Sean A., "Formation and evaporation of regular black holes", *Phys.Rev.Lett.*, **96**, 031103 (2006). [DOI], [arXiv:gr-qc/0506126 [gr-qc]]. (Cited on pages 65 and 88.)

[36] Hossenfelder, Sabine, "What black holes can teach us", *arXiv*, e-print, (2004). [arXiv:hep-ph/0412265 [hep-ph]]. (Cited on pages 20, 22, 23, and 87.)

[37] Hossenfelder, Sabine, "Minimal Length Scale Scenarios for Quantum Gravity", *Living Reviews in Relativity*, **16**(2) (2013). [DOI]. URL (accessed September 2014): http://www.livingreviews.org/lrr-2013-2. (Cited on page 24.)

[38] Isi, Maximiliano, Mureika, Jonas and Nicolini, Piero, "Self-Completeness and the Generalized Uncertainty Principle", *JHEP*, **1311**, 139 (2013). [DOI], [arXiv:1310.8153 [hep-th]]. (Cited on pages 27 and 75.)

[39] Isi, Maximiliano, Mureika, Jonas and Nicolini, Piero, "Self-Completeness in Alternative Theories of Gravity", *arXiv*, e-print, (2014). [arXiv:1402.3342 [hep-th]]. (Cited on pages 27 and 75.)

[40] Kanti, Panagiota, "Black holes in theories with large extra dimensions: A Review", *Int.J.Mod.Phys.*, **A19**, 4899–4951 (2004). [DOI], [arXiv:hep-ph/0402168 [hep-ph]]. (Cited on page 19.)

[41] Kanti, Panagiota and Winstanley, Elizabeth, "Hawking Radiation from Higher-Dimensional Black Holes", *arXiv*, e-print, (2014). [arXiv:1402.3952 [hep-th]]. (Cited on page 73.)

[42] Kempf, Achim, Mangano, Gianpiero and Mann, Robert B., "Hilbert space representation of the minimal length uncertainty relation", *Phys.Rev.*, **D52**, 1108–1118 (1995). [DOI], [arXiv:hep-th/9412167 [hep-th]]. (Cited on pages 27 and 75.)

[43] Kiefer, Claus, "Quantum gravity: General introduction and recent developments", *Annalen Phys.*, **15**, 129–148 (2005). [DOI], [arXiv:gr-qc/0508120 [gr-qc]]. (Cited on page 77.)

[44] Kiefer, Claus, *Quantum gravity*, International series of monographs on physics, 136, (Oxford Univ. Press, Oxford [u.a.], 2007), 2. ed. edition. (Cited on page 77.)

[45] Knipfer, Marco, *Generalized Uncertainty Principle inspired Schwarzschild Black Holes in Extra Dimensions*, Bachelor thesis, (Goethe-Universität, Frankfurt, 2014). (Cited on page 27.)

[46] Koch, Benjamin, *Black hole production and graviton emission in models with large extra dimensions*, Ph.D. thesis, (Goethe-Universität, Frankfurt, 2007). [ADS]. (Cited on page 10.)

[47] Koch, Benjamin, Bleicher, Marcus and Hossenfelder, Sabine, "Black hole remnants at the LHC", *JHEP*, **0510**, 053 (2005). [DOI], [arXiv:hep-ph/0507138 [hep-ph]]. (Cited on pages 20, 22, and 87.)

[48] Köppel, Sven, Iso, Maximiliano, Knipfer, Marco, Mureika, Jonas and Nicolini, Piero, "Self-Completeness and the Generalized Uncertainty Principle in Extra Dimensions", in preparation, (2014). (Cited on pages 27, 41, and 75.)

[49] Maldacena, Juan Martin, "Black holes in string theory", *arXiv*, e-print, (1996). [arXiv:hep-th/9607235 [hep-th]]. (Cited on page 77.)

[50] Misner, Charles, Thorne, Kip and Wheeler, John, *Gravitation*, (W. H. Freeman, New York, 1973). (Cited on pages 10, 11, 14, 16, 62, and 64.)

[51] Modesto, Leonardo, "Loop quantum black hole", *Class.Quant.Grav.*, **23**, 5587–5602 (2006). [DOI], [arXiv:gr-qc/0509078 [gr-qc]]. (Cited on page 76.)

[52] Modesto, Leonardo, "Super-renormalizable Quantum Gravity", *Phys.Rev.*, **D86**, 044005 (2012). [DOI], [arXiv:1107.2403 [hep-th]]. (Cited on page 74.)

[53] Modesto, Leonardo, Moffat, John W. and Nicolini, Piero, "Black holes in an ultraviolet complete quantum gravity", *Phys.Lett.*, **B695**, 397–400 (2011). [DOI], [arXiv:1010.0680 [gr-qc]]. (Cited on pages 27, 39, 65, and 74.)

[54] Myers, Robert C., "Tall tales from de Sitter space", in Gomberoff, A. and Marolf, D., eds., *Lectures on Quantum Gravity*, Series of the Centro De Estudios Científicos, p. 12345. Springer, (2006). (Cited on page 18.)

[55] Nicolini, Piero, "Noncommutative Black Holes, The Final Appeal To Quantum Gravity: A Review", *Int.J.Mod.Phys.*, **A24**, 1229–1308 (2009). [DOI], [arXiv:0807.1939 [hep-th]]. (Cited on page 74.)

[56] Nicolini, Piero, "Entropic force, noncommutative gravity and un-gravity", *Phys.Rev.*, **D82**, 044030 (2010). [DOI], [arXiv:1005.2996 [gr-qc]]. (Cited on page 74.)

[57] Nicolini, Piero, "Nonlocal and generalized uncertainty principle black holes", *arXiv*, e-print, (2012). [arXiv:1202.2102 [hep-th]]. (Cited on pages 27 and 39.)

[58] Nicolini, Piero, Mureika, Jonas, Spallucci, Euro, Winstanley, Elizabeth and Bleicher, Marcus, "Production and evaporation of Planck scale black holes at the LHC", *arXiv*, e-print, (2013). [arXiv:1302.2640 [hep-th]]. (Cited on page 20.)

[59] Nicolini, Piero, Smailagic, Anais and Spallucci, Euro, "Noncommutative geometry inspired Schwarzschild black hole", *Phys.Lett.*, **B632**, 547–551 (2006). [DOI], [arXiv:gr-qc/0510112 [gr-qc]]. (Cited on pages 30 and 74.)

[60] Nicolini, Piero and Spallucci, Euro, "Holographic screens in ultraviolet self-complete quantum gravity", *arXiv*, e-print, (2012). [arXiv:1210.0015v2 [hep-th]]. (Cited on pages 56 and 57.)

[61] Nicolini, Piero and Spallucci, Euro, "Holographic screens in ultraviolet self-complete quantum gravity", *Adv.High Energy Phys.*, **2014**, 805684 (2014). [DOI], [arXiv:1210.0015 [hep-th]]. (Cited on pages 33, 42, 43, 44, 46, 53, 59, and 69.)

[62] Nicolini, Piero and Winstanley, Elizabeth, "Hawking emission from quantum gravity black holes", *JHEP*, **1111**, 075 (2011). [DOI], [arXiv:1108.4419 [hep-ph]]. (Cited on page 74.)

[63] Niedermaier, Max and Reuter, Martin, "The Asymptotic Safety Scenario in Quantum Gravity", *Living Reviews in Relativity*, **9**(5) (2006). [DOI]. URL (accessed September 2014): http://www.livingreviews.org/lrr-2006-5. (Cited on page 76.)

[64] Penrose, Roger, *The large, the small and the human mind*, (Cambridge Univ. Press, Cambridge, 1997). (Cited on pages 7 and 87.)

[65] Perez, Alejandro, "The Spin-Foam Approach to Quantum Gravity", *Living Reviews in Relativity*, **16**(3) (2013). [DOI]. URL (accessed September 2014): http://www.livingreviews.org/lrr-2013-3. (Cited on page 76.)

[66] Peters, Antje, *Determination of* $\Lambda_{\overline{MS}}$ *from the static quark-antiquark potential in momentum space*, Master's thesis, (Goethe-Universität, Frankfurt, 2014). [ADS]. (Cited on page 15.)

[67] Reuter, M., "Nonperturbative evolution equation for quantum gravity", *Phys.Rev.*, **D57**, 971–985 (1998). [DOI], [arXiv:hep-th/9605030 [hep-th]]. (Cited on page 76.)

[68] Rizzo, Thomas G., "Noncommutative Inspired Black Holes in Extra Dimensions", *JHEP*, **0609**, 021 (2006). [DOI], [arXiv:hep-ph/0606051 [hep-ph]]. (Cited on pages 30 and 74.)

[69] Rovelli, Carlo, "Loop Quantum Gravity", *Living Reviews in Relativity*, **11**(5), 12345 (2008). [DOI]. URL (accessed September 2014): http://www.livingreviews.org/lrr-2008-5. (Cited on page 76.)

[70] Scardigli, Fabio and Casadio, Roberto, "Gravitational tests of the Generalized Uncertainty Principle", *arXiv*, e-print, (2014). [arXiv:1407.0113 [hep-th]]. (Not cited.)

[71] Spallucci, Euro and Smailagic, Anais, "Black holes production in self-complete quantum gravity", *Phys.Lett.*, **B709**, 266–269 (2012). [DOI], [arXiv:1202.1686 [hep-th]]. (Cited on page 26.)

[72] Spallucci, Euro and Smailagic, Anais, "Semi-classical approach to quantum black holes", *arXiv*, e-print, (2014). [arXiv:1410.1706 [gr-qc]]. (Cited on page 26.)

[73] Stephani, Hans, Kramer, Dietrich, Maccallum, Malcolm, Hoenselaers, Cornelius and Herlt, Eduard, *Exact Solutions of Einstein's Field Equations*, Cambridge Monographs on Mathematical Physics, (Cambridge University Press, Cambridge, 2003). (Cited on page 15.)

[74] Susskind, Leonard, "Trouble for remnants", *arXiv*, e-print, (1995). [arXiv:hep-th/9501106 [hep-th]]. (Not cited.)

[75] Susskind, Leonard, "Singularities, Firewalls, and Complementarity", *arXiv*, e-print, (2012). [arXiv:1208.3445 [hep-th]]. (Not cited.)

[76] Susskind, Leonard and Uglum, John, "Black hole entropy in canonical quantum gravity and superstring theory", *Phys.Rev.*, **D50**, 2700–2711 (1994). [DOI], [arXiv:hep-th/9401070 [hep-th]]. (Not cited.)

[77] Thiemann, Thomas, "Lectures on loop quantum gravity", *Lect.Notes Phys.*, **631**, 41–135 (2003). [DOI], [arXiv:gr-qc/0210094 [gr-qc]]. (Cited on page 76.)

[78] Thiemann, Thomas, "Loop Quantum Gravity: An Inside View", *Lect.Notes Phys.*, **721**, 185–263 (2007). [DOI], [arXiv:hep-th/0608210 [hep-th]]. (Cited on page 76.)

[79] Wagner, Marc, "Quantum Field Theory II", lecture notes, (2013). (Cited on pages 76 and 80.)

[80] Wald, Robert M., *General Relativity*, (The University of Chicago Press, Chicago and London, 1984). (Cited on pages 10, 11, 16, 64, and 85.)

[81] Wald, Robert M., "Teaching general relativity", *arXiv*, e-print, (2005). [arXiv:gr-qc/0511073 [gr-qc]]. (Cited on page 10.)

[82] Winstanley, Elizabeth, "Hawking radiation from rotating brane black holes", *arXiv*, e-print, (2007). [arXiv:0708.2656 [hep-th]]. (Cited on page 22.)

[83] Witten, Edward, "Anti-de Sitter space, thermal phase transition, and confinement in gauge theories", *Adv.Theor.Math.Phys.*, **2**, 505–532 (1998). [arXiv:hep-th/9803131 [hep-th]]. (Not cited.)

Acknowledgement

First of I all, I want to thank Piero Nicolini for his patience and availability in the past year. His knowledge in people and papers was a great help to navigate in the Quantum Gravity landscape.

Second, I would like to thank Marcus Bleicher for kind FIAS hospitality and group supervision.

Erklärung

Ich versichere hiermit, die vorliegende Arbeit selbständig verfasst und keine anderen als die angegebenen Quellen und Hilfsmittel vewendet zu haben. Alle Stellen der Arbeit, die wörtlich oder sinngemäß aus Veröffentlichungen oder aus anderen fremden Texten entnommen wurden, sind von mir als solche kenntlich gemacht worden. Ferner erkläre ich, dass die Arbeit nicht – auch nicht auszugsweise – für eine andere Prüfung verwendet wurde.

Frankfurt am Main, im Dezember 2014

Sven Köppel